



UNRAVELLING THE PIVOTAL METABOLIC PATHWAYS OF MALIGNANT GLIOMAS

DAVID ALEXANDRE DIAS VAN DER KELLEN

A dissertation submitted in partial fulfillment of the requirements for the Degree of Masters in Biomedical Research (Specialization Area: Oncobiology) at Faculdade de Ciências Médicas | NOVA Medical School of NOVA University Lisbon

September, 2021

UNRAVELLING THE PIVOTAL METABOLIC PATHWAYS OF MALIGNANT GLIOMAS

David Alexandre Dias van der Kellen Supervisors: Jacinta Serpa, Assistant Professor at NOVA Medical School Luís Gonçalves, Invited Researcher at Instituto de Tecnologia Química e Biológica

A dissertation submitted in partial fulfillment of the requirements for the Degree of Masters in Biomedical Research (Specialization Area: Oncobiology)

September, 2021

Acknowledgments

Em primeiro lugar, gostaria de agredecer à Faculdade de Ciências Médicas e ao grupo de docentes do Mestrado em Investigação Biomédica por terem criado este mestrado e pela formação que é, e foi dada, não só a mim, mas a todos os meus colegas ao longo do percurso.

Aos meus orientadores, Doutora Jacinta Serpa, por me ter aceite no grupo, pela enorme ajuda que me deu ao longo deste ano e por toda a paciência, e Doutor Luís Gonçalves, pela ajuda importante dada na área de NMR e pela paciência em esclarecer todas as perguntas que fiz. A ambos, muito obrigado.

Às minhas colegas de laboratório, um obrigado. À Ana Hipólito, por servir de exemplo pela sua dedicação. À Cindy Mendes, principalmente pela orientação que me deu quando estive em rotação laboratorial no grupo. À Isabel Lemos, pela companhia no ITQB e também pela ajuda que me deu. Por fim, e não menos importante, pelo contrário, à Filipa Martins. Recebeu-me de braços abertos no primeiro dia e sempre esteve disponível para me ajudar, tendo sido muito important para o trabalho que desenvolvi durante este ano. Para além disto, também agradeço pela companhia na viagem de volta do IPO.

A um nível mais pessoal, quero agradecer a todos os meus amigos que estiveram comigo nas diferentes etapas da minha vida. Aos amigos que trouxe de Queluz, obrigado pela amizade que construímos e conseguimos manter. Aos amigos do ISA, por tudo o que sempre me ensinaram e pela companhia que me fazer. Aos amigos que conheci durante o NBR, por me mostrarem o que é trabalhar arduamente e lutarem todos os dias pelo vosso sonho, algo que eu não consegui fazer. Sem vocês esta etapa teria sido muito mais difícil do que tem sido.

À minha família, especialmente aos meus irmãos, por me terem permitido continuar a estudar sem ter de me preocupar com mais nada. Esta frase é pequena, mas a ajuda dos familiares que vivem comigo foi enorme.

Por fim, quero agradecer à minha namorada, companheira de todas as horas, Ana Correia Matos. Sem ela o meu percurso teria sido totalmente diferente. Pela ajuda que me deu desde que estamos juntos, especialmente durante este ano que passou. Pela paciência que tem em aturarme. Quero também agradecer à família Correia, por me aceitarem e, sobretudo à Isabel Correia, por me tratar como um filho e por toda a ajuda que meu.

A todos, obrigado.

Resumo

Glioblastomas (GBM) são o subtipo tumoral mais frequente do sistema nervoso central. Apesar das opções terapêuticas actuais e inespecíficas, os GBM são caracterizados pela sua elevada morbidade e mortalidade. Posto isto, é necessário desenvolver terapias mais eficazes. Neste contexto, o metabolismo de tumores é um alvo atraente para novas terapias.

O metabolismo tumoral permite que o tumor progrida, nas mais diversas condições, sendo o resultado da interação entre diversos factores, nomeadamente o tecido de origem e o microambiente tumoral. Compostos como glucose, glutamina, glutamata e acetoacetato, essenciais ao normal funcionamento do cérebro, são interessantes no contexto de GBM.

O objetivo desta tese é revelar as principais vias metabólicas de GBM. Para o atingir, estudámos a influência da disponibilidade dos diferentes nutrientes sobre as características celulares de GBM, o seu metabolismo e a expressão de genes metabólicos importantes. Para tal, foram utilizadas como modelos *in vitro* de GBM as linhas celulares U-251 e U-87.

Os nossos resultados revelaram que a glucose e a glutamina mostram ter um papel central no fenótipo em ambas linhas celulares. Em linha com isto, nós observámos que a proliferação celular apenas aumentou na presença de glucose. No entanto, apenas glucose não é suficiente sendo também necessário a presença de glutamina ou glutamato, sugerindo papéis complementares na proliferação celular. Para além disso, mostramos que a capacidade migratória de células de GBM é promovida pela glucose e glutamina. A nível metabólico, a metabolómica, baseada em NMR, revelou que o metabolismo é suficiente para distinguir as duas linhas celulares. Além disto, enquanto as amostras de U-87 não agruparam de acordo com nutriente específico, revelando plasticidade metabólica reduzida, o metabolismo das células U-251 foi afetado pela presença glucose ou glutamina. Curiosamente, em amostras com glucose encontrámos metabolitos aumentados, como a alanina, glicina, e acetato, que podem explicar o aumento da proliferação e migração. Além disto, a análise à expressão genética revelou que as principais vias desreguladas, de ambas as linhas celulares, estão envolvidas no metabolismo da glucose e glutamina. Isto mostra que as adaptam-se à biodisponibildade do composto orgânico

Este estudo revela que as duas linhas celulares são distintas ao nível de malignidade e de metabolismo, sublinhando assim a heterogeneidade existente entre subtipos tumorais. Os nossos resultados demonstram um possível papel da via dos fosfatos de pentose e do metabolismo de um carbono nestes tumores. Apesar de serem específicos à linha celular, as nossas observações destacam as características individuais e detalhes metabólicos que podem ser importantes no tratamento de GBM, num contexto de medicina personalizada.

Palavras-chave: Glioblastoma, Metabolismo tumoral, Microambiente tumoral, Glucose, Glutamina, Glutamato, Acetoacetato, Biodisponibilidade de nutrientes

Abstract

Glioblastomas (GBM) are the most frequent tumor sub-type in the central nervous system. Despite current and unspecific therapy options, GBM are still characterized by high morbidity and mortality. As such, there is a need to develop new therapies. In recent years, cancer metabolism as grown as an attractive target for the design of new therapies.

Cancer metabolism and metabolic remodeling are important mechanisms that allow tumors to grow and progress, even in unfavorable conditions. Cancer metabolism is a result of important factors that include selective pressures from the microenvironment and the tissue of origin. Thus, the setting in which the tumor develops is important. Due to their origin, the metabolism of important metabolites for the physiological brain function are interesting in the context of GBM. These compounds include glucose, glutamine, glutamate and acetoacetate.

The objective of this thesis is to disclose the main metabolic pathways of GBM. To achieve our aim, we studied if the bioavailability of glucose, glutamine, glutamate and acetoacetate influenced the characteristics of GBM cells, their metabolism and the expression of important genes in the metabolism of the previous organic compounds. Therefore, an *in vitro* study was developed using two GBM cell lines, U-251 and U-87.

Our results revealed that glucose and glutamine appear to have a central role in the GBM cells. We found that proliferation only increased when glucose was available. However, it was not enough since glutamine or glutamate were also required, suggesting complementary roles, to sustain cellular proliferation. Furthermore, we also show that the migratory capacity of GBM cells is promoted by glucose and glutamine. At the metabolic level, NMR-based metabolomics revealed that cellular metabolism was sufficient to distinguish between cell lines. Furthermore, while U-87 samples did not cluster according to a particular nutrient, revealing reduced metabolic plasticity, the metabolism of U-251 cells was specifically affected by the presence of glucose or glutamine. In glucose-containing samples we found important metabolites, such as alanine, glycine, and acetate to be increased, which might underlie the increase in proliferation and migratory rates. Furthermore, gene expression analysis revealed that the main deregulated pathways are involved with the metabolism of glucose and glutamine, in both cells. This observation reinforces the ability of cells to adjust to the bioavailability of organic compounds.

This study revealed that both cell lines are distinct in terms of malignancy and metabolism, highlighting the heterogeneity in tumor sub-types. In addition, the pentose phosphate pathway and the one carbon metabolism appeared to have an important role in these tumors. Although cell line-specific, our results underscore, in the context of personalized medicine, that specific individual traits and metabolic details can be important for the treatment of GBM.

Key words: Glioblastoma, Cancer metabolism, Tumor microenvironment, Glucose, Glutamine, Glutamate, Acetoacetate, Nutrient bioavailability.

Funding

The project entitled as *Unravelling the Pivotal Metabolic Pathways of Malignant Gliomas* was developed at the Cancer Metabolism and Microenvironment (IPO | CEDOC | NMS) and it was not funded by any public, or private, organization.

Index

Acknowledgments	I
Resumo	II
Abstract	III
Funding	IV
Introduction	1
Cancer – Overview	1
Benign vs malignant tumor	1
Cancer Biology	1
Cancer hallmarks – an update	2
Brain cancer – Overview	4
Grading of gliomas	4
Molecular biomarkers used in the diagnosis and prognosis of gliomas	5
Brain metabolism - main metabolic pathways	6
Glucose metabolism	7
Glutamine metabolism	8
Ketone bodies metabolism	9
Malignant gliomas metabolic rewiring	11
Glucose metabolism	11
Glutamine metabolism	14
Ketone bodies metabolism	16
Clinical management of malignant glomas	16
Metabolism-based therapeutic approaches	16
Hypothesis and objective	18
Materials and Methods	19
Cell culture	19
Cell death assay	19
Cell proliferation assay	20
Wound healing assay	21

RNA extraction and Reverse transcription and real-time quantitative PCR (RT-qPCR) 21
Nuclear magnetic resonance (NMR) spectroscopy
Statistical Analysis
Results
Glioblastoma cells are able to adapt to the availability of different organic compounds 25
Glucose is the main contributor to sustain the metabolic needs associated to cellular proliferation
Cell migration is positively influenced by glucose and glutamine
Glucose and glutamine have a primary influence in glioblastoma cells
Transport of the supplied nutrients and production of related organic compounds 38
Gene expression is affected by nutrient availability
Gene expression reveals differences between cell lines
Discussion
Conclusions
Future Prespectives
References
Supplementary Figures and Tables
Supplementary Figure 176
Supplementary Figure 2
Supplementary Figure 3
Supplementary Table 185
Supplementary Table 2
Supplementary Table 390

Introduction

Cancer - Overview

Cancer is a major health problem worldwide that accounted for an estimated 19.3 million new cases and almost 10 million deaths in 2020¹. This disease arises when the regulatory mechanisms, that tightly control the replication and proliferation of healthy cells, fail and is defined by its ability of continuous proliferation, and dissemination^{2,3}.

Benign vs malignant tumor

A tumor (benign or malignant) arises from a single cell or a group of cells that proliferate autonomously within a certain microenvironment. Both types of tumors may present uncontrolled cell proliferation, however their agressiveness enables its distinction. Benign tumors often present no cell atypia, low proliferation rates and, importantly, they lack aggressiveness, meaning that they are not able to invade nearby tissue or metastazise⁴. Normally they are harmless, but if these tumors compress the surrounding tissues, due to excessive growth, or produce high levels of hormones, it can lead to adverse effects⁴. Tumors are considered malignant, also called cancer, when their cells lose normal morphology and attain the ability to invade the surrounding tissue and dessiminate into distante sites (metastasis)^{4,5}. Cancer-associated adverse effects are dependent on the primary tumor size and localization, invasion into neighbouring tissue and metastasis location⁴.

Cancer Biology

For a cell to transform, it is required to accumulate mutations in several genes and to acquire epigenetic alterations in order to evade mechanisms that do not allow cells to become autonomous^{6,7}. Moreover, both mutations and epigenetic alterations will ultimately provide transformed cells with selective advantage in comparison to normal cells. Tumor formation is promoted by mutations that typically occur into three classes of gene, oncogenes, tumor suppressor genes and stability genes^{3,8}. Mutations in oncogenes render active pathways that stimulate tumor growth. In contrast to oncogenes, tumor suppression genes are subjected to loss-of-function mutations resulting in the inactivation of mechanisms that control cell proliferation and replication. Although oncogenes and tumor suppressor genes promote tumor formation, growth and progression in a similar manner, stability genes promote tumorigenesis by enabling cells to acquire more mutations. Stability genes are a subset of tumor suppressor genes and include genes involved in DNA repair mechanism, mismatch repair, nucleotide-excision repair and base-excision repair. Thus, impairment of these mechanisms will lead to a higher rate of mutations⁹. At the chromatin level, tumorigenesis can be promoted by alterations in the epigenetic status of the previous gene classes⁷. These alterations can be caused by aberrant DNA methylation, histone

modifications and chromatin remodeling, leading to profound phenotypic changes by directly affecting the expression of oncogenes and tumor suppressor genes^{7,10,11}.

Tumors acquire the previous alterations throughout disease progression, confering important phenotypic changes. The newly acquired characteristics provides cells with selective advantange, in comparison to the surrounding tissue, and are known as cancer hallmarks^{12,13}.

Cancer hallmarks – an update

To better understand the complexity of cancer biology, Hanahan and Weinberg initially introduced six traits that normal cells acquire while progressing into malignancy¹². These traits: sustaining proliferative signaling, evading mitogenic suppressors, resisting cell death, enabling replicative immortality, inducing angiogenesis, and activating invasion and metastasis; are known as the cancer hallmarks and provided a basis for cancer research. Consequentially, with the increase in scientific knowledge, the hallmarks have been refined in order to include key traits, in cancer progression and maintenance, that were not previously recognize^{13,14}. As such, avoiding immune surveillance, interactions with the tumor microenvironment (TME), and cancer metabolism and its remodeling, have also been included in the hallmarks of cancer. Among the several hallmarks, which are currently needing an update, the TME and cancer metabolism and metabolic remodeling show a prominent importance.

Cancer metabolism and metabolic remodeling confer growth advantage to transformed cells, promoting disease establishement and progression, both in nutrient replete and poor conditions. Altered metabolic activities in cancer are a consequence of intrinsic and extrinsic factors. These include, in a general manner, the tissue of origin, mutations in proliferation control genes (which will affect the expression of key metabolic genes), epigenetics and interactions with the TME¹⁵. Moreover, the metabolism of the patient, influenced by genetics, diet, and, if appliable, metabolic disorders, also contribute to the metabolic phenotype of the tumor¹⁵, however this influence is far from being completely understood. Alterations in cancer metabolism are known to occur in different stages of tumorigenesis and can either be involved in all the steps of the disease: initiation, progression and recurrence^{16,17}. These alterations enable transformed cells to meet their biosynthetic and bioenergetic demands, while also maintaining cellular homeostasis, and encompass increased uptake of nutrients, nutrient metabolization through pathways that contribute to the acquisition and maintenance of tumorigenic properties, and paracrine communication between cancer and stroma cells in the TME^{14–17}.

Besides its role in sustaining cellular needs during carcinogenesis and tumor progression, the importance of cancer metabolism and metabolic remodeling is also highlighted by the fact that it is linked to other hallmarks of cancer¹⁸, for instance sustaining proliferative signaling. In contrast to unicellular organisms, our cells are not able to activate pathways that enables them to grow and proliferate in the absence of extracellular signals, such as growth factors, even in the

presence of abundant nutrients¹⁹. However, cancer cells are able to avoid this, usually through mutations in receptor tyrosine kinases (RTKs) or in the downstream effectors, or through loss-of-function in negative regulators of these pathways, rendering them independent of extracellular stimuli. RTKs are usually activated by specific growth factors, which stimulates several signaling pathways, such as the PI3K/AKT pathway, leading to the expression of genes involved in cellular proliferation and other cellular functions²⁰. Accordingly, these pathways also regulate nutrient uptake and metabolism, and macromolecules biosynthesis. PI3K/Akt signaling regulates glucose metabolism by promoting the expression of glucose transporter 1 (*GLUT1*)^{21,22}, and by increasing the activity of hexokinase (HK), and of phosphofructokinase (PFK), ultimately resulting in an increased glucose uptake and oxidation^{23,24}. Furthermore, PI3K/AKT activation increases the amino acid flux across the plasma membrane, activation of the mammalian target of rapamycin 1 (mTORC1), an activator of protein synthesis and inhibitor of catabolic reactions, and also stimulates fatty acid synthesis^{16,18}. Thus, constitutive activation of RTKs or of its downstream targets, can promote substantial changes in cellular metabolism, improving cellular fitness and promoting tumor formation and progression.

Hypoxia is a feature that is common to many solid tumors, arising from the ineficient tumor vasculature and high proliferative rate of cells^{25–27}. Furthermore, it can have an important role in metabolic rewiring^{28,29}. The cellular response to hypoxia is orchestrated by the hypoxia inducible factors (HIF) family, in specific the O₂-regulated α subunit (HIF-α) and the constitutively expressed β (HIF- β) subunit^{30–33}. Under hypoxic conditions, the HIF- α subunits become stable and are able to translocate into the nucleus where they will dimerize with HIF-B, exerting its function as a transcription factor^{25,30}. HIF will then promote the expression of genes, being some of them involved in the regulation of metabolism²⁸. At the level of glucose metabolism, glucose transporters, such as GLUT1, are HIF-1α targets resulting in an increase in glucose uptake 18,32,33 . In addition to the high rate of glycolysis, HIF-1 α prevents the entry of most glucose into the tricarboxilic acid (TCA) cycle. This occurs through the upregulation of pyruvate dehydrogenase kinase 1 (PDK1), which inhibits the enzyme pyruvate dehydrogenase (PDH), preventing the oxidation of pyruvate into acetyl-CoA^{32–34}. As such, lactate becomes the main fate of glucose (glycolysis). This processes is also facilitated by the HIF-1α-mediated upregulation of glycolytic enzymes, such as HK I and II, lactate dehydrogenase (LDH) A, and of lactate transporters, monocarboxylate transporters (MCT) 1 and 4, sustaining the high glycolytic flux^{35–} ³⁷. Aside from its effect on glucose metabolism, HIF can also increase amino acid transport, through the upregulation of large-neutral-amino-acid-transporter (LAT) 1 and other transporters^{38,39}; promote lipogenesis, through the upregulation of fatty acid synthase (FASN)⁴⁰; and impact other aspects of cellular metabolism²⁸.

The TME results from the interaction between tumoral and non-tumoral cells, which depend on and can impact the fate of each other^{41,42}. Moreover, the microenvironment applies a selective pressure that favors cells with increased proliferation and spread advantage, ultimately promoting cancer progression. Cancer metabolism can directly influence the microenvironment, but at the same time it can be affected by nutrient availability and interactions with non-tumoral cells in the TME^{17,42}. Tumoral cells often alter the microenvironment composition through the release of high amounts of lactate, causing the TME to become more acidic¹⁷. The increase in acidity can lead to an immune-permissive microenvironment^{43,44}. Moreover, increased levels of lactate are also crucial to promote the formation of new blood vessels (neo-angiogenesis)^{45,46}. In the other hand, the non-tumoral cells in the TME, which include endothelial cells, cancer associated adipocytes, cancer associated fibroblasts and tumor associated macrophages, among others, release soluble factors that influence the proliferation, invasion, metastasis and metabolism of cancer cells⁴⁷.

Taken all together, tumor metabolism and metabolic remodeling show a central importance in cellular transformation, tumor growth and progression. These alterations enable cells to meet their bioenergetic and biosynthetic demands, and to achieve cellular homeostasis ¹⁶. Therefore, understanding the complexity of factors that underly the metabolic adaptation reported in tumors, can point to metabolic liabilities worth to be explored as disease biomarkers and therapeutic targets.

Brain cancer - Overview

Gliomas are brain tumors that originate from glia or precursor cells. This type of tumors is rare but, among over 100 histological types of central nervous system (CNS) tumors, it is the most common, accounting for approximately 25% of the reported cases. Importantly, 80% of these neoplasms are malignant⁴⁸. Gliomas comprise astrocytoma (including glioblastoma, GBM), ependymoma, oligodendroglioma, oligoastrocytoma, among other histological types⁴⁸, and are characterized by a high mortality rate that is justified by its unreachable localization, high proliferative rate, invasive capacity^{48,49} and also due to the lack of effective therapies⁵⁰.

Grading of gliomas

Gliomas and other tumors from the CNS are not staged, unlike other types of tumor⁴⁸. Instead, these tumors are graded according to the 2016 World Health Organization (WHO) Classification of Tumors of the Central Nervous System⁵¹. According to the WHO grade system, gliomas can be graded from I to IV and is based on predicted clinical behaviour according to characteristics such as mitoses, necrosis, and microvascular proliferation⁵⁰. Accordingly, tumors with higher grade (IV being the highest) are associated to increased anaplasia and poorer clinical outcome^{48,52}. Furthermore, gliomas can be classified as low-grade gliomas (Grade I and II) and high-grade gliomas (Grade III and IV)⁵¹.

Molecular biomarkers used in the diagnosis and prognosis of gliomas

Brain tumors have been classified, during the past century, according to their histological similarities between the cells of origin. However, starting from 2016, the WHO classification⁵¹ has been used, enabling a more accurate diagnosis of gliomas. The current classification not only is based in the phenotypic characteristics mentioned above, but also in the molecular features of the tumor. Specifically, gliomas diagnosis must include molecular information relative to mutations in the isocitrate dehydrogenase (*IDH*) 1/2 genes, and to the 1p/19q codeletion status^{48,52}. As such, adult gliomas are generally divided into 3 major molecular groups: *IDH* wildtype, *IDH* mutant with intact 1p/19q and *IDH* mutant with 1p/19q codeleted⁵³.

Mutations in the metabolic enzymes *IDH1/2* are frequent in gliomas, particularly in *IDH1*, with a prevalence of up to 80 to 90% of grade II and III gliomas⁵⁴. Thus, the assessment of *IDH* mutation status represents one of the first steps for the diagnosis of gliomas. The presence or absence of a mutation in these enzymes also exhibit significant prognostic value. Indeed, *IDH*-mutated gliomas (astrocytoma, oligodendroglioma and secondary GBM) are associated to improved prognosis when compared to *IDH* wild type gliomas (GBM), independently of tumor grade^{48,50,55}.

To further differentiate *IDH*-mutant gliomas, the codeletion of 1p/19q is also assessed. It refers to the loss of the short arm of the chromosome 1 and the long arm of chromosome 19 and has been long recognized as a glioma biomarker^{56–58}. Specifically, the 1p/19q codeletion is used in order to distinguish *IDH*-mutant tumors between astrocytoma and oligodendroglioma⁵⁰. Loss of 1p/19q and mutated *IDH* co-occur in the vast majority of oligodendrogliomas and are associated to the best prognosis between the different glioma subtypes^{59,60}.

Even though the recognition of mutant *IDH* and 1p/19q codeletion as biomarkers helped improve glioma diagnosis, the 2016 WHO classification still presents limitations regarding the heterogeneity of this type of tumors⁵¹. Nevertheless, efforts have been made in order to identify new biomarkers that could contribute for a better diagnosis and prediction of clinical behaviour. *MGMT* (O-6-methylguanine-DNA methyltransferase) promoter methylation status, *PTEN* (phosphate and tensin homologue) mutations or deletions, *EGFR* (epithelial growth factor receptor) amplification or mutations are examples of potential biomarkers that could be incorporated into the current classification. Alterations in these genes are frequent and can be good indicators for prognosis and radio- and chemotherapy response⁶¹. For instance, the methylation status of the *MGMT* promoter can be used as a predictive and prognostic biomarker in GBM. Tumors presenting *MGMT* methylation have been found, in most cases, to be sensitive to temozolomide (TMZ) and radiation. Moreover, independently of the treatment received, patients with tumors that harbour this alteration survive longer than patients with tumors without *MGMT* promoter methylation⁶².

Brain metabolism - main metabolic pathways

The brain is a very complex organ that metabolically depends mostly on glucose, and, in certain areas, on glutamine. While, glucose is the primary source of energy for ATP generation and maintenance of its normal functions⁶³, glutamine is mainly used for the synthesis of the neurotransmitters glutamate and γ -aminobutyric acid (GABA)⁴⁹. In certain conditions, such as nutrient deprivation, the brain can also use other substrates to satisfy its metabolic needs. Ketone bodies, for instance, can function as an alternative and important source of energy during fasting conditions⁶⁴. The physiological metabolic network of the brain is represented in **Fig 1**.

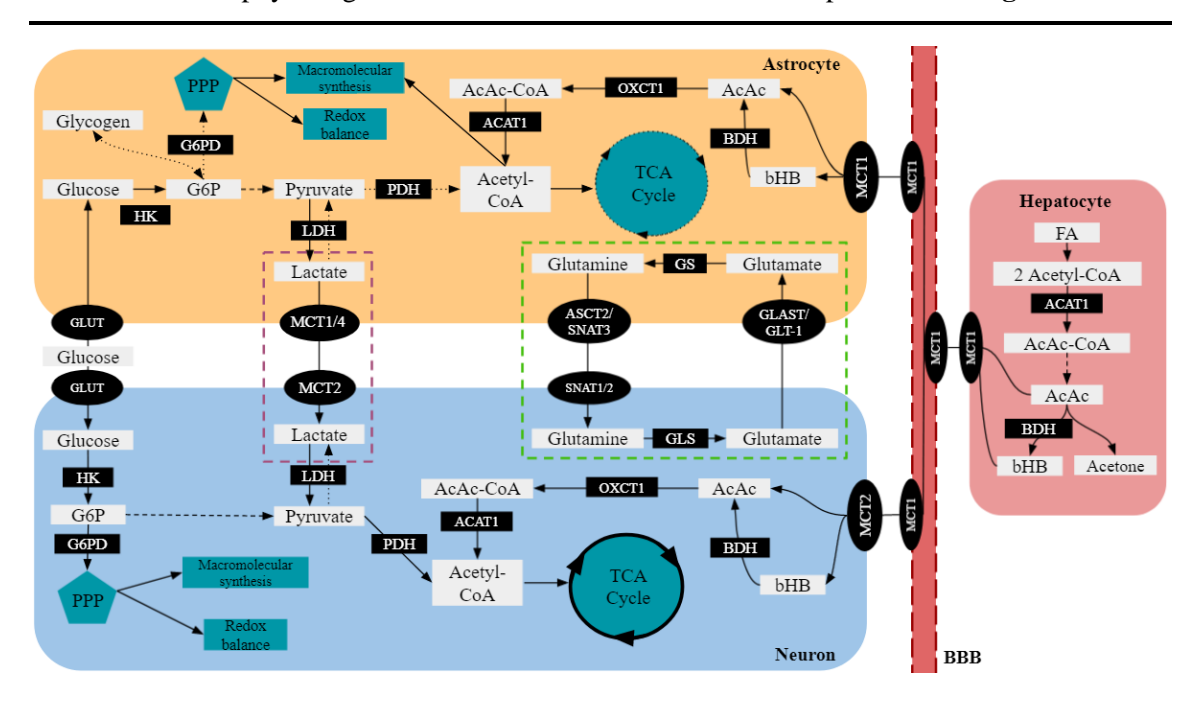


Fig 1. The physiological metabolic network of the brain. Glucose is the brain's main metabolic fuel and, depending on cell type, it is used differently. While neurons are mainly oxidative, i.e. predominantly oxidize glucose oxidative phosphorylation (OXPHOS), astrocytes are characterized as glycolytic, mainly utilize in the glycolytic pathway, having lactate as an important final product. Glucose enters the cell through membrane transporters of the glucose transporter (GLUT) family. Inside the cell, glucose is quickly phosporylated by hexokinases (HK) into glucose-6-phosphate (G6P), which can either be redirected to the pentose phosphate pathway (PPP), by glucose-6-phosphate dehydrogenase (G6PD), or be transformed into pyruvate, through several reactions. In the case of astrocytes, G6P can be stored as glycogen. To note that, intermediate metabolites between G6P and pyruvate can also serve as precursors for several different compounds. If redirected into the PPP, G6P is used to sustain biosynthetic reactions and in regulating oxidative stress. This pathway is particularly important in the regulation of redox homeostasis because NADPH, generated in the PPP, is mainly utilized in the synthesis of glutathione. When pyruvated is generated it can be transformed into lactate (mainly in astrocytes), or follow the tricarboxylic (TCA) cycle (predominantly in neurons). Lactate produced in astrocytes can be shuttled into neurons (Astrocyte-Neuron Lactate Shuttle - Purple dashed rectangle) and transformed by lactate dehydrogenase (LDH) into pyruvate, being able to follow the TCA cycle. In the TCA cycle, pyruvate is used to produce ATP, carbon skeletons and reducing power. Glutamine takes a specific role in neurons and astrocytes, participating predominantly in the glutaminergic cycle (Green dashed rectangle). In this cycle, glutamate is released by neurons, during neuronal activity, into the synaptic cleft. Excess glutamate is cleared by astrocytes, through the glutamate asparate transporter (GLAST) and glutamate transporter 1 (GLT-1), and glutamine synthase (GS) amidates glutamate, generating glutamine. Glutamine is then released. Through the alanine/serine/cysteine transporter 2 (ASCT2) and sodium-coupled neutral amino acid 3 (SNAT3) and taken up by neurons, through SNAT1 and 2. Here, glutaminase (GLS) uses glutamine to synthesize glutamate, which will be released again during neuronal activity. (Continues on the next page)

Fig 1. (Continuation) During starvation, ketone bodies (Acetoacetate – AcAc; β-hydroxybutyric acid – bHB; Acetone) can be used as an alternative fuel to glucose. These molecules are mainly produced (ketogenesis) in hepatocytes and originate from the oxidation of fatty acids (FA). FA undergo β-oxidation, giving origin to acetyl-CoA. Two molecules of acetyl-CoA are then condensed by the enzyme acetoacetyl-CoA thiolase (ACAT1) and, through several steps, originating AcAc. This molecule can be spontaneously decarboxylated, originatic acetone, or used to synthesize bHB by β-hydorxybutyrate dehydrogenase (BDH). Ketone bodies leave hepatocytes, cross the blood brain barrier (BBB) and enter brain cells through the monocarboxylate transporter 1 (MCT1). In these cells, the reverse process (Ketolysis) occurs. BDH catalyzes the reverse reaction of bDH into AcAc, which is metabolized into acetoacetyl-CoA (AcAc-CoA) by 3-oxoacid CoA-transferase 1 (OXCT1). The enzyme ACAT1 further metabolizes AcAc-CoA into Acetyl-CoA, which allows it to be oxidized through the TCA cycle or to be used in the synthesis of FA. To note that, acetone is not represented as being transported into neurons because it has a minimal metabolic input⁶⁵. Solid arrows – Main metabolic pathway; Dotted arrows – Secondary/down-regulated metabolic pathways; Dashed arrows – Hidden intermediary steps; Grey squares – Metabolites; black squares – Enzymes; Elipses – transporters; Dark blue shapes – Metabolic pathways;

Glucose metabolism

Glucose is the primary oxidative fuel for the adult brain, mainly being used to produce ATP and meet the energetic demands associated to brain function⁶⁶. Indeed, the energy that is consumed in neuronal signalling processes (resting and action potentials, glutamate cycling, post-synaptic receptors, among others) accounts for ~70% of energy consumption. Glucose can also be used for the generation of intermediates for lipid synthesis, amino acids for the synthesis of proteins, neurotransmitters and neuromodulators, pentoses for *de novo* nucleotide synthesis and also to protect cells against oxidative stress^{63,66}. The transport of glucose through the blood brain barrier (BBB) into and from brain cell occurs via different glucose transporters, such as GLUT1 that localizes to endothelial cells and astrocytes, and GLUT3 and GLUT4 which localize to neurons⁶⁷⁻⁶⁹.

Depending on the cell type, glucose will have different fates. While neurons are characterized as oxidative cells, astrocytes are mainly glycolytic^{63,66}. In neurons, glucose is oxidized mainly through oxidative phosphorylation (OXPHOS). Upon uptake, glucose is phosphorylated by HK to generate glucose-6-phosphate (G6P) preventing its efflux back to the extracellular space. Through a series of reactions, glucose is ultimately converted into pyruvate. This last metabolite can be further imported to the mitochondria where it will be converted into acetyl coenzyme A (acetyl-CoA) and further oxidized in the TCA cycle. The electrons released during the different enzymatic reactions are used in order to reduce NAD⁺ and FAD, respectively into NADH and FADH₂, and then shuttled to the electron transport chain, generating an electrochemical gradient that fuels the synthesis of ATP. Neurons also metabolize glucose via the pentose phosphate pathway (PPP)⁶³. This pathway is the first branching point of glycolysis in which G6P can be used to generate ribose-5-phosphate, a component of nucleotides, and NADPH, used in the control of oxidative stress and biosynthetic reactions⁶³.

As mentioned above, astrocytes are mainly glycolytic⁶⁶, and a glucose/lactate-dependent metabolic symbiosis may work between astrocytes and neurons. Glucose is predominantly

converted into lactate, but a fraction of G6P is used in the PPP and converted into glycogen⁷⁰. The difference between astrocytes and neurons, arises due to the expression of certain enzymes and transporters that regulate glucose metabolism. The different expression pattern of these proteins promotes a glycolytic phenotype in astrocytes. While astrocytes express high levels of 6-phosphofructo-2-kinase/fructose-2,6-bisphosphatase 3 (PFKFB3), this enzyme is subjected to continuous ubiquitin-dependent proteasomal degradation in neurons⁷¹ PFKFB3 regulates the levels of fructose 2,6-bisphophate (F2,6P) and promotes glycolysis through allosteric activation of PFK by F2,6P⁷². Moreover, the conversion of pyruvate to acetyl-CoA is limited due to the increased expression of pyruvate dehydrogenase kinase 4 (PDK4)⁷³ which reduces the activity of pyruvate dehydrogenase (PDH)⁷⁴. The production of lactate, from pyruvate, in astrocytes is also promoted by the expression of lactate dehydrogenase (LDH) 5^{75,76}. This final reaction is accompanied by the oxidation of NADH to NAD+ that further will sustain continuous glycolysis⁶⁶.

Initially thought as a waste product, lactate is currently known to have important functions in the brain. At the metabolic level, the current evidence suggests that lactate can be shuttled from astrocytes to neurons in a phenomenon known as astrocyte-neuron lactate shuttle (ANLS) model^{63,76}. This model states that the glutamate released, during neuronal activity, promotes the uptake of glucose and lactate production in astrocytes. Lactate is then released by astrocytes to be used by neurons^{75,77}. The ANLS model is not fully accepted, but is strongly supported by several evidences. These include differential expression of LDHs and MCTs between neurons and astrocytes^{75,78}, necessity of lactate released by astrocytes and imported by neurons to sustain neuronal activity, among other evidence^{76,79–81}.

Glutamine metabolism

Glutamine is a non-essential, highly abundant, amino acid that plays important roles in the organism. In most proliferating cells, glutamine can be a very versatile nutrient as it can be both an important source of carbon and/or nitrogen to several pathways^{17,82}. Glutamine-derived carbon can be used in order to replenish the TCA cycle, through the production of glutamate-derived α-ketoglutarate, to sustain lipid synthesis through reductive carboxylation, and the synthesis of other macromolecules. Moreover, glutamine is also directly and indirectly involved in the synthesis of two of the three amino acids that compose glutathione (GSH), glutamate and glycine, the most important reactive oxygen species (ROS) scavenger^{16,83}. In addition, glutamate can be transported through the xCT antiporter in exchange with cystine⁸⁴, which is quickly reduced to cysteine inside the cell⁸⁵, the third component of GSH. Glutamine-derived nitrogen is instead used in nicotinamide adenine dinucleotide phosphate (NADPH), protein and *de novo* nucleotide synthesis, and to support the levels of several amino acid pools. Furthermore, it can also be used as a pH regulator through the balance of the NH₃/NH₄+ pair^{86,87}.

In the brain, glutamine concentration can reach a concentration of 500 µM88 and is a crucial player in neurotransmission as it serves as the precursor for the synthesis of glutamate, an excitatory neurotransmitter, and the precursor of GABA, the main inhibitory neurotransmitter^{89,90}. Specifically, glutamine is involved in the glutaminergic cycle, where it is constantly recycled between glutamine and glutamate, across neurons and astrocytes⁹¹. Glutaminergic neurons (glutamate-releasing neurons) release glutamate into the synaptic cleft, through exocytosis, which is cleared afterward by astrocytes, mainly via excitatory amino acid transporter 1 (EAAT1) and EAAT2, also known as glutamate aspartate transporter (GLAST) and glial glutamate transporter 1 (GLT1), respectively. In the astrocytes, glutamate is amidated to form glutamine by glutamine synthetase (GS). Glutamine will then be exported through the system A amino acid transporter 3 (SNAT3), and alanine/serine/cysteine transporter 2 (ASCT2) and taken up by presynaptic neurons by SNAT1 and SNAT2. In these neurons, glutamine will then be hydrolyzed into glutamate by glutaminase (GLS), where it can be released again into the synaptic cleft^{49,90}. Astrocytes are of significant relevance in this cycle as they are responsible for glutamate homeostasis. This occurs through glutamate clearance from the synaptic cleft and also through the conversion of glutamate into glutamine^{89,92}. This reaction is particularly important because neurons do not express GS⁹³ and pyruvate carboxylase (PC)⁹⁴, resulting in the inability to synthesize glutamine from glutamate, and to de novo synthesize glutamate or GABA from glucose, respectively. Indeed, astrocytes are responsible for 90% of total glutamate uptake from the synaptic cleft⁹⁵, and more than 70% of the synaptic glutamate derives from the glutaminergic cycle 96,97.

Ketone bodies metabolism

Under physiological conditions, such as starvation, hepatic fatty acid β-oxidation occurs, generating acetyl-CoA to fuel the TCA cycle⁹⁸. However, the rate by which acetyl-CoA is generated, is higher than its metabolization through the TCA cycle. The surplus of acetyl-CoA is then used for the synthesis of ketone bodies (KBs), primarily acetoacetate, which can be converted into β-hydroxybutyrate (bHB) and acetone⁹⁸. These organic compounds are transported to extrahepatic tissue for energy production, *de novo* lipid synthesis and fulfil other physiological functions^{64,99,100}. In the case of the brain, KBs constitute an important alternative source of energy as they account for 60% to 70% of the energy supply during starvation^{64,101}. The synthesis of KBs, ketogenesis, occur primarily in the mitochondria of hepatocytes, but astrocytes and other cells are also capable of performing ketogenesis, though to a lesser extent⁹⁸.

The first step of ketogenesis is the condensation of two molecules of acetyl-CoA. This is a reversible reaction catalyzed by the acetyl-CoA acetyltransferase 1 (ACAT1) and originates acetoacetyl-CoA. Next, hydroxymethylglutaryl-CoA synthase (HMGCS2) couples the third acetyl-CoA to acetoacetyl-CoA, converting it into 3-hydroxy-3-methylglutaryl-CoA (HMG-CoA), in an irreversible manner. This molecule is then converted into acetoacetate, a KB, by

hydroxymethylglutaryl-CoA lyase (HMGCL) realising acetyl-CoA. Finally, acetoacetate is converted in its majority into bHB by β-hydroxybutirate dehydrogenase (BDH), a reversible reaction accompanied by the oxidation of NADH, and, in a smaller proportion, into acetone by spontaneously decarboxylation 98,102. While acetone can be exhaled through the lungs, acetoacetate and bHB can be delivered to extrahepatic tissues through the blood 103. The uptake of KBs by other tissues can occur via MCT1, which is expressed in glial cells 104–106. In the case of bHB, once inside the target tissue, BDH converts it back to acetoacetate. Then, 3-oxoacid CoA-transferase (OXCT1, also known as SCOT) utilizes the CoA from succinyl-CoA to synthesize acetoacetyl-CoA from acetoacetate, bypassing the irreversible reaction catalyzed by HMGCS2. Acetoacetyl-CoA is finally converted back into two acetyl-CoA which can, for instance, fuel the TCA cycle for ATP production 102. Biochemically, KBs can also be used in fatty acids (FA) synthesis for biomass production, however this has not been explored for decades 107,108. In this pathway, HMGCS2 is the rate-limiting enzyme in ketogenesis, as it is tightly regulated, and OXCT1 is the key ketolytic enzyme since it allows the usage of KBs as an energy, and putatively biomass, substrate 98.

Besides their ability to serve as a major alternative energy supply to the brain, KBs can act as signal molecules and have neuroprotective effects ^{102,103}. KBs have been shown to exert its signalling functions through several mechanisms. By activating at least two G-protein-coupled receptors (GPCRs), KBs can reduce lipolysis, sympathetic tone and metabolic rate ^{109,110}. Moreover, KBs can influence the protein acetylation status through direct inhibition of histone deacetylases (HDACs)¹¹¹ and by indirectly promoting protein hyperacetylation, through the increase in intracellular acetyl-CoA, increasing its availability for both enzymatic and non-enzymatic protein acetylation¹⁰².

Regarding its neuroprotective effects, KBs have been shown to play roles in the modulation of oxidative stress and inflammatory response. However, while showing both attenuations of oxidative stress and anti-inflammatory effects, it has also been reported increased oxidative stress and inflammatory response in exposition to KBs¹⁰³. Nevertheless, the therapeutical effect of KBs have been long recognized and ketogenic diets (KDs; a high-fat, low-carbohydrate diet that promotes ketogenesis) are used in several neurological diseases¹⁰³. For example, in epilepsy, KDs is used to reduce oxidative damage and seizure frequency, and in traumatic brain injuries, KBs have been shown to reduce brain damage and improve neuronal function^{112,113}.

The metabolism of KBs is tightly regulated through several mechanisms⁹⁹. HMGCS2, the rate-limiting enzyme in ketogenesis, is regulated transcriptionally and through post-translational modifications^{102,114}. At the transcriptional level, KBs metabolism can be regulated by at least two nutrient-sensing mechanisms. One pathway involves the forkhead box transcription factor

FOXA2. When active, FOXA2 binds to the promoter of HGCS2 and promotes transcription¹¹⁵. FOXA2 activity is regulated by insulin and glucagon levels. Whereas insulin inactivates FOXA2 through phosphorylation, leading to cytoplasmic sequestrion, glucagon activates FOXA2 through p300-mediated acetylation^{116,117}. Accordingly, while the first inhibits lipolysis and stimulates glucose influx and oxidation, glucagon promotes lipolysis, the release and transport into the liver, and oxidation of FA, followed by ketogenesis^{98,118,119}. Additionally, deacetylation of FOXA2 can be controlled by NAD+-dependent deacetylase sirtuin 1 (SIRT1), rendering it inactive¹¹⁷. The second regulatory mechanism of HMGCS2 transcription concerns the interaction between mTORC1 and peroxisome proliferator-activated receptor α (PPAR α)^{120,121}. PPAR α is a major transcription factor that promotes the expression of genes involved in FA uptake and oxidation and in the synthesis and import of KBs⁹⁸. Moreover, mTORC1 is an important regulator of PPARa function. mTORC1 inhibits PPARα transcriptional activity under physiological conditions, resulting in the inhibition of \(\beta \)-oxidation and ketogenesis \(\frac{120}{20} \). However, under conditions of, for instance, low glucose levels, mTORC1 is repressed, allowing PPARα-induced expression of ketogenic genes, including HMGCS2. At the level of post-translational modifications, HMGCS2 can be regulated by acetylation¹²² and succinvlation¹²³. In the inverse pathway, ketolysis, OXCT1 is the key enzyme as it enables the use of KBs. However, unlike HMGCS2, little is known regarding OXCT1 regulation. The expression of OXCT1 is potentially regulated by PPARαdependent mechanisms and its activity is regulated by acetylation and nitration post-translational modifications^{99,124}.

Malignant gliomas metabolic rewiring

Metabolic plasticity is an important characteristic of many tumors, including malignant gliomas ¹²⁵. Across the intricate metabolic network, cancer cells commonly reprogram pathways involved in bioenergetics, biosynthesis and redox homeostasis ¹⁶. Furthermore, the metabolic phenotype of tumors is dependent on several factors, including tissue of origin, TME, among others ¹⁵. As such, the metabolism of glucose, glutamine and KBs show special interest in malignant gliomas. The main rewired metabolic pathways in malignant gliomas are resumed in **Fig 2**.

Glucose metabolism

Similarly to many tumors, gliomas transform the majority of its glucose supply into lactate^{83,126,127}. This phenomenon is known as the Warburg effect, or aerobic glycolysis, and is the classical metabolic remodeled pathway in tumors¹²⁸. The Warburg effect describes a switch in the metabolism of glucose from OXPHOS, even in aerobic conditions, resulting in the metabolization of the majority of glucose into lactate, the latter being secreted into the extracellular space¹²⁹. Despite being an inefficient process to produce ATP, the main advantage of the Warburg effect

is to produce glycolytic intermediates at a faster rate, in order to supply supplementary pathways, helping proliferanting cells to meet their metabolic demands¹⁷. Indeed, the several branching points of the glycolytic pathways connects glycolytic intermediates into biosynthetic and energetic pathways, while also being involved in cellular redox balance^{16,42}.

As mentioned previously, the first branching point occurs at the second step of glycolysis where it connects with the PPP¹³⁰. G6P is converted by glucose-6-phosphate dehydrogenase (G6PD), the rate-limiting step of PPP, enabling the use of glucose as a precursor for amino acid and nucleotides. Moreover, the NADPH generated throughout this pathway can be used to maintain cellular redox balance and to sustain FA synthesis^{17,131–133}. These products will ultimately improve cell survival and proliferation, and high rates of PPP have been associated to therapy resistance¹³³. Moreover, PPP has been reported to be upregulated in proliferating glioma cells and down regulated in migratory cells^{134,135}.

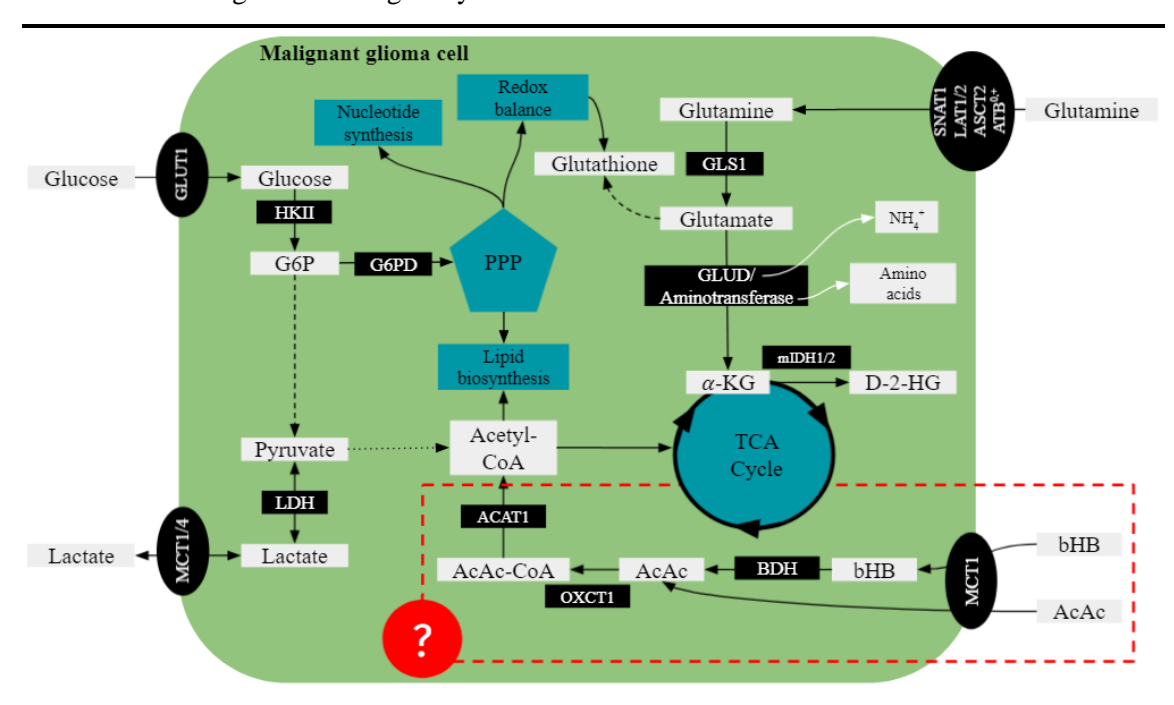


Fig 2. Main remodelled metabolic pathways in malignant gliomas. In malignant gliomas, glucose is mainly used to produce lactate. This phenomenon is known as the Warburg effect and it is common between many solid tumors. Glucose enters the cell through glucose transporter 1 (GLUT1), known to be upregulated in malignant gliomas, and is immediately phosphorylated by hexokinase II (HKII), commonly upregulated in cancers, into glucose-6-phosphate (G6P). Higher glycolytic rates results in increased amounts of intermediate metabolites that can be deviated into subsidiary metabolic pathways to sustain biosynthetic needs and maintain redox homeostasis. The pentose phosphate pathway (PPP) is one examples, being particular important since it sustains lipid and nucleotide biosynthesis, while also sustaining the production of glutathione, the main reactive oxygen species scavenger. The deviation from the glycolytic pathway to the PPP is caused by glucose-6-phosphate dehydrogenase (G6PD) activity. Once glucose is transformed into pyruvate, a small portion is redirected to the tricarboxylic acid (TCA) cycle, and the majority is converted by lactate dehydrogenase (LDH) to lactate. This metabolite is then exported by the monocarboxylate transporters 4 (MCT4), but can be imported back into the cell, through MCT1, to sustain the TCA cycle. Malignant gliomas are known to upregulate glutamine metabolism in order to sustain energetic and biosynthetic needs, but also to regulated oxidative stress. **(Continues on the next page)**

Fig 2. (Continuation) Glutamine is transported into the cell by transporters that are often upregulated in tumors, sodium-coupled neutral amino acid 1 (SNAT1), L-type amino acid transporter 1 and 2 (LAT1/2) and Amino Acid Transporter ATB0+ (ATB^{0,+}). Afterwards, glutamine is converted into glutamate, by glutaminase, which can then be used for the synthesis of glutathione or α -ketoglutarate (α -KG). This last metabolite can be synthesized by two different enzymes, glutamate dehydrogenase (GLUD) and aminotransferases having as by-products NH₄⁺ and amino acids, respectively. α-KG enters the TCA cycle to sustain most of the cell's energetic needs. In the case of *IDH*-mutant GBM the mutated enzyme isocitrate dehydrogenase 1 or 2 (mIDH1/2) acquires a new activity. Instead of catalyzing the reaction of α-KG to isocitrate, mIDH1/2 will convert α-KG into D-2-hydroxyglutarate (D-2-HG). This neo-enzymatic acitivity is believed to be pro-tumorigenic. The metabolism of ketone bodies (KBs; β-hydroxybutyric acid – bHB; Acetoacetate – AcAc) is still unclear in malignant gliomas. Some studies show that these tumors are able to metabolize KBs, but other studies demonstrate the opposite. KBs are imported into the cell through MCT1. Inside the cell, \(\mathcal{B}-\) hydorxybutyrate dehydrogenase (BDH) converts bHB into AcAc, which in turn is converted to Acetoacetyl-CoA (AcAc-CoA) by 3-oxoacid CoA-transferase 1 (OXCT1). AcAc-Coa is broken down to acetyl-CoA by acetoacetyl-CoA thiolase (ACAT1), being able to fuel the TCA cycle or to sustain lipid biosynthesis. Acetone, another KB, is not represented due to its minimal metabolic contribution⁶⁵. Solid arrows - Main metabolic pathway; Dotted arrows -Secondary/down-regulated metabolic pathways; Dashed arrows - Hidden intermediary steps; White arrows - Reaction by-products; Grey squares - Metabolites; black squares - Enzymes; Elipses - transporters; Dark blue shapes -Metabolic pathways;

Glioma cells can oxidize glucose through OXPHOS and glycolysis during exponential tumour growth¹³⁶. However, as mentioned above, IDH1/2 mutations are common in gliomas^{50,51,53}. Wildtype IDH1 and IDH2 are enzymes that catalyse the oxidative carboxylation of isocitrate to α-ketoglutarate (α-KG), NADP⁺ as a cofactor, and are involved in major metabolic processes, such as the TCA cycle, glutamine metabolism, lipid biosynthesis and redox homeostasis 137-139. While IDH1 is found in the cytoplasm and peroxisomes, IDH2 is located in the mitochondrial matrix⁹⁰. Mutations in specific sites, R132 in IDH1 and R172 in IDH2, can lead to a neoenzymatic activity. Instead of catalysing the previous reaction, mutated IDH1/2 further convert α-ketoglutarate into D-2-hydroxyglutarate (D-2-HG), which is accompanied by NADPH consumption 140,141. Gain-of-function IDH mutations has been described as pro-tumorigenic and an early event in gliomagenesis 142-144. The mechanism by which D-2-HG may promote tumor formation is not fully understood, but it has been shown to induce changes in cellular metabolism, cancer biology and, as mentioned, to promote carcinogenesis 145,146. Indeed, the new acquired function of IDH1/2 leads to a depletion of α-KG and of NADPH, which can have widespread effects across the cell at the levels of metabolic pathways, redox homeostasis, and also in gene expression¹⁴⁷. In the context of cellular metabolism, the new acquired function of IDH1/2 leads to a depletion of α -KG, preventing its metabolization through the TCA cycle¹⁴⁸, and consumption of NADPH, which will not be available for the synthesis of FA^{149,150}. Facing these substantial changes, and the fact that glucose is mainly metabolized through glycolysis, cells are required to compensate for the loss of α -KG, and NADPH through the use of different carbon sources ^{151,152}. Glutamine, which will be reviewed in greater detail later, is a solution for these problems in several tumors, including gliomas^{49,82,153}. Indeed, this amino acid can be a source of carbon to replenish the TCA cycle, and also to sustain lipid synthesis⁸². Mutated IDH1/2 can also impact the function of several dioxygenases that require α-KG as a cosubstrate. Inhibition of these enzymes could have pleotropic effects as they are involved in the gene expression through regulation of epigenetic marks. Moreover, the increase in D-2-HG, and consequent depletion of α -KG, might also lead to a constitutive activation of HIF, an important regulator of glycolysis, through inhibition of prolyl hydroxylases¹⁵⁴. These enzymes are important regulators of HIF- α stability and are dependent on α -KG to exert its function¹⁴⁷.

The glucose metabolism is regulated by allosteric and transcriptional regulatory mechanisms¹⁵⁵. At the level of allosteric regulation, the different glycolytic enzymes can be positively and negatively regulated by their own products or by downstream glycolytic metabolites. For instance, HKII, the most expressed isoform in cancer, is negatively regulated by G6P, its own product. However, due to the high glycolytic rate of tumor cells, HKII is not likely to be inhibited by its reaction product¹⁵⁶. At the transcriptional level, glucose metabolism is regulated by several pathways that are often deregulated in cancer. The PI3K/Akt/mTORC pathway plays an important role in the regulation of glucose metabolism^{157,158}. In normal cells this pathway is regulated through activation of RTKs and by its negative regulator PTEN^{157,159}. In gliomas, this pathway is often constitutively active through mutations in EGFR, PI3K or PTEN^{61,160}. Activation of the PI3K/Akt/mTORC pathway leads to the upregulation of glycolysis through the expression of glucose transporters (GLUT), in particular GLUT-1^{22,161,162}, and also, in cooperation with c-MYC, through the activation of the HIF pathway which also increases de expression of GLUT-1 and the synthesis of several glycolytic enzymes, such as HKII^{163,164}. Moreover, the HIF pathway is frequently active in cancer due to the hypoxic conditions of the TME¹⁶⁵. The tumor suppressor p53 (*TP53*) regulates glycolysis by repressing the transcription of GLUT-1 and GLUT-4, reducing glucose uptake. Through other regulatory mechanisms, p53 can also upregulate the TCA cycle. Thus, gliomas presenting mutations in the TP53 can upregulate glycolysis leading to a more aggressive phenotype¹⁵⁸.

Glutamine metabolism

Glutamine is a very versatile nutrient that can be used as a carbon and nitrogen donor to support bioenergetis, biosynthesis and cellular homeostasis^{42,82}. Glutamine can be transported into the cell through several transporters such as ATB^{0,+} (*SLC6A14*), ASCT2 (*SLC1A5*), LAT1 (*SLC7A5*), LAT2 (*SLC7A8*) and SNAT1 (*SLC38A1*), which are frequently upregulated in tumors¹⁶⁶. In the cytoplasm, glutamine is converted into glutamate by GLS 1 or 2¹⁶⁷. Whereas GLS1 is considered pro-tumoral, GLS2 is considered tumor suppressive. In the context of malignant gliomas, GLS2 is often found to be downregulated while GLS1 is upregulated^{49,168,169}. Thus, due to its importance in glutaminolysis, GLS1 plays a key role in the survivability and growth of tumors¹⁷⁰.

Glutamine can serve as an anaplerotic compound through the synthesis of α -KG¹⁵³. This reaction can be catalyzed either by glutamate dehydrogenase (GLUD), which is an ammonia-

releasing process, or through several aminotransferases, having several different amino acids as by-products. These amino acids can then be used for the synthesis of nucleotides or proteins and ROS control. α-KG can be used to maintain the TCA cycle, using it as an energy-generating substrate, or be used for lipid synthesis through reductive carboxylation. Because the redox control is crucial in cancer, glutamate can be directly used in the synthesis of GSH, the most relevant ROS scanveger^{171,172}. In addition, and as mentioned previously, glutamine can also be used to synthesize glycine, and glutamate can be be exchanged through the xCT antiporter by cystine⁸², the remaining constituents of GSH. For these reasons, similar to glucose, glutamine is considered to be crucial in cancer metabolism and, in some cases, it can completely replace glucose⁸³.

The current knowledge about glutamine metabolism points to a very heterogeneous role of this amino acids in cancer, which is affected by extrinsic and intrinsic factors ranging from culture conditions to oncogene status⁸⁶. Depending on the glutamine needs, gliomas can be divided as glutamine dependent and independent tumors^{49,90}. The dependence on this amino acid is, at least in part, reflected by the expression of glutamine synthetase (GS), which synthesizes glutamine *de novo* from glutamate¹⁷³, and increased expression of ASCT2 and SNAT3^{174,175}. While high expression of GS enables the synthesis of glutamine from glucose-derived glutamate, low expression of GS causes gliomas to be dependent on an external source of glutamine due to their inability to synthesize it^{86,90}.

The regulation of glutamine metabolism involves signaling pathways, oncogenes and tumor supressors that are shared with the regulation of glucose metabolism. c-MYC is a key regulator of glutamine metabolism, being associated to its upregulation⁸². This oncogene is known to regulate the expression of GLS and of high-affinity glutamine importers, such as ASCT2, leading to an increased glutamine uptake and metabolization ^{176,177}. MAPK signaling pathway is also considered a major regulator of glutamine transport and metabolism⁴². This is highlighted by the fact that KRAS-driven tumor cells exhibit glutamine dependency^{178–180} and also because this type of tumors present high levels of glutamine-derived metabolites 180-183. The PI3K/Akt/mTOR signaling pathway have also been shown to regulate glutaminolysis through mutations of its negative regulator PTEN, which increased the expression of GLS¹⁸⁴, and is often activated in gliomas⁶¹. Glutamine uptake can also activate several signaling pathways through the mTOR complex, which activates anabolic pathways under nutrient rich conditions 16. Moreover, the tumor supressors p53 and retinoblastoma (Rb) protein are also involved in the regulation of glutamine metabolism. The action of p53 is required for the expression of GLS2¹⁸⁵ and Rb regulates the expression of ASCT2, and GLS1, and through the regulation of the catalytic subunit of γ -glutamylcysteine ligase (GCLC), can modulate glutathione synthesis¹⁸⁶.

Ketone bodies metabolism

Research on the role of ketone bodies in cancer, including gliomas, has brought contrasting results. In gliomas, a number of studies indicate that these tumors are not able to oxidize KBs, being justified by the downregulation of enzymes required in KBs metabolism^{187–189}. However, at the same time, several papers indicate the opposite. Gliomas express the required enzymes and are able to metabolize KBs^{190–193}. Thus, further studies are needed to address this problem.

KBs can have anti- and pro-tumoral properties through different mechanisms, which can be attributed to the properties of KBs as signaling molecules¹⁰² or attributed to the effects of KDs¹⁹⁴. These include reduction of glucose and insulin levels¹⁹⁴, decreasing the availability of glucose to cancer cells, modulation of oxidative stress^{195,196}, improving the response to chemo and ratiotherapy, enhancing the anti-tumor immunity¹⁹⁷, by increasing the innate and adaptive immune responses, among others¹⁹⁴. However, KBs can promote tumor progression as some tumors can utilize them as fuel or it could be favoured through the strengthening of signaling cascades in BRAFV600E mutated tumors^{198,199}.

Clinical management of malignant glomas

The standard of care for malignant glioma involves maximal safe resection of the tumor, followed by adjuvant radiation and chemotherapy with TMZ⁵⁰. However, the overall survival (OS) of these patients remains low (average OS 15 months)⁶¹. Even though radiation plus TMZ brought a significant improvement in OS²⁰⁰, the poor prognosis is justified by several limitations in the standard therapy. These includes potential neurological damage due to the removal of brain parenchyma²⁰¹, radiation inefficiency due to hypoxic TME²⁰² and low TMZ response in tumors presenting a non-methylated *MGMT* promoter, which is responsible for the reparation of TMZ-induced DNA damage^{203,204}. Besides radiation plus TMZ, the only FDA-approved therapies are tumor treating fields plus TMZ and bevacizumab, an antiagiogenic compound, plus TMZ. While tumor treating fields show survival benefit and progression free survival (PFS)^{205,206}, bevacizumab only presented PFS improvement^{207,208} but with high response rate²⁰⁹. Even though the approval of these therapeutical modalities for the treatment of malignant gliomas was an advance in the therapy of this type of tumors, new and more efficient therapies are required in order to improve the progonostic of these patients. In this context, several therapies targeting metabolic liabilities have been studied has an option for the treatment of malignant gliomas.

Metabolism-based therapeutic approaches

Aerobic glycolysis is a feature of many malignant gliomas^{83,126,127}. Therefore, research has been done in order to exploit enzymes, transporters and the main signaling pathways involved in aerobic glycolysis as metabolic liabilities in these tumors. HKII plays a crucial role in

glycolysis and is the most expressed HK in cancer^{164,210}. Thus, it is an attractive target and its inhibition in gliomas resulted in the suppression of glycolysis and tumor formation, and induced differentiation of glioma stem cells²¹¹. As mentioned above, GLUT-1 is regulated by several pathways that are constitutively active in gliomas^{22,161,162} and high expression of this transporter was detected in glioma patients²¹². GLUT-1 inhibition blocked glutamine metabolism resulting in the decrease proliferation and invasion of glioma cells²¹³. At the level of signaling pathways, the PI3K/Akt/mTORC pathway is often constitutively active through mutations in upstream or downstream effectors^{157,159}. Thus, it has been pointed out as an appealing target. In addition, other glycolytic enzymes and transcription factors have been pointed out as putative therapeutic targets²¹⁴.

Due to the relevance of glutamine to gliomas, several efforts, with different approaches, have been made in order to identify new therapeutical targets⁴⁹. Targeting the enzymes GS, GLS and GLUD have been a focus of interest due to their central role in glutamine metabolism and in cancer^{49,82}. Inhibiting these enzymes, individually, resulted in, depending on the study, decreased proliferation and increased sensitivity to oxidative stress^{49,173,215–217}. Moreover, GLS2, described as a tumor suppressor, reduced cell proliferation, migration and increased oxidative stress and TMZ sensitivity^{218–220}. The glutamine transporter ASCT2 is often found to be upregulated in gliomas¹⁷⁴. As such, targeting this transporter with a therapeutical point of view has been explored by several studies and resulted in tumor growth inhibition²²¹. Beside these targets, other approaches including the inhibition of glutamate transport and uptake, depletion of glutamine and the use of glutamine analogs have also been studied⁴⁹. However, malignant gliomas are very heterogenous and a therapeutical approach, for instance GS inhibition, can have anti-cancer effects in a group of gliomas but have no effect in other groups^{222,223}. Thus, highlighting the need for a better understanding of these tumors biology.

As mentioned above, the role of KBs in cancer is unclear. However, a few trials have been performed in order to assess the effect of KDs over gliomas²²⁴. These studies are based on the premise that ketone bodies are an ineffective fuel for gliomas. Thus, by reducing glucose leves, while increasing the concentration of KBs, tumors would be deprived from an efficient energetic fuel, alting its progression¹⁹⁴. KDs are high fat, low carbohydrate diets that have the objective to reduce systemic glucose levels, inducing a starvation-like metabolic state which promotes ketogenesis¹⁹⁴. Several preclinical studies have reported therapeutic effects of KDs in the treatment of gliomas. In these studies, it was reported an increase in median OS^{196,197,225}, and in PFS and a decrease in tumor growth²²⁶. Importantly, it was also demonstrated a synergistic effect of KDs with radiation²²⁷ and with TMZ²²⁸. In humans, there is a need for more and robust studies. While it has been reported improved OS and PFS^{229–231}, the number of participants in these studies is too small to consider efficient for clinical use.

Hypothesis and objective

Malignant gliomas are characterized by a poor clinical outcome. The current therapy brought a significant prognostic improvement, but is still rather inefficient. Therefore, there is an urgent need for the development of new and more efficient therapies. As mentioned before, cancer metabolism plays a central role in the establishment of the disease and in its progression, presenting itself as an attractive therapeutic target. It results from the interplay of intrinsic factors, such as disturbed endogenous metabolism and signaling pathways, and extrinsic factors, such as the tissue of origin and the bioavailability of organic and signaling molecules in the TME ¹⁵. Furthermore, the ability of cancer cells to remodel their metabolism confers them adaptative advantage to different microenvironmental conditions and selective pressures.

The same pathway can have different inputs in order to sustain cellular needs. For instance, the TCA cycle can be sustained by glucose, glutamine, FA and other fuels^{16,82,232}. The synthesis of different macromolecules, e.g. proteins and FA, can be carried out in the presence of glucose, essential and nonessential aminoacids, scavanged proteins and lipids from the extracellular space, among other important molecules^{16,82,233–235}. Taking this into consideration, we hypothesize that malignant gliomas are able to rewire their metabolism according to nutrient availability. Our objective is to explore if malignant gliomas rewire their metabolism when presented with different substrates, glucose, glutamine, glutamate and acetoacetate, and the impact of metabolic rewiring on cellular characteristics.

The main objective will be achieved using in vitro models and according to the specific aims:

- 1. Assess the metabolic profile of glioblastoma cell lines exposed to glucose, glutamine/glutamate and acetoacetate;
- 2. Assess the expression of key genes involved in the metabolism of glucose, glutamine/glutamate and acetoacetate;
- 3. Assess the metabolic conditions impact on cellular characteristics.

Materials and Methods

Cell culture

Two commercial glioblastoma cell lines, U-251 (09063001, European Collection of Authenticated Cell Cultures (ECACC)) and U-87 (HTB-14, American Type Culture Collection (ATCC)), were used during this study. Both cell lines were maintained in a humidified environment of 5% CO₂ at 37 °C and cultured in Dulbecco's modified Eagle medium F-12 (DMEM/F-12; 11330-032, Gibvo, Life Technologies), supplemented with 10% fetal bovine serum (FBS; p40-37500, PAN Biotech), 1% Antibiotic-Antimycotic (AA; P06-07300, PAN Biotech) and 50 μg/mL gentamicin (15750-060, Gibco, Life Technologies). Cells were cultured until an optical confluence of 75-100%. Then, 0.05% trypsin-EDTA (25300-054, Invitrogen, Thermo Fisher Scientific) was applied, at 37 °C for approximately 5 min, in order to detach the cells, which were divided and maintained in culture flasks or cultured in new plates for experimental procedures. Furthermore, before seeding, cell number was assessed through the use of a Bürker counting chamber.

Before *in vitro* assays, adherent cells were washed with phosphate-buffered saline (PBS) 1X and synchronized under starvation (culture medium without FBS) overnight. After starvation, culture medium was substituted and cells were maintained in DMEM/F-12 without glucose, without L-glutamine and without hepes (L0091-500), with 1% FBS, during the duration of the assay. Experimental conditions comprised 5 mM glucose (G8270, Sigma), 6 mM glutamate (63382-010, Sigma Aldrich), 6 mM glutamine (25030-024, Gibco) and 7.5 mM lithium acetoacetate (LiAcAc; A8509, Sigma Aldrich), separately or in combinations. Lithium chloride (7.5 mM; L9650, Sigma Aldrich) was used as a control for the effects of lithum. Baseline conditions without adition of any supplement to the DMEM/F-12 + FBS media, are, henceforth, mentioned as control conditions. All cell lines were previously tested for mycoplasma contaminants with Universal Mycoplasma Detection Kit (30-1012K, ATCC).

Cell death assay

In order to assess the effect of nutrient availability on cellular viability, we analysed cell death through flow cytometry. Here, we applied the FITC annexin V/propidium iodide (PI) staining to distinguish between live cells and apoptotic/necrotic cells. Annexin V is an intracellular protein that binds, in a calcium-dependent manner, to phosphatidylserine (PS), a membrane component^{236–238}. While PS are normally found in the inner leaflet of the plasma membrane, these molecules become exposed on the outer leaflet in apoptotic cells²³⁹. As such, fluorochrome-labelled annexin V (FITC annexin V) is used as a marker for early apoptotic cells^{240,241}. Furthermore, using PI, a membrane-impermeable dye that binds to nucleic acids^{241,242},

it is possible to differentiate early apoptotic cells from cells with a permeabilized membrane, for instance, late apoptotic cells and necrotic cells²⁴³.

Cells were seeded at a concentration of 2 x 10⁵ cells/mL in 24-well plates (0.5 mL/well). Cells were starved overnight and then exposed to the experimental conditions during 24 h. Afterwards, the culture medium was collected, and adherent cells detached with 0.05% trypsin-EDTA. Cells were then collected into the tube of the corresponding supernatant and centrifuged at 255 ×g during 5 min. The supernatant was discarded, and the pellet washed with 300 μL PBS 1X with 0.1% (v/w) bovine serum albumin (BSA) and centrifuged at 255 ×g during 5 min. The supernatant was discarded, and cells were incubated with 0.5 μL annexin V-fluorescein isothiocynate (FITC; 640906, BioLegend), in annexin V binding buffer 1X (10mM Hepes (pH 7.4; 391333, Milipore), 140 mM sodium chloride (NaCL; 106404, Merck), 2.5 mM calcium chloride (CaCl₂; 449709, Sigma) for 15 min in the dark, at room temperature. Then, 200 μL PBS 1X with 0.1% (v/w) BSA was added and centrifuged at 255 ×g for 5min. The supernatant was discarded and cells were resuspended in annexin V binding buffer 1X and 2.5 μL μL propidium iodide (PI; 50 μg/mL; P4170, Sigma-Aldrich) was added prior acquisition. Samples were acquired by flow cytometry in a FACScalibur (Becton Dickinson) and data treated using FlowJo X 10.0.7 (http://flowjo.com) software.

Cell proliferation assay

The cell proliferation assay is an assay that can be performed through different methodologies. In our case, it was performed by counting cells in determined time points. Proliferative rate can be an indirect measurement of metabolic fitness and plasticity¹⁷. As such, we applied this method to assess which nutrients confer proliferative advantage to cells.

Cells were seeded at a concentration of 1 x 10⁵ cells/mL in 24-well plates (0.5 mL/well), starved overnight, and collected at 0 h, 4 h, 12 h, 24 h, 32 h and 48 h after exposure to experimental conditions. As in the cell death assay, the culture medium was collected, cells were detached with 0.05% trypsin-EDTA and collected into the respective tube. Cell concentration at each time point was calculated using a Bürker counting chamber and cell viability was assessed using 0.4% (w/v) trypan blue stain (15250-061, Gibco), at a ratio of 1:5. Three replicates were used for each experimental condition and cell line. Population doubling time (DT) was determined according to the American Type Culture Collection (ATCC) animal cell culture guide (http://www.uab.cat/doc/ATCCguide), using the following formula:

$$DT = Tln2/ln(\frac{Xe}{Xh})$$

T stands for the duration of the assay in any units, Xb is the cell number at the time point 0h (beginning of the assay) and Xe represents the cell number at the final time point (end of the assay).

Wound healing assay

The wound healing assay is a method applied to measure the 2D migratory capacity of cells *in vitro*²⁴⁴. Being simple and relatively inexpensive, it is a reliable assay to study the effect of our experimental conditions over cell migration.

Cells were seeded at 80-90% confluency (U251 - 3 x 10⁵ cells/mL; U-87 MG - 2 x 10⁵ cells/mL). Before exposure to experimental conditions, cells were incubated with mitomycin-C (M4287, Sigma) during 1 h (U251) and 2 h (U-87 MG), in the dark. Mitomycin-C is an alkylating agent that inhibits DNA synthesis, thus it inhibits cell proliferation. As such, by incubating cells with this compound we reduce the contribution of cell proliferation in wound closure²⁴⁴. To note that, in this assay, cells were not starved. After mitomycin-C treatment, a scratch/wound across the well diameter was made using a P200 pipette tip. Then, the culture medium was discarded, to remove cells and debris in suspension, and experimental conditions were applied. Wound closure was monitored by taking bright-field images, of each well, using an Olympus IX53 Inverted Microscope, during 48 h, at the following time points: 0 h, 4 h, 8 h, 10 h, 24 h, 32 h and 48 h. Wound closure was quantified using the ImageJ software.

RNA extraction and Reverse transcription and real-time quantitative PCR (RT-qPCR)

Reverse transcription and real-time quantitative PCR (RT-qPCR) is a method utilized to assess gene expression²⁴⁵. Aided by specialized thermocyclers, and dyes used as a nucleic acid stain that intercalate with double-stranded DNA (e.g., SYBR Green), it allows us to amplify genetic material and quantify it simultaneously^{246,247}. In this project, we utilized this technique in order to assess the effect of nutrient availability over the expression of metabolism-related genes.

Cells were seeded at a concentration of 2 x 10⁵ cells/mL in 6-well plates (2 mL/well) and, after starvation, experimental conditions were applied. Total RNA extraction was performed using RNeasy Mini Extraction kit (74104, Qiagen), according to the manufacturer's protocol. cDNA was synthesized from 1 μg RNA, using SuperScript II Reverse Transcriptase (18080e44, Invitrogen), as indicated in the manufacturer's protocol. To quantify the amount of DNA in our samples, we performed a real-time quantitative PCR (qPCR) using the SYBR Green PCR Master Mix (04707516001, Roche), according to the manufacturer's instructions. The experiment was carried out in a Lightcycler[®] 480 System instrument (05015243001, Roche. Primers for the following genes were used: *HKII* (For: 5'-GGAGAGGGGACTTTGATATCG-3'; Rev: 5'-CGCATCTCTTCCATGTAGCAG-3'), *G6PD* (For: 5'-GGCAACAGATACAAGA ACGTGAAG-3'; Rev: 5'-GCAGAAGACGTCCAGGATGAG-3'), *PDHA1* (For: 5'-GCTAACC

AGGGCCAGATATTC-3'; Rev: 5'-CTTGTAGTAATCAGTGCTGGC-3'), SLC2A1 (here also called GLUT1, For: 5'-CACGGCCTTCACTGTCGTG-3'; Rev: 5'-GGACATCCAGGGTAGCT GC-3'), SLC16A1 (here also called MCT1, For: 5'-GCTGGGCAGTGGTAATTGGA-3'; Rev: 5'-CAGTAATTGATTTGGGAAATGCAT-3'), SLC16A4 (here also called MCT4, For: 5'-CACAA GTTCTCCAGTGCCATTG-3'; Rev: 5'-CGCATCCAGGAGTTTGCCTC-3'), GLS1 (For: 5'-CT TCTACTTCCAGCTGTGCTC-3'; Rev: 5'-CACCAGTAATTGGGCAGAAACC-3'), GLNS (For: 5'-GAATGGTCTGAAGTACATCGAGG-3'; Rev: 5'-GTTAGACGTCGGGCATTGTC-3'), SLC1A2 (here also called GLT-1, For: 5'-GGGATGAACGTCTTAGGTCTG-3'; Rev: 5'-GGGGAGAGTACCACATGATC-3'), GLAST (For: 5'-CACCGCTGTCATTGTGGGTAC-3', Rev: 5'-CCGCCATTCCTGTGACAAG-3'), SLC7A5(here also called LAT1 (For: 5'-CATCCTC CAGGCTCTTCTTC-3'; Rev: 5'-CGTCATCACACACGTGAACAC-3'), SLC38A2 (here also called SNAT1, For: 5'-CATTCTATGACAACGTGCAGTCC-3'; Rev: 5'-CAGCAACAATGAC AGCCAGC-3'), SLC38A2 (here also called SNAT2, For: 5'-CTGAGCAATGCGATTGTGGG-3'; Rev: 5'-CTCCTTCATTGGCAGTCTTC-3'), SLC38A3 (here also called SNAT3, For: 5'-CAC AGACAGCATACACCATCC-3'; Rev: 5'GACAGGTTGGAGATGTGCTGC-3'), OXCT1 (For: 5'-GGCCGCTCTTGAGTTTGAGG-3'; 5'-CGTGGATATGGACCCAAACC-3'), ACAT1 (For: 5'-GTATTGGGTGCAGGCTTACC-3'; Rev: 5'-CATTGGACATGCTCTCCATCC-3'), ACADS (For: 5'-CCCTCGATTGTGCTGTGAAC-3'; Rev: 5'-GCCAACTTGAACTGGATGC C-3'), ACADM (For: 5'-GCTACTTGTAGAGCACCAAGC-3'; Rev: 5'-CCAAGCTGCTCTCT GGTAAC-3') and FASN (For: 5'-GCTCGGCATGGCTATCTTC-3'; Rev: 5'-GGAACACCGT GCACTTGAGG-3'). As housekeeping we TGACACTGGCAAAACAATGCA-3'; Rev: 5'-GGTCGTTTTTCACCAGCAAGCT-3')

Nuclear magnetic resonance (NMR) spectroscopy

NMR is one of the main analytical methods used in the field of metabolomics, which is due to important advantages in comparison to similar methods^{248,249}. For instance, samples can be prepared with ease and can also be reutilized for further analyses. In addition, NMR allows compound quantification and presents high reproducibility between experiments. This technique also presents several disadvantages that should not be overlooked, such as, relatively low sensitivity (µM), high maintenance costs and scarce bioinformatic tools for spectra analysis²⁴⁹. NMR is also a versatile tool that allows the analysis of the general metabolic network, and to follow the utilization of organic compounds when aided by isotopically enriched molecules²⁴⁸. In this study, NMR was used to study the impact over the metabolic network of malignant gliomas cells caused by nutrient availability.

Cells were seed in 175 cm² culture flasks at a concentration of 2.6 x 10⁷ cells/flask. After overnight starvation, cells were exposed to the experimental conditions during 24 h. Supernatants

were then collected and cells were scraped in PBS 1X, harvested, into a different tube, and centrifuged at $155 \times g$ during 10min. The supernatant of this suspension was discarded and pellets were weighted. To separate aqueous and organic phases, methanol and chloroform extraction, respectively, was performed on ice. Cold methanol was added to cell pellets (4 mL/1 g cell pellet), followed by water (twice the volume of methanol). Then, after a 5 min incubation, 1 volume of chloroform was added, followed by 1 volume of water. Samples incubated during 10 min and, afterwards, centrifuged at $1700 \times g$ for 15 min at 4 °C. Aqueous and organic phases were collected, into separate eppendorfs, using a glass pipette and stored at -20 °C until sample acquisition. Aqueous phase (methanol/water extracts containing water soluble compounds), organic phase (chloroform extracts containing insoluble water compounds) and cell culture media (supernatants) were analyzed through ¹H-NMR spectroscopy. Extracts were lyophilized in a SpeedVac Plus system. Aqueous samples were dissolved in 430 μL deuterated water (D₂O), 30 μL of 0.16 mM 3-(trimethylsilyl)propionic-2,2,3,3-d4 acid (TSP), as chemical shift reference, and in 140 µL of 0.35 mM potassium phosphate buffer in D₂O (KPi pH 7.4) with 2 mM sodium azide (NaN₃) and organic samples were dissolved in 600 µL deuterated chloroform (CD₃Cl). For supernatants, 30 μL of TSP and 30 μL of 0.35 mM KPi (pH 7.4) with 2 mM NaN₃ were added to 540 μL of supernatants. ¹H-NMR spectra of aqueous and supernatant samples were obtained at 25 °C in a 800 MHz magnetic field in a UltrashieldTM 800 Plus Spectrometer (Bruker) with a 5 mm TCI cryo-probe, using noesygppr1d pulse program, in which water pre-saturation occurred during mixing time and relaxation delay. Acquisition parameters were the following: 128 scans for the aqueos extracts and 40 scans for the supernatants, relaxation delay of 4 s, mixing time of 10 ms, spectral width of 20.0237 ppm and free induction decay (FID) size of 128k points. Organic samples spectra were acquired in a 500 MHz magnetic field in the 500 UltraShieldTM Spectrometer (Bruker) using a5 mm TCI-z (5mm); using zg pulse program. Acquisition parameters were: 40 scans, relaxation delay of 3 s, spectral width of 11.7616 ans FID of 48k points. For the purpose of spectral assignment, 2D NMR spectra were acquired for some samples: ¹H-¹³C HSQC (hsqcetgpsisp2 pulse sequence, 512 points in F1 and 2048 points in F2; 128 scans; relaxation delay of 1.5 s; sweep width of 33,207.441 Hz in F1 and 12820.513 Hz in F2) and ¹H J-resolved (jresgpprqf pulse sequence, 100 points in F1 and 8192 points in F2; 16 scans; relaxation delay of 2 s; sweep width of 78.113 Hz in F1 and 133,68.984 in F2). Spectra were acquired and processed using TopSpin 4.0.7 software (Bruker). All FIDs signals were multiplied by an exponential function, followed by Fourier Transformation. Spectra were manually phase and baseline corrected. Chemical shifts were adjusted according to the chemical shift of TSP at 0.00 ppm. Compound identification of aqueous and supernatant spectra was made with the use of the Human Metabolme database (HMDB; http://www.hmdb.ca/) and Chenomx NMR Suite software version 8.1 (Chenomx Inc.), that is also used for quantification. Organic spectra were processed through the NMR*ProcFlow* 1.4 software (nmrprocflow.org) and bucket assignment to each functional group or lipidic constituent was performed based on Amiel *et al.* 2019²⁵⁰.

Statistical Analysis

For most experiments, all data were analyzed using Student's t-teste, on-way ANOVA or two-way ANOVA in GraphPad Prism v7 (http://www.graphpad.com). These assays were performed with a minimum of 3 biological replicates for each condition and the differences were considered to be significant when p value < 0.05.

For the NMR results, Partial Least Square-Discriminant Analysis (PLS-DA) and Principal Component Analysis (PCA) were performed through the SIMCA v13.0.3.0 software. NMR spectroscopy was performed with 1 biological replicate and 2 technical replicates, for each condition

Results

Glioblastoma cells are able to adapt to the availability of different organic compounds

Adaptation to different microenvironmental conditions is a crucial characteristic of cancer cells that allows its progression²⁵¹. As such, we decided to study the effect of the availability of different organic compounds, relevant for both normal and malignant glioma cells, over cellular viability (**Fig 3**). To achieve this, we exposed GBM cells to different metabolites, 5 mM glucose, 6 mM glutamine, 6 mM glutamate, 7.5 mM LiCl and 7.5 mM LiAcAc separately or in combination, during 24 h. Our control (CTRL) comprised cells exposed to DMEM-F12 without glucose and without glutamine.

Overall, the U-251 cells were more resistant, and more adapted to the different conditions, than the U-87 cells (**Fig 3**). This is highlighted by the lower percentage of cell death of the first cell line, which is consistent across most conditions (**Fig 3A-E**). The viability of U-251 cells was affected negatively by the presence of LiCl (**Fig 3E**), which was not completely reverted by glucose (**Fig 3E**). In the case of LiAcAc (**Fig 3E**), lithium may have caused a slight, but not significant, increase in cell death. The effect of lithium, included in LiAcAc, might impact cell viability. U-87 total cell death was unaffected by the presence, or absence, of different metabolites (**Fig 3F-J**). Even though these cells presented lower cellular viability than U-251 cells, they were able to adapt to all conditions. The only differences seen in U-87 cells are not significant, the lowest percentage of cell death was achieved by glucose.

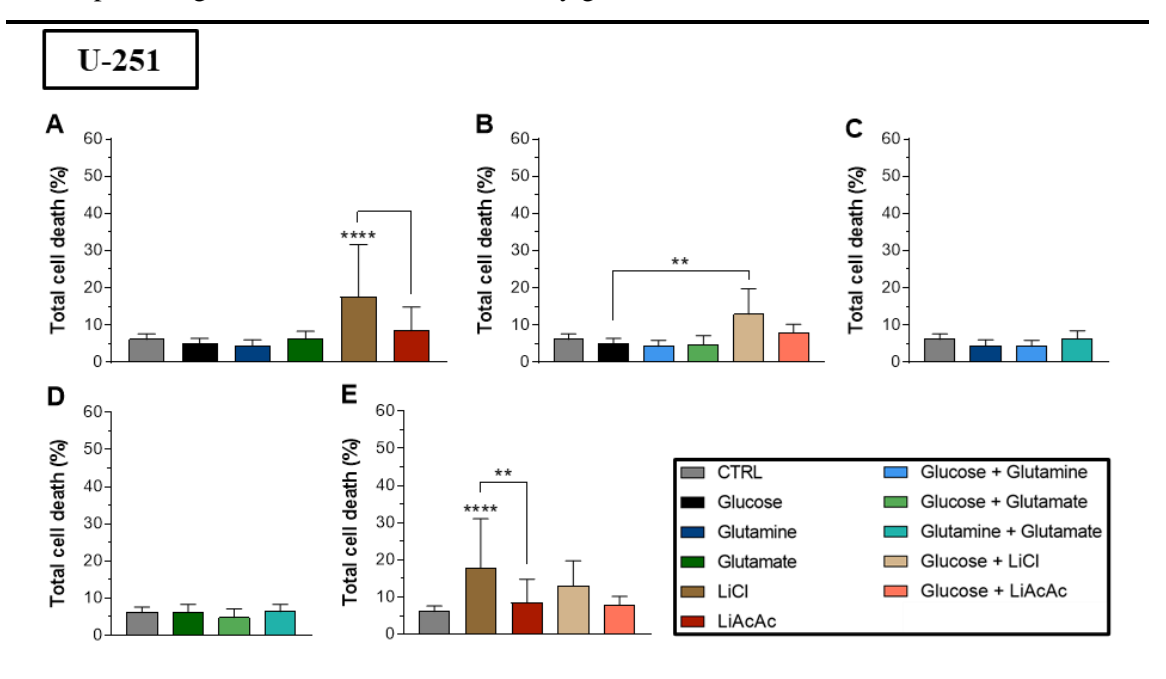


Fig 3. (Continues on the next page)

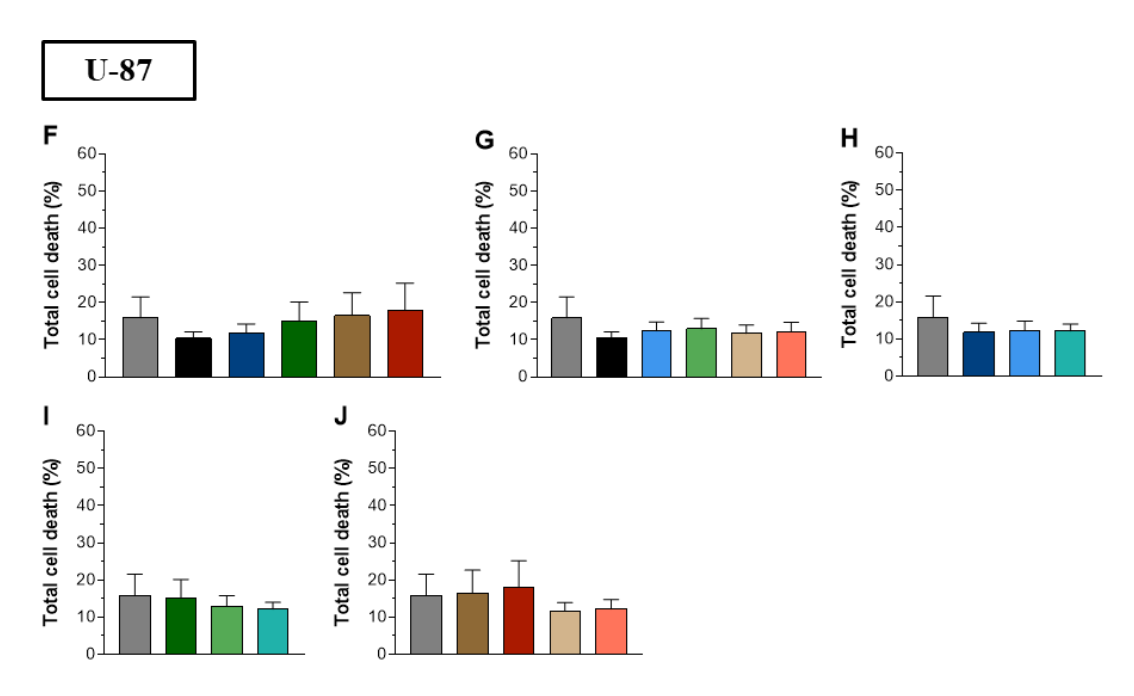


Fig 3. (**Continuation**) Effect of nutrient availability over $(\mathbf{A} - \mathbf{E})$ U-251 and $(\mathbf{F} - \mathbf{J})$ U-87 cell lines viability. Cells were exposed to different metabolites in separate or in combinations of the different nutrients, $(\mathbf{A} \text{ and } \mathbf{F})$ Control conditions, i.e., only one metabolite was supplied, $(\mathbf{B} \text{ and } \mathbf{G})$ Glucose and related conditions, $(\mathbf{C} \text{ and } \mathbf{H})$ Glutamine and related conditions, $(\mathbf{D} \text{ and } \mathbf{I})$ Glutamate and related conditions, $(\mathbf{E} \text{ and } \mathbf{J})$ Ketone bodies, in the form of lithium acetoacetate (LiAcAc), and related conditions. Lithium chloride (LiCl) is the control of the potential effects of lithium present in LiAcAc. CTRL – Control, cells exposed to culture medium (DMEM-F12) without glucose and glutamine. Cells were exposed to the experimental conditions for a period of 24 h. Assay was performed with a minimum of n=3. Results are shown as mean \pm SD. *p<0.05, **p<0.01, ****p<0.001, ****p<0.0001.

Glucose is the main contributor to sustain the metabolic needs associated to cellular proliferation

Cellular proliferation is a characteristic that depends directly on nutrient import, the main nutrients being glucose and glutamine^{16,17}. As such, we decided to study how our cells profilerate in presence to the availability of different nutrients. The approach was similar to the previous experiments, where we exposed cells to different combinations of the metabolites, with the difference that cells were harvested and counted at specific time points, 0 h, 4 h, 12 h, 24 h, 32 h and 48 h.

Between both cell lines, the U-251 presented a higher proliferation rate. Furthermore, most conditions did not impact cell proliferation, in both cell lines (**Fig 4A-J**). In U-251 cells, the only conditions that increased cell proliferation, in comparison to the CTRL, were glucose + glutamine and glucose + glutamate (**Fig 4B**). To note that, while glucose + glutamine significantly increased cell proliferation, when compared to glutamine (**Fig 4C**), there was no difference to glucose (**Fig 4B**). Furthermore, glucose + glutamate significantly increased cell proliferation in comparison to glucose (**Fig 4B**) and glutamate (**Fig 4D**). Regarding the U-87 cells (**Fig 4F-J**), the only condition that increased cell proliferation was glucose + glutamine, which was only significantly higher to the CTRL and glutamine (**Fig 4H**). These suggests that glucose could

contribute more to sustain proliferation than glutamine, even though when glucose is the only nutrient available might not be sufficient. Accordingly, the presence of glutamine or glutamate improves proliferation.

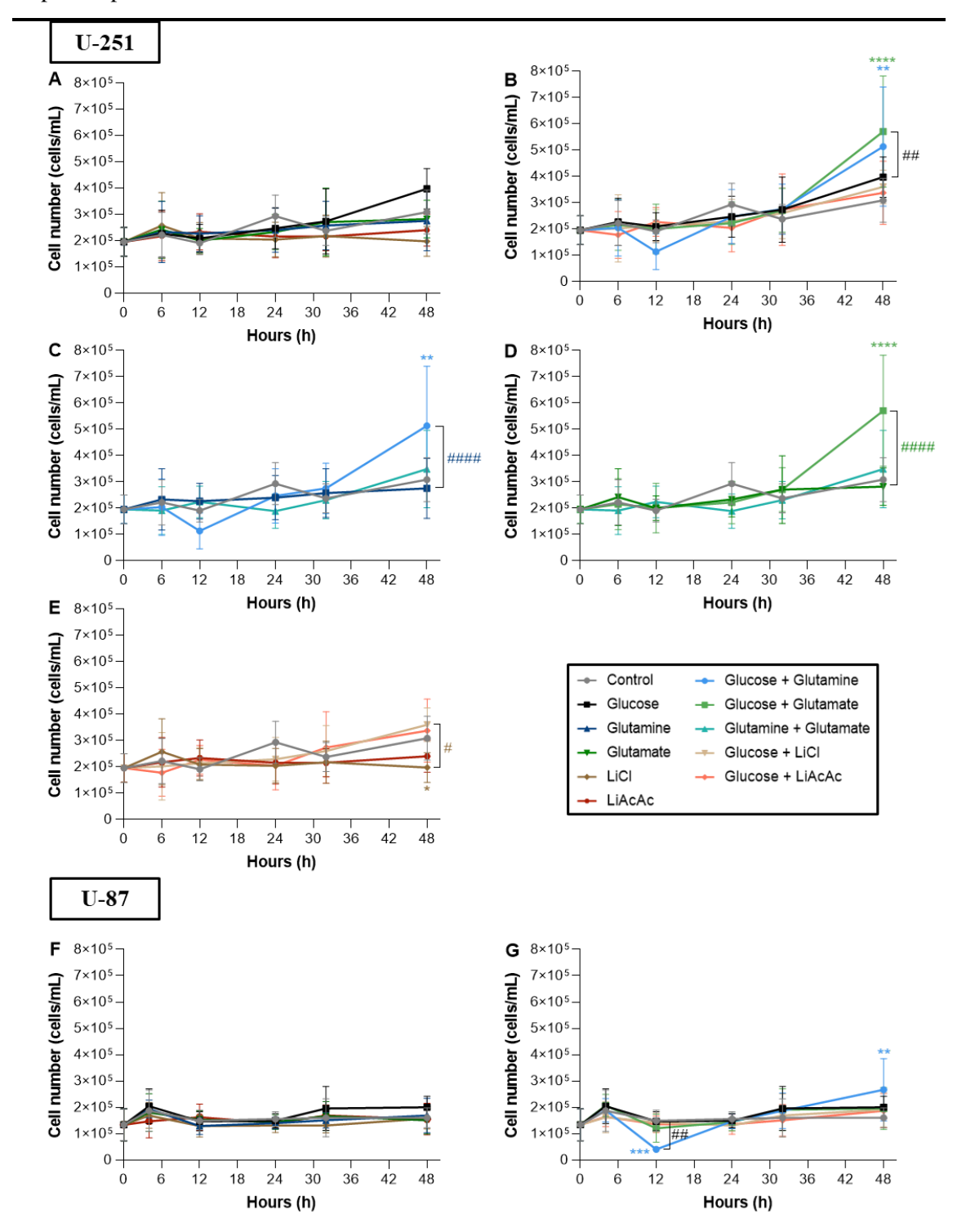


Fig 4. (Continues on the next page)

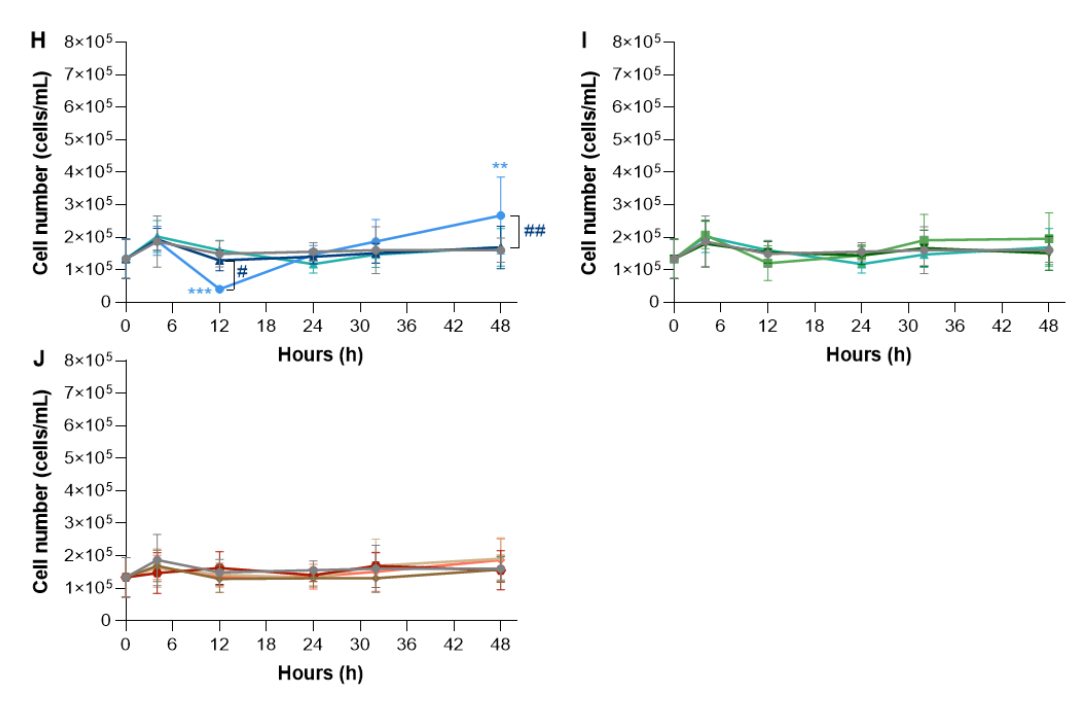


Fig 4. (Continuation) Cellular proliferation is mainly sustained by glucose. (A - E) U-251 and (F - J) U-87 cell lines proliferation. Cells were exposed to different metabolites in separate or in combinations of the different nutrients (A and F) Control conditions, i.e., only one metabolite was supplied, (B and G) Glucose and related conditions, (C and C) Glutamine and related conditions, (C and C) Glutamine and related conditions, (C and C) Retone bodies, in the form of lithium acetoacetate (LiAcAc), and related conditions. Lithium chloride (LiCl) is the control of the potential effects of lithium present in LiAcAc. CTRL – Control, cells exposed to culture medium (DMEM-F12) without glucose and glutamine. Cells were exposed to the experimental conditions for a period of 0 h, 4 h, 12 h, 24 h, 32 h, and 48 h. Results are shown as mean \pm SD. *p<0.05, **p<0.01, ***p<0.001, ****p<0.0001. The symbol # has the same meaning as *, but indicates significant differences versus the condition indicated by the color of #. The symbol * always indicated significant differences versus CTRL.

Cell migration is positively influenced by glucose and glutamine

The migratory capability is an important characteristic of malignant tumors²⁵². It allows these tumors to invade nearby and distant tissue, being dependent on several cell features including metabolic plasticity^{253,254}. For this reason, we evaluated how the availability of different nutrients affects tumor cell migration (**Fig 5**). To achieve this objective, we exposed cells to different combinations of organic compounds, similar to the previous experiments, after blocking the ability to proliferate with mitomycin C. With this approach, we were able to ensure that the wound closure was a result of cell migration, instead of cell proliferation (**Supplementary Figure 1 and 2** shows the wound healing process).

In this experiment, the two cell lines were clearly different. While, the U-87 cells (**Fig 5F-J**) were able to fully close the wound in almost every condition, U-251 (**Fig 5A-E**) cells only closed a maximum of 20% of the wound. In the U-251 cell line, glucose and glutamine were the only control conditions that significantly increased cell migration (**Fig 5A**). These differences only started to be notable at 32 h (for glutamine) and 48 h (for glucose). Glucose + glutamine was the

condition that promoted the highest increase, which is significantly different when compared to both glucose and glutamine (**Fig 5B and C**). While glucose + glutamate and glutamine + glutamate, also increased migration, when compared to the CTRL, the increase was similar to glucose (**Fig 5B**), glutamine (**Fig 5C**) and glutamate (**Fig 5D**), depending on the condition. LiCl and LiAcAc separately, or in combination with glucose, had no effect in cell migration (**Fig 5E**).

In the case of U-87 almost all conditions promoted the full closure of the wound (**Fig 5F-J**). This by itself presents the high migratory capability of this cell line. The exceptions are LiCl and LiAcAc (**Fig 5J**), which without glucose, were not able to promote cell migration. Glucose + glutamine was the condition were the wound was able to close faster (**Fig 5G and H**). To note that, in this condition, it is possible to identify significant differences as early as 8 h in U-87 cells. There was no difference between glucose + glutamate, glucose + LiCl and glucose + LiAcAc *vs* glucose (**Fig 5G and J**), and glutamine + glutamate *vs* glutamine (**Fig 3I**). These results indicate that glucose and glutamine are the main contributors for the increase of cell migration. Furthermore, glucose and glutamine have a synergistic effect (**Fig 5G and H**), being the first condition to promote the full closure of the wound, at 24 h.

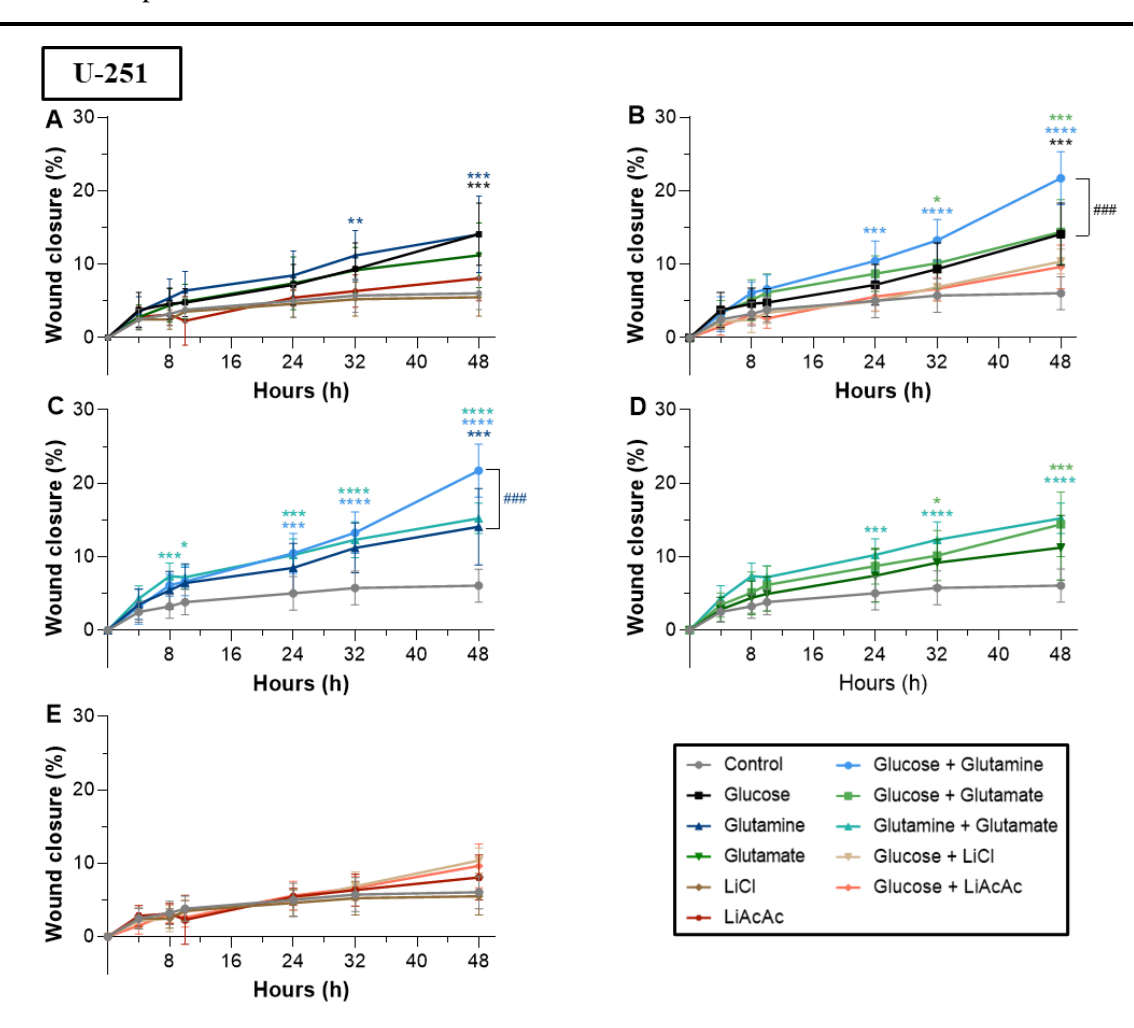


Fig 5. (Continues on the next page)

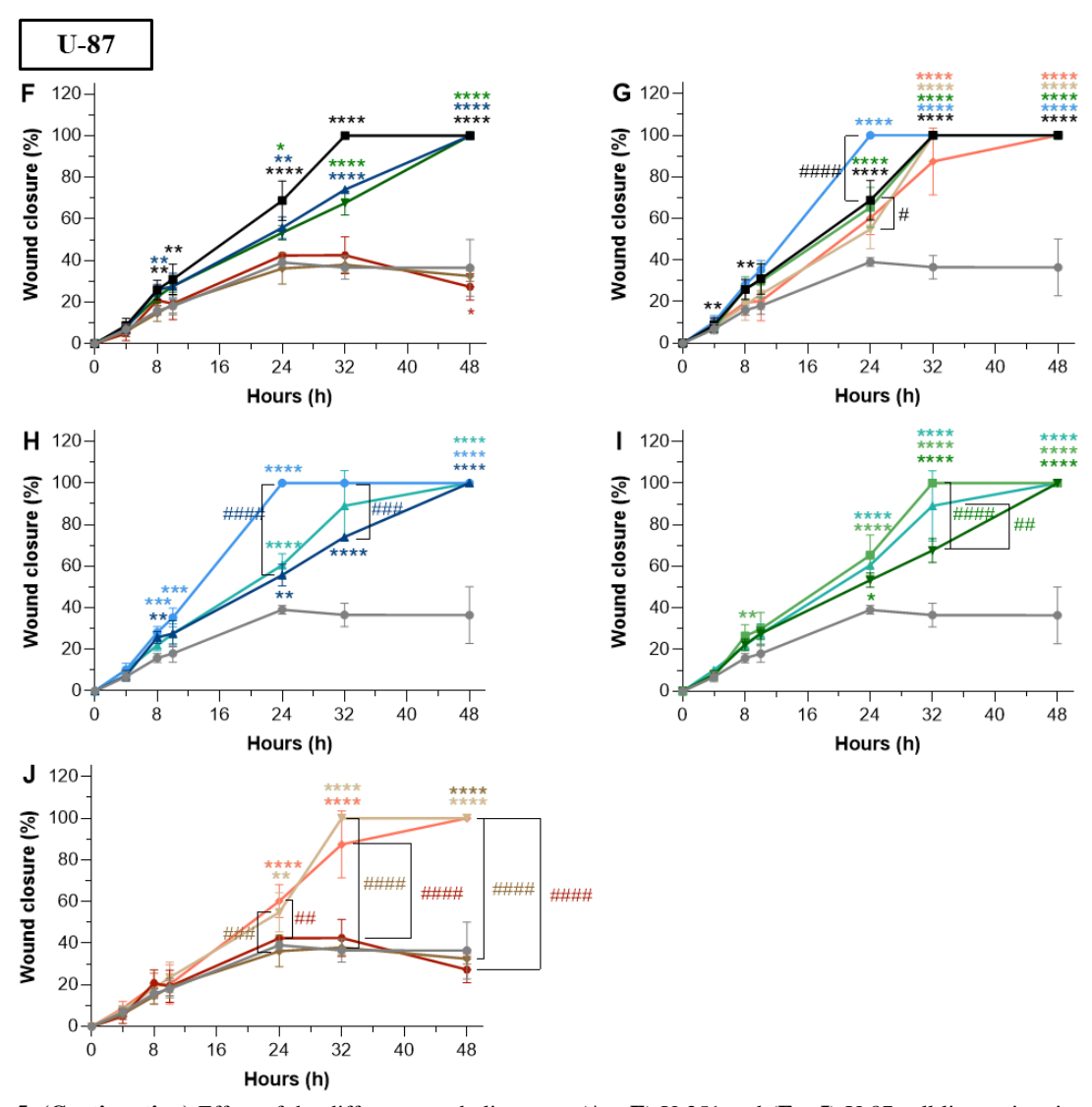


Fig 5. (Continuation) Effect of the different metabolites over $(\mathbf{A} - \mathbf{E})$ U-251 and $(\mathbf{F} - \mathbf{J})$ U-87 cell lines migration. Cells were exposed to different metabolites in separate or in combinations of the different nutrients $(\mathbf{A}$ and $\mathbf{F})$ Control conditions, i.e., only one metabolite was supplied, $(\mathbf{B}$ and $\mathbf{G})$ Glucose and related conditions, $(\mathbf{C}$ and $\mathbf{H})$ Glutamine and related conditions, $(\mathbf{D}$ and $\mathbf{I})$ Glutamate and related conditions, $(\mathbf{E}$ and $\mathbf{J})$ Ketone bodies, in the form of lithium acetoacetate (LiAcAc), and related conditions,. Lithium chloride (LiCl) is the control of the potential effects of lithium present in LiAcAc. CTRL – Control, cells exposed to culture medium (DMEM-F12) without glucose and glutamine. Results are shown as mean \pm SD. Cells were exposed to the experimental conditions for a period of 0 h, 4 h, 8 h, 10 h, 24 h, 32 h and 48 h.*p<0.05, **p<0.01, ***p<0.001, ****p<0.0001. The symbol # has the same meaning as *, but indicates significant differences versus the condition indicated by the color of #. The symbol * always indicated significant differences versus CTRL.

Glucose and glutamine have a primary influence in glioblastoma cells

To explore if and how nutrient availability impacts the metabolic signature of GBM cells, we resorted to Nuclear Magnetic Resonance (NMR) spectroscopy. Here, we applied the same experimental conditions and for each condition three samples were collected: culture media, intracellular aqueous extract and intracellular organic extracts. The culture media samples (supernatants) correspond to the culture media after 24 h of culture on our experimental conditions. These samples are composed by the metabolites present culture medium initial

composition and by metabolites exported by the cells. The remaining two samples are the cellular aqueous and organic phases. While the aqueous phase contains water soluble compounds, the organic phase contains insoluble water compounds. One-dimensional ¹H-NMR spectra of the different sample types were acquired and utilised for quantitative analysis. Metabolite assignment was aided by two-dimensional ¹H *J*-RESolved (JRES) and ¹³C-¹H heteronuclear single quantum coherence (HSQC) spectra. Representative ¹H-NMR spectra of each type of sample and cell line are shown in **Fig 6.** Metabolite concentration was used to perform multivariate analysis: Principal Component Analysis (PCA), to study how the metabolic variance between the different conditions, and Partial Least Square-Discriminant Analysis (PLS-DA), to discriminate between the different conditions and cell line.

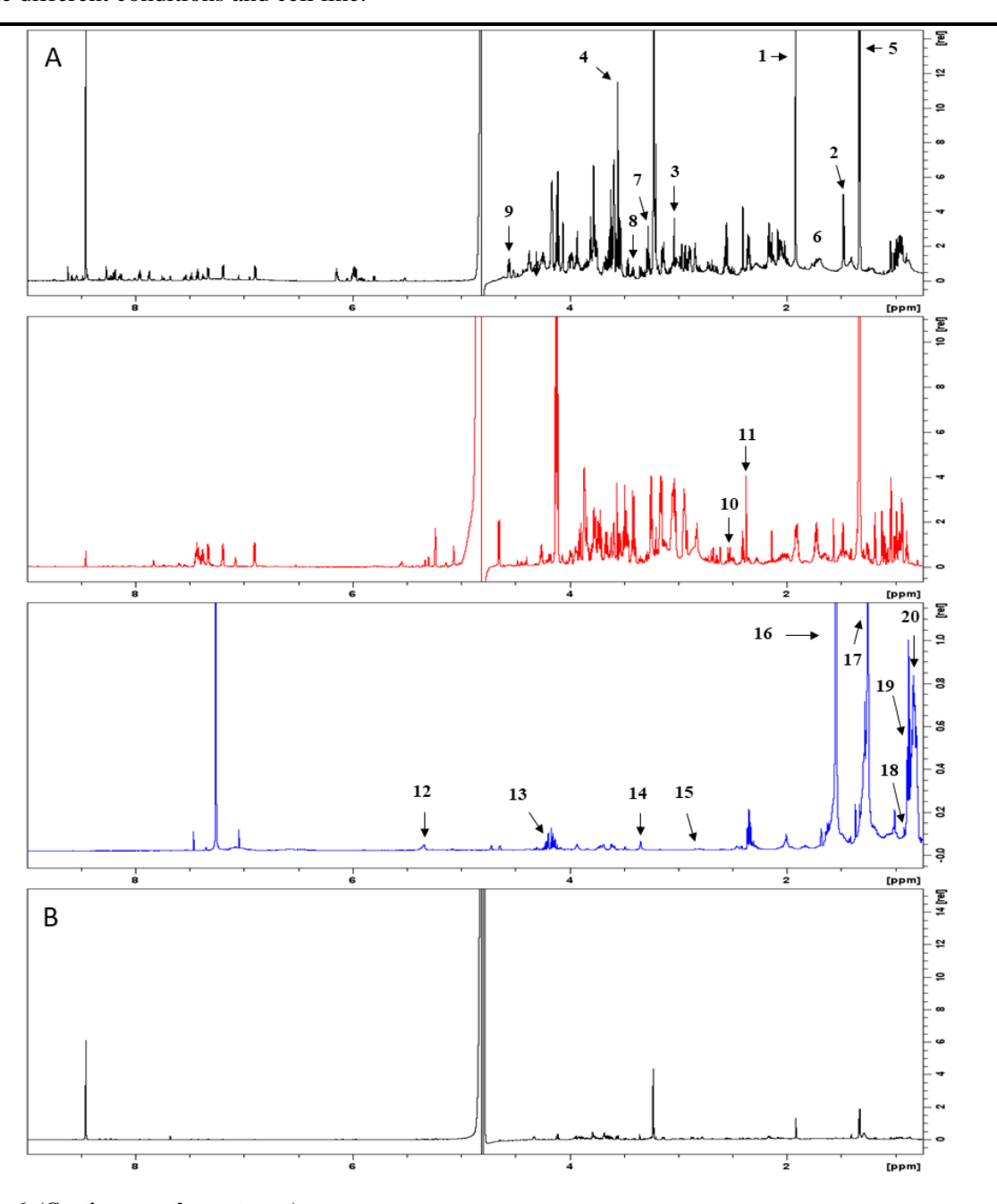


Fig 6. (Continues on the next page)

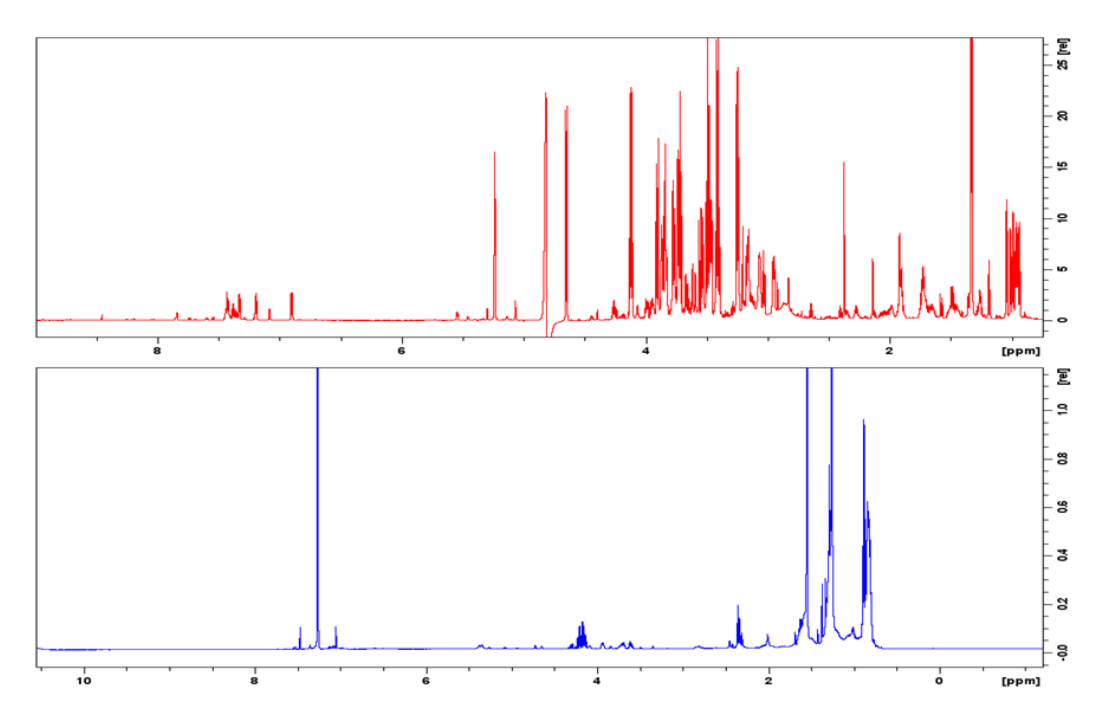


Fig 6. (Continuation) Representative ¹H-NMR spectra of glucose samples of (A) U-251 and (B) U-87. Only the spectral region between 0.75 and 9 ppm is shown. Black spectra – Aqueous samples; Red spectra – Supernatant samples; Blue spectra – Organic samples. 1 – Acetate; 2 – Alanine; 3 – Creatine; 4 – Glycine; 5 – Lactate; 6 – Leucine; 7 – Myo-inositol; 8 – Proline; 9 – Glutathione; 10 – Citrate; 11 – Pyruvate; 12 – Unsaturated Fatty Acids; 13 – Glycerol; 14 – Phosphatydilcholine; 15 – Polyunsaturated Fatty Acids; 16 – Fatty Acids; 17 – CH₂-from Fatty Acids; 18 – Esterified Cholesterol; 19 – Free Cholesterol; 20 – CH₃-from Fatty Acids. Cells were exposed to the experimental conditions for a period of 24 h.

The first step was to perform a PCA (**Fig 7A and B**) in order to assess if our samples grouped according to the cell line or culture condition. In both type of samples, aqueous and supernatant, we found that the main clustering factor was the cell line. Accordingly, the PLS-DA confirmed that it is possible discriminate the two cell lines, both in aqueous (**Fig 7C**) and supernatant (**Fig 7D**) samples, despite the culture conditions. Furthermore, U-251 samples were more scattered and U-87 samples grouped in a narrower cluster. These results demonstrate that both cells can be distinguishable by their metabolisms and that U-87 cells have a more homogeneous metabolic signature, regardless of which nutrients are provided, in comparison to U-251 cells. While differences between cell lines could be explained by the first component, differences within cell-specific samples, in specific U-251 samples, could be justified by the second component.

Each cell line was analyzed alone by PCA. U-251 samples, both aqueous (**Fig 8A**) and supernatant (**Fig 8E**), appear to be separated according to the presence or absence of glucose and glutamine. The differences between samples with glucose and samples without glucose appears to be explained by the principal component 1 (PC1). PC2 could account for the separation of glutamine-containing samples, from samples without glutamine. In the intracellular aqueous fraction (**Fig 8A**), the amino acids alanine, glycine, leucine and proline; and the organic compounds acetate, creatine, glutathione, inosine, myo-inositol and NAD⁺ were more important

in the separation of samples with and without glucose (**FIG 8B**). An univariate analysis confirmed the importance of this compounds, most of them are significantly increased in glucose-containing samples (**Fig 8C**). The exceptions being leucine, proline and creatinewhich do not show a significant difference but have a tendency to be increased. To note that the mentioned amino acids and myo-inositol are present in the culture media (consult **Supplementay Table 1** for media formulation), suggesting its increased import. Indeed, in the respective loadings scatter plot of U-251 supernatant samples (**Fig 8F**), the same compounds are negatively correlated with glucose-containing samples. Furthermore, NAD⁺ was found to have similar values (**Fig 8C**) and inosine was not found in glucose-containing conditions (**Supplementary Table 2**).

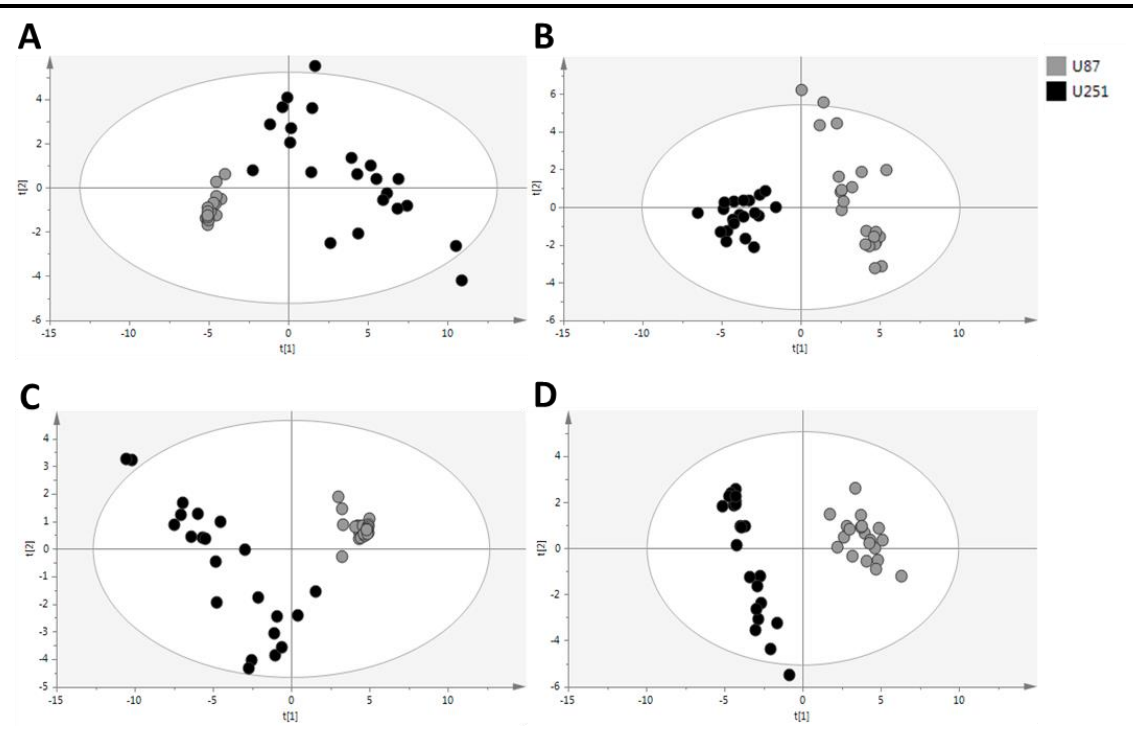


Fig 7. Discrimination between U87 and U-251 based on the ¹H-NMR metabolic profile. Principal Component Analysis (PCA) score plots of (**A**) aqueous and (**B**) supernatant samples, and Partial Least Square-Discriminant Analysis (PLS-DA) score plots of (**C**) aqueous and (**D**) supernatant samples. Statistical analysis was based on ¹H-NMR spectra acquired from the previous type of samples. Cells were exposed to the experimental conditions for a period of 24 h.

Although glycine is the only molecule to be significantly decreased in supernatant samples, supplemented with glucose (**Fig 8D**), leucine shows a tendency to be decreased, supporting the idea that they are being transported in high amounts into the cell. Proline and myo-inositol have no differences and alanine is instead increased in conditions with glucose. The positive correlation of intracellular acetate, creatine and glutathione, in glucose-containing samples, indicate that these compounds are being synthesized in higher amounts when glucose is supplied. This observation is supported by the increase of acetate and glutathione (**Fig 8C**) in aqueous extracts from cells exposed to glucose. Glutamine also appears to play an important role, in the metabolism of U251 cells, as they are separated from samples that are not supplied with it, even though there is a clear separation between the three conditions (glutamine, glutamine + glucose and glutamine

+ glutamate). In these samples, aspartate, AMP and glutamate appear to be more important while dimethyl sulfone, *O*-phosphocholine and sn-glycero-3-phosphocholine are less important. Accordingly, aspartate and glutamate are increased in glutamine-containing samples and *O*-phosphocholine is decreased (**Fig 8G**). AMP, dimethyl sulfone and sn-glycero-3-phosphocholine are present in similar amounts in samples with and without glutamine (**Fig 8H**).

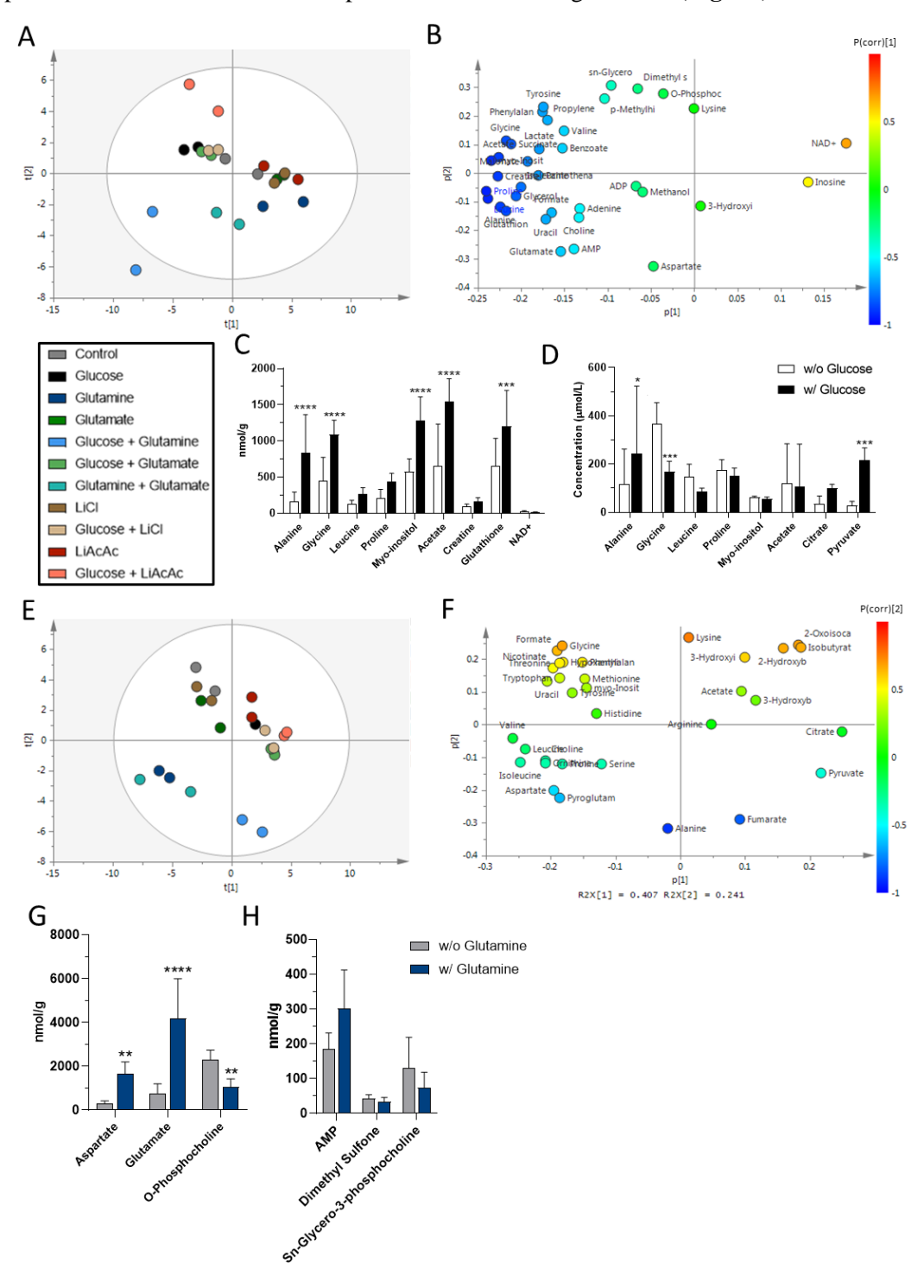


Fig 8. (Continues on the next page)

Fig 8. (Continuation) Glucose and Glutamine impacts the metabolism of U-251 cells. (A) Principal Component Analysis (PCA) score plot of U-251 aqueous samples and (B) the respective loadings scatter plot. (C) amount, per gram of biomass, of organic compounds with importance in the separation of samples with glucose, from samples without glucose, present in the aqueous phase, (D) concentration of the previous compounds present in the supernatant, (E) PCA score plot of U-251 supernatant samples and (F) the respective loadings scatter plot. (G and H) amount, per gram of biomass, of organic compounds important in the separation of samples with glutamine, from samples without glutamine, present in the aqueous phase. Figure G and H are shown in different scales because the amount, per gram of biomass, in H is low in comparions to G. As such, having the six organic compounds in the same figure would difficult the interpretation of these two figures. Lithium chloride (LiCl) is the control for the potential effects of lithium present in Lithium acetoacetate (LiAcAc). CTRL – Control, cells exposed to culture medium (DMEM-F12) without glucose and glutamine. Cells were exposed to the experimental conditions for a period of 24 h. Results are shown as mean \pm SD. **p<0.01, ****p<0.001, *****p<0.0001.

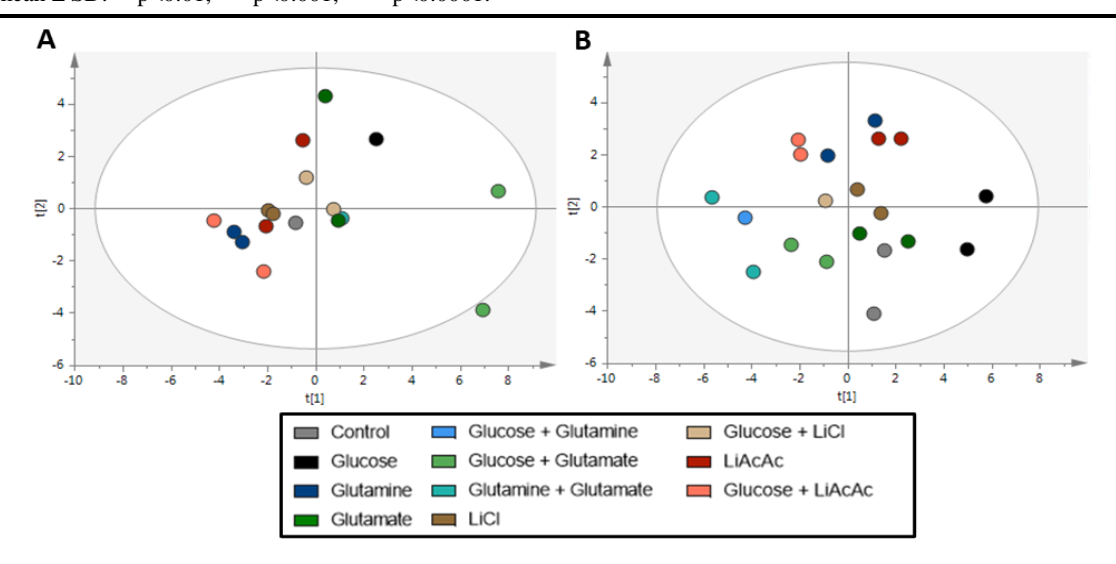


Fig 9. The metabolism of U-87 cells is not affected by the availability of a particular nutrient. (**A**) Principal Component Analysis (PCA) score plots of U-87 aqueous samples, (**B**) PCA score plots of U87 supernatant samples. Lithium chloride (LiCl) is the control for the potential effects of lithium present in Lithium acetoacetate (LiAcAc). CTRL – Control, cells exposed to culture medium (DMEM-F12) without glucose and glutamine. Cells were exposed to the experimental conditions for a period of 24 h.

In U-87 cells, aqueous samples were initially tightly clustered (Supplementary Figure 3) with the exception of one sample from four different conditions, CTRL, glucose, glucose + glutamine and glutamine + glutamate. As such, we considered them to be outliers and decided to exclude these samples from our analysis, resulting in a more interpretable PCA (Suplementary Figure 3 and Fig 9A, respectively). It is important to state that, at the level of the spectra (not shown) there was no indication (e.g. poor spectra quality, bad shimming and baseline errors) to exclude the previous four samples. Furthermore, these samples were not excluded from the supernatant and organic type of samples. Unlike U-251 samples, samples from U-87 samples did not cluster according to a particular organic compound, both in aqueous (Fig 9A) and supernatant (Fig 9B) samples. This could be explained by a lower metabolic plasticity of U-87 cells (in comparison to U-251 cells), or by the lower biomass in U-87 samples in comparison to U-251 samples (Supplementary Figure 2 and 3), which results in spectra with a relative low signal potentially affecting sample analysis.

Organic spectra of each cell line were analyze with the open-source software NMRProcFlow. With this approach we were able to identify the following functional groups and lipid constituents: -CH₂- from fatty acids (FA), -CH₃-from FA, esterified cholesterol (ChoE), free cholesterol (ChoF), total cholesterol (ChoT), glycerol from triacylglycerol (Gly), FA, -CH=CH-(unsaturated FA - UFA), -CH=CH-CH₂-CH=CH- (polyunsaturated FA - PUFA) and phosphatidylcholine (PhCho). Overall, there was no significant changes in the organic fraction, among conditions, in both cell lines (**Fig 10 and 11**). The only exception was PhCho in U-251 cells (**Fig 10A**). This lipid constituent was increased in the control conditions glutamine, glutamate and LiCl. Interestingly, when these conditions are combined with glucose, the relative levels of PhCho return to basal levels. Combination of glutamine and glutamate had the same effect has glucose supplementation.

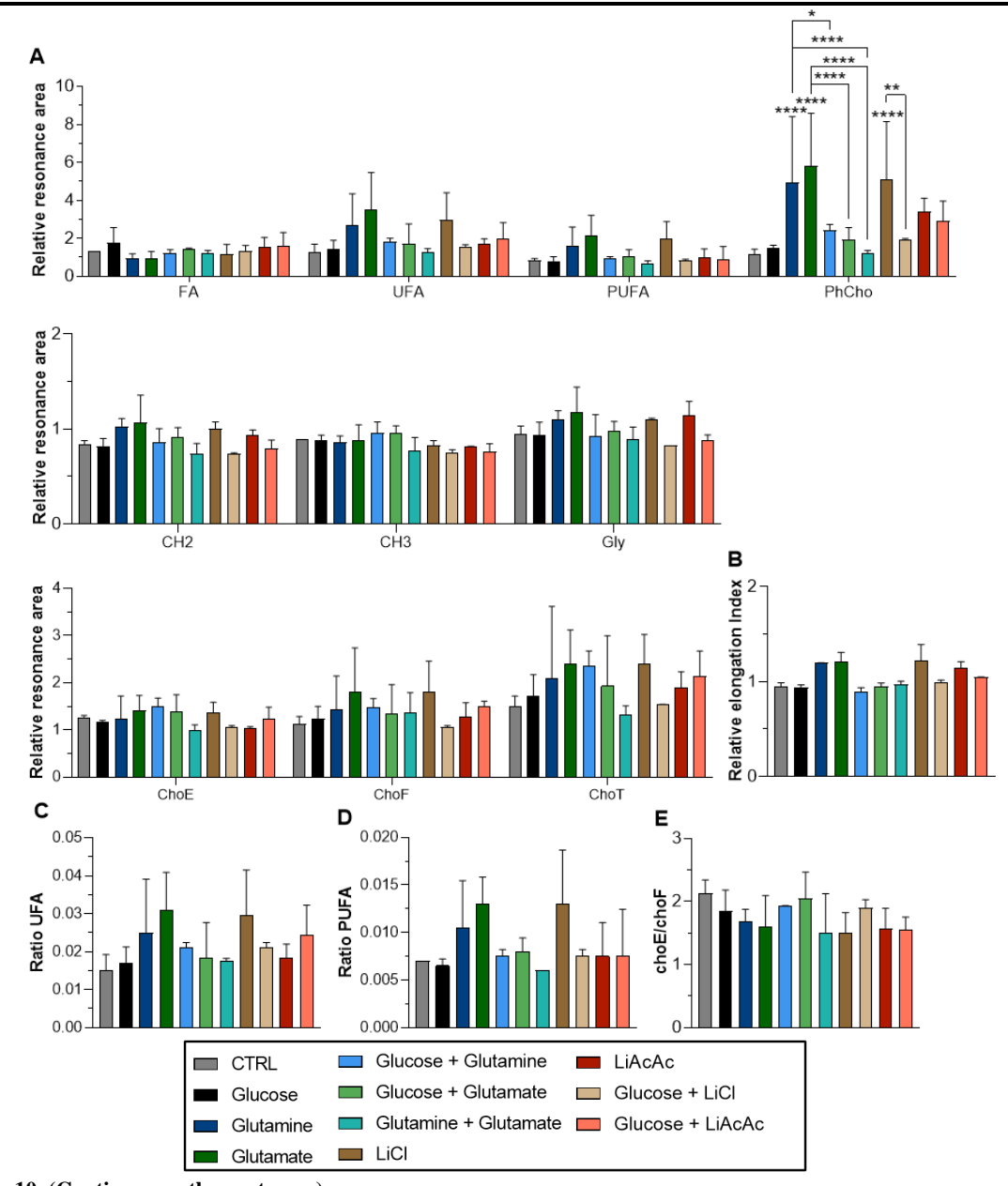


Fig 10. (Continues on the next page)

Fig 10. (**Continuation**) Lipid dynamics in U-251 cells exposed to different conditions. (**A**) Indentified functional groups and lipid constituents in organic samples. (**B**) Relative elongation index of fatty acids (FA), calculated through the levels of CH₂ and CH₃, (**C**) Unsaturated FA (UFA) ratio, (**D**) Polyunsaturated FA (PUFA) ratio, (**E**) Relation between esterified cholesterol (choE) and free cholestrol (choF). ChoT – Total cholesterol Gly – Glycerol; PhCho – Phosphatidylcholine. Lithium chloride (LiCl) is the control for the potential effects of lithium present in Lithium acetoacetate (LiAcAc). CTRL – Control, cells exposed to culture medium (DMEM-F12) without glucose and glutamine. Cells were exposed to the experimental conditions for a period of 24 h. Results are shown as mean \pm SD. *p<0.05, **p<0.01, ****p<0.001, ****p<0.0001.

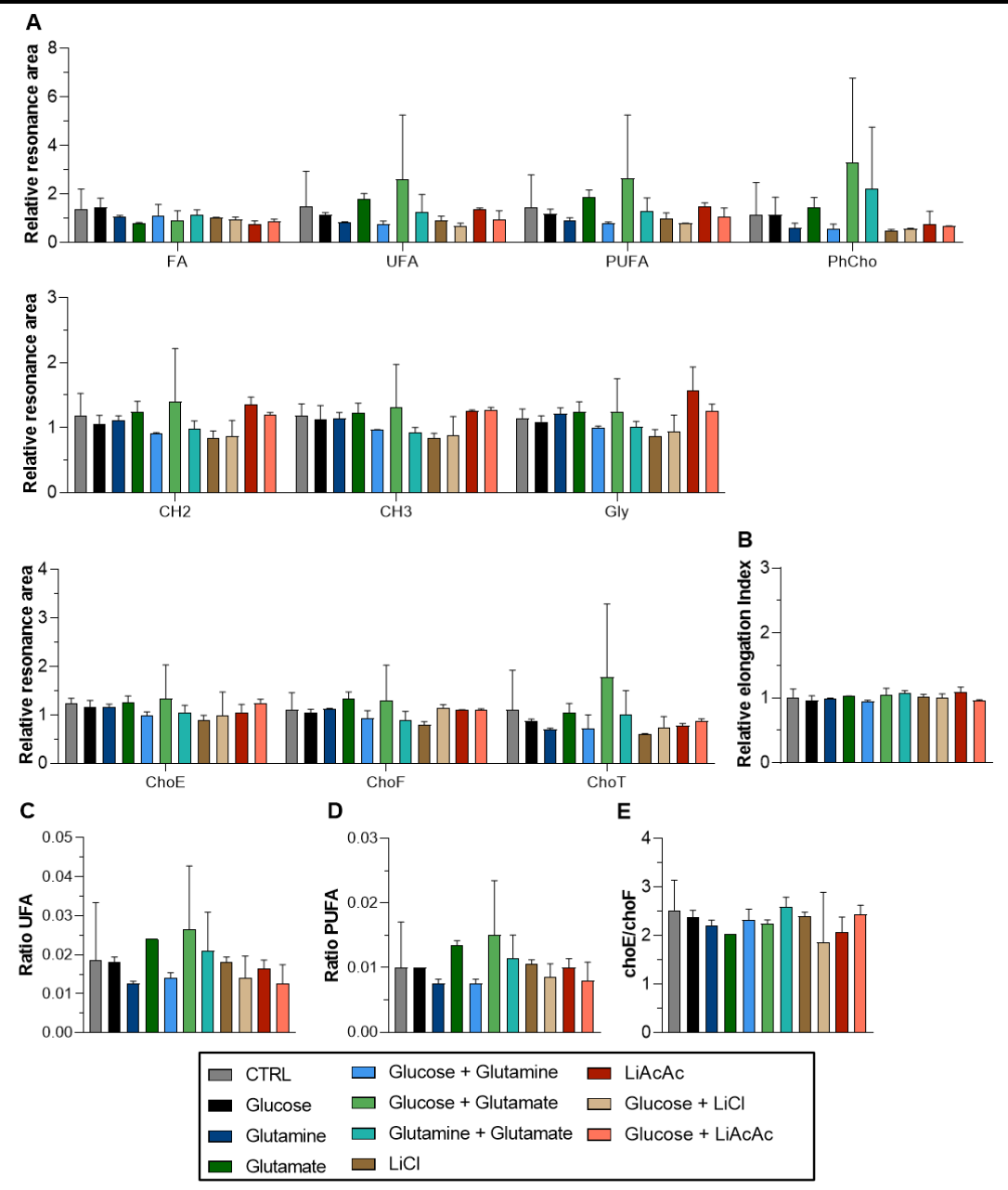


Fig 11. The dynamics of lipids from U-87 cells remains similar, independently of culture conditions. (A) Indentified functional groups and lipid constituents in organic samples. (B) Relative elongation index of fatty acids (FA), calculated through the levels of CH2 and CH3, (C) Unsaturated FA (UFA) ratio, (D) Polyunsaturated FA (PUFA) ratio, (E) Relation between esterified cholesterol (choE) and free cholestrol (choF). ChoT – Total cholesterol Gly – Glycerol; PhCho – Phosphatidylcholine. Lithium chloride (LiCl) is the control for the potential effects of lithium present in Lithium acetoacetate (LiAcAc). CTRL – Control, cells exposed to culture medium (DMEM-F12) without glucose and glutamine. Cells were exposed to the experimental conditions for a period of 24 h. Results are shown as mean \pm SD. *p<0.05, **p<0.01, ***p<0.001, ****p<0.0001.

Transport of the supplied nutrients and production of related organic compounds

Due to the inherent capacity of NMR spectroscopy to quantify organic compounds that are present in relative high amounts in samples, we also evaluated the concentration of the supplied nutrients, in supernantant samples (**Fig 12**). With this information we can infer if a given nutrient is being differently transported to the cell in different conditions. Furthermore, we also evaluated the concentrations of lactate in aqueous and supernatant samples, in order to have a idea of its production.

Overall, the concentration of glucose, glutamine, glutamate and AcAc in the supernatant stays similar among conditions where these nutrients were supplied (**Fig 12**). The only significant difference corresponds to glucose concentration in U-251 samples (**Fig 12A**). In this case, glutamine, glutamate and LiCl appear to decrease the concentration of glucose in medium, suggesting that it is being transported in higher amounts. This effect is more pronounced when glutamine is present (glucose + glutamine).

Table 1. Glioblastoma cells are able to transport acetoacetate and potentially metabolize it. LiAcAc – Lithium acetoacetate.

Cell line	Condition	Aqueous Samples (nmol/g)	Supernatant Samples (µmol/L)	
		Acetoacetate	3-Hydroxybutyrate	Acetoacetate
U-251	LiAcAc	22.550	253.111	2931.111
	LiAcAc	10.480	222.889	2783.111
	Glucose + LiAcAc	25	291.111	2790.889
	Glucose + LiAcAc	0	266.000	2829.444
U-87	LiAcAc	0	0	4428.556
	LiAcAc	0	0	4415.111
	Glucose + LiAcAc	44.019	0	4221.778
	Glucose + LiAcAc	8.902	0	4534.778

Lactate was found to be produced in relatively high amounts by U-251 cells (**Fig 13A** and B), in comparison to U-87 cells (**Fig 13C** and D). However, this difference could be again related by the low biomass in U-87 cells. In U251 samples we found that there is a clear increase in lactate production when glucose is supplied. Indeed, **Fig 13B** shows us that lactate concentration, in conditions with glucose, is significantly higher than in the respective controls. In the aqueous fraction (**Fig 13A**), even though the differences are not statistically significant, glucose conditions appears to have the tendency to increase lactate quantity. Lactate production in U-87 cells does not seem to change considerably between conditions.

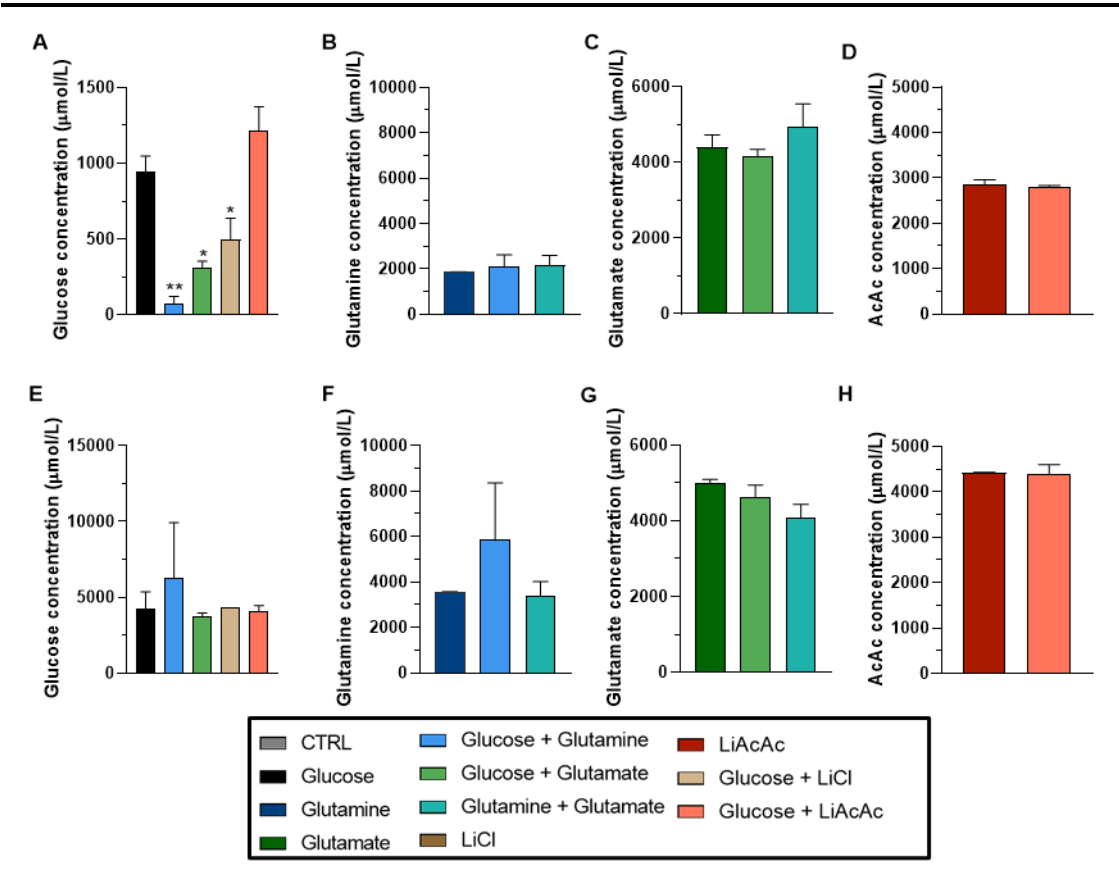


Fig 12. Transport of supplied (A) Glucose, (B) Glutamine, (C) Glutamate and (D) Acetoacetate. Graphics A - D correspond to U-251 supernatant samples and graphics E - H correspond to U-87 supernatant samples. Lithium chloride (LiCl) is the control for the potential effects of lithium present in Lithium acetoacetate (LiAcAc). CTRL – Control, cells exposed to culture medium (DMEM-F12) without glucose and glutamine. Cells were exposed to the experimental conditions for a period of 24 h. Results are shown as mean \pm SD. *p<0.05, **p<0.01.

At the substrate level, we found AcAc in supernatant and in the aqueous samples (**Table 1**). This finding indicates that AcAc is being imported, both in U251 and U87 cells. Furthermore, we also found 3-hydroxybutyrate (also known as bHB) exclusively in supernatant samples that contain LiAcAc, but only in U251 samples (**Table 1**) This particular finding is interesting because it may suggest that the metabolism of AcAc is active in the cell line U251.

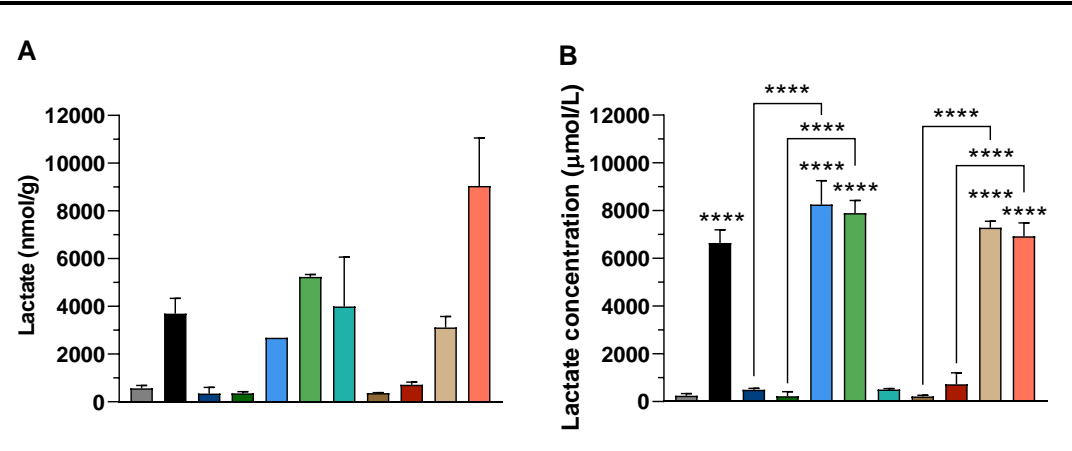


Fig 13. (Continues on the next page)

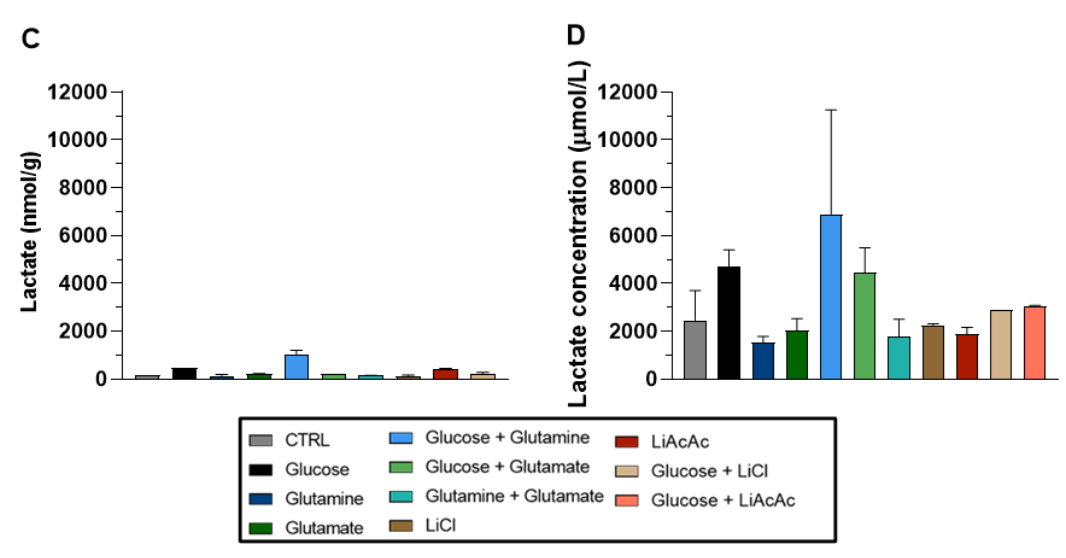


Fig 13. (Continuation) Lactate is found to be increased when cells are exposed to glucose. U-251 (A) Aqueous and (B) Supernatant samples, U-87 (C) Aqueous and (D) Supernatant samples. Lithium chloride (LiCl) is the control for the potential effects of lithium present in Lithium acetoacetate (LiAcAc). CTRL – Control, cells exposed to culture medium (DMEM-F12) without glucose and glutamine. Cells were exposed to the experimental conditions for a period of 24 h. Results are shown as mean \pm SD, ***p<0.001, ****p<0.0001.

Gene expression is affected by nutrient availability

To understand how GBM metabolism is affected by nutrient availability, we assessed the impact of the different culture conditions over the expression of rate-limiting enzymes and transporters involved in metabolic pathways, both important to the tumor and to the central nervous system. These metabolic pathways include the metabolism of glucose, glutamine/glutamate and acetoacetate. In glucose and lactate metabolism we decided to assess the expression of the enzymes *HKII*, *G6PD*, and *PDHAI*, and the expression of the transporters *GLUT1* and *MCT1* and *4*. In glutamine/glutamate metabolism the expression of the enzymes *GLS1* and *GLNS* was assessed, together with the expression of the transporters *GLT-1*, *GLAST*, *LAT1*, *SNAT1*, 2 and 3. Ketone bodies metabolism was assessed through the expression of the enzymes *OXCT1*, *ACAT1* and the ketone bodies main transporter, MCT1. Furthermore, due to the inherent connection between these metabolic pathways, we also assessed the expression of enzymes involved in the synthesis of FA, *FASN*, and their degradation, Acyl-CoA Dehydrogenase Short Chain (ACADS – *ACADS*) and Acyl-CoA Dehydrogenase Medium Chain (ACADM – *ACADM*).

In U-251 cells, glucose metabolism (**Fig 14A**) was mainly affected by lithium. In its presence, glucose consumption may increase, as suggested by the increased expression of *HKII* and *PDHA1*, even though the expression of *GLUT1* was mostly unaffected. *GLUT1* was only affected by AcAc, which increased its expression. Furthermore, glucose appears to potentiate the effect of lithium (present in LiCl and LiAcAc) in the expression of *HKII*. The deviation of glucose into PPP may be blocked upon glutamine + glutamate exposure, since it significantly reduced the

expression of *G6PD*. The transport of lactate (MCT1 and MCT4) is mainly affected by the presence of glutamine and glutamate but only in the presence of another organic compound. The expression of *MCT1* and *MCT4* is also affected by the presence of lithium itself, and seemingly not AcAc.

The metabolism of glutamine/glutamate (**Fig 14B**) is mainly affected at glutamate transport level. Indeed, the expression of *GLAST* is consistently downregulated in the presence of glutamine. This suggests that glutamine impairs glutamate import.

Besides the transport of AcAc, the expression of genes involved in its metabolism (**Fig 14C**) was mostly unaffected. Nonetheless, the combination of glutamine and glutamate appears to promote the degradation of AcAc, since it upregulates the expression of *OXTC1* and *ACAT1*. The expression of MCT1 however, is reduced in the same condition and, as previously said, it was mainly affected by glutamine and glutamate. ACAT1 expression is also affected by the control condition glutamine, and by glucose + LiCl.

Degradation of FA (**Fig 14D**) may be significantly increased in the presence of lithium, seen by the increased expression of *ACADS*. At the same time, in the presence of glutamine and glutamate, the expression of FASN increases (**Fig 14D**), potentially increasing the synthesis of FA.

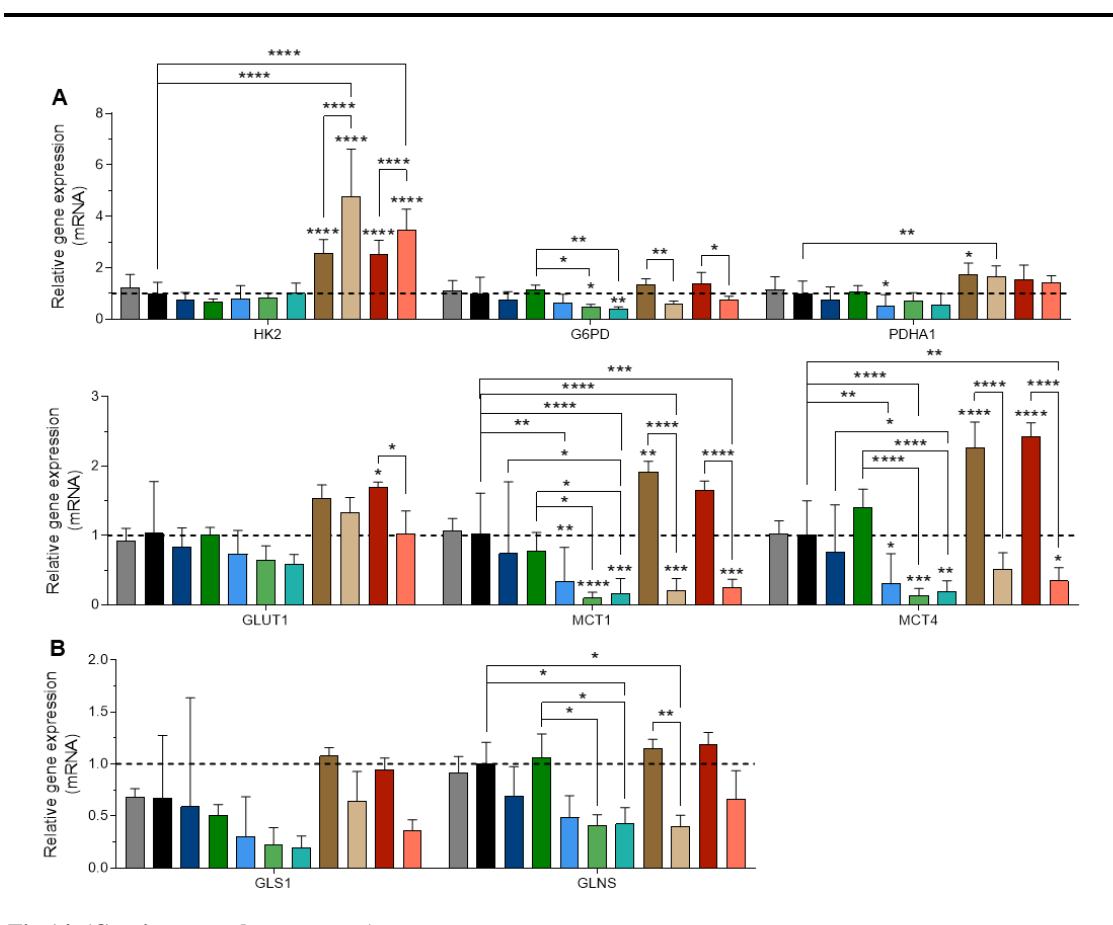


Fig 14. (Continues on the next page)

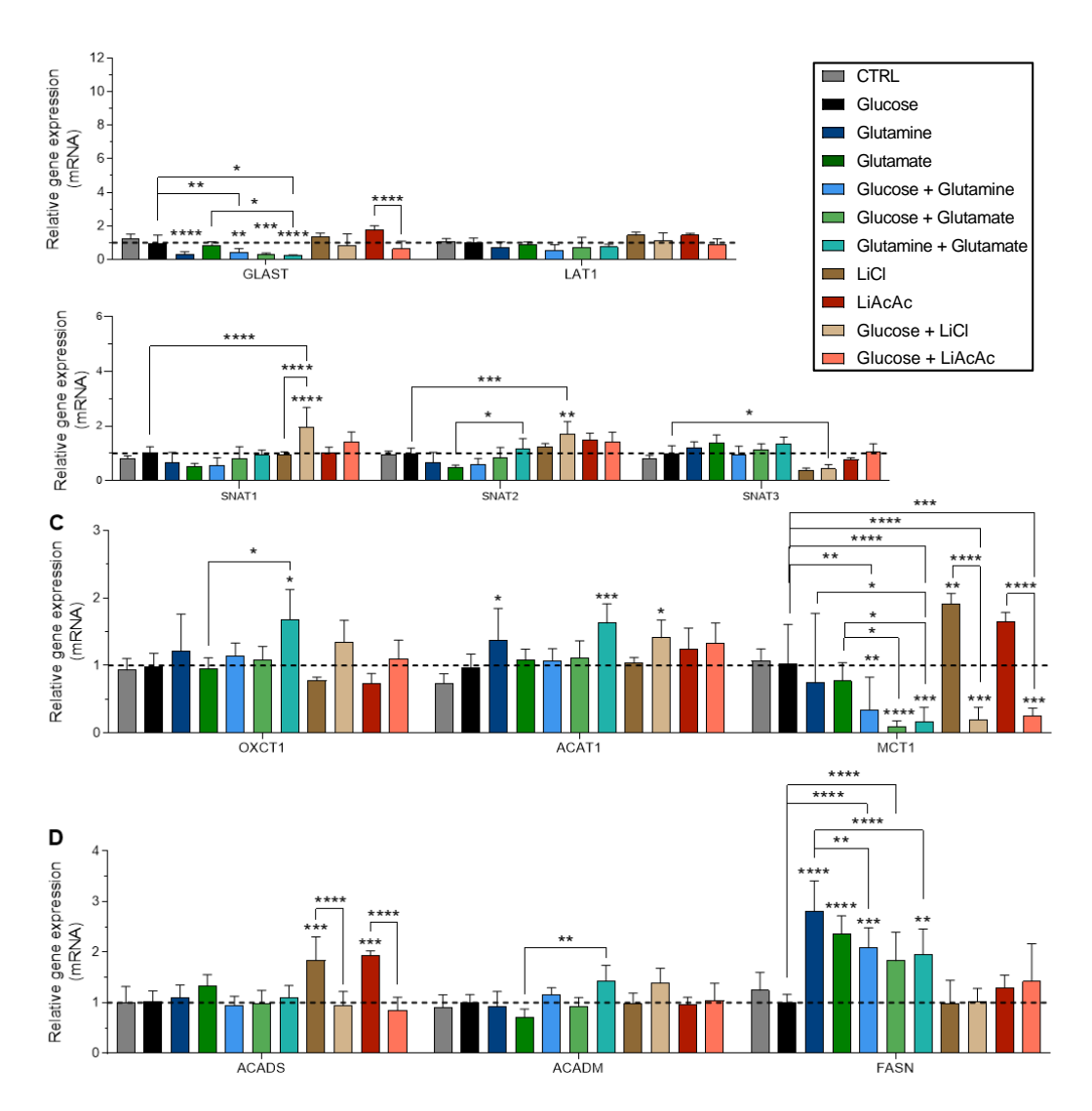


Fig 14. (Continuation) Nutrient availability impacts the expression of genes involved in nutrient transport and its metabolism, in U-251 cells. We studied the expression of genes related to (A) glucose metabolism, HKII (Hexokinase 2), G6PD (Glucose-6-Phosphate Dehydrogenase), PDHA1 (Pyruvate Dehydrogenase E1 Subunit Alpha 1), SLC2A1 (Glucose Transporter-1, GLUT1), SLC16A1 (Monocarboxylate Transporter 1, MCT1) and SLC16A4 (Monocarboxylate Transporter 4, MCT4), (B) glutamine/glutamate metabolism, GLS1 (Glutaminase 1), GLNS (Glutamine synthetase), SLC1A3 (Glutamate Aspartate Transporter, GLAST), SLC7A5 (L-type amino acid transporter 1, LAT1), SLC38A1 (Sodium-Coupled-Neutral-Amino-Acid-Transporter 2, SNAT2) and SLC38A3 (Sodium-Coupled-Neutral-Amino-Acid-Transporter 3, SNAT3), (C) ketone bodies metabolism OXCT1 (3-Oxoacid CoA-Transferase 1), ACAT1 (Acetyl-CoA Acetyltransferase 1) and MCT1, and (D) lipid metabolism, ACADS (Acyl-CoA Dehydrogenase Short Chain), ACADM (Acyl-CoA Dehydrogenase Medium Chain) and FASN (Fatty Acid Synthase). Lithium chloride (LiCl) is the control for the potential effects of lithium present in Lithium acetoacetate (LiAcAc). CTRL – Control, cells exposed to culture medium (DMEM-F12) without glucose and glutamine. Cells were exposed to the experimental conditions for a period of 24 h. Results are shown as mean ± SD. *p<0.05, **p<0.01, ****p<0.001, *****p<0.001.

In U-87 cells, glucose metabolism (**Fig 15A**) was mainly downregulated by glucose, as seen in the expression of *HKII*, *G6PD* and *PDHA1*. Furthermore, glutamate also lead to decreased expression of *HKII*. While the expression of these enzymes decreased, the expression of glucose and lactate transporters was consistent across most conditions. Nevertheless, glucose + glutamine

increased the expression of both *GLUT1* and *MCT4*. The expression of *MCT4* was also increased by glucose + glutamate. *MCT1* expression was only increased by AcAc.

The expression of genes involved in the metabolism of glutamine and glutamate (**Fig 15B**) was mostly downregulated. However, in the presence of both glutamine and glutamate (in combination) all genes, but *GLS-1* and *LAT1*, are upregulated. These results are interesting because when cells are exposed separately to glutamine or glutamate most genes are either downregulated or do not suffer any difference. Glucose also downregulated most genes in every condition where it is present, with a few exceptions. The main exception being *GLS1* expression, which was not affected by glucose. LiCl decreased the expression of *GLAST*, but it was reverted to CTRL levels when glucose was added. *LAT1* expression was not influenced by LiCl and Glucose + LiCl. To note that, even though lithium appears to be responsible for differences in the expression of several genes, in this case, AcAc may instead be responsible for the upregulation of *LAT1* and *SNAT1*.

The expression of genes related to ketone bodies metabolism (**Fig 15C**) was only slightly affected. The most differences can be found in the expression of *ACAT1*, where the presence of glucose leads to its downregulation. *MCT1* was only affected by AcAc and *OXCT1* expression was not affected by any condition.

Unlike U-251 cells, the lipid metabolism of U-87 (**Fig 15D**) was mostly downregulated. In specific, every condition significantly reduced the expression of *ACADS* and *ACADM*. This might suggest that β-oxidation is downregulated when nutrients are available. *FASN* expression was downregulated by glucose but upregulated by AcAc.

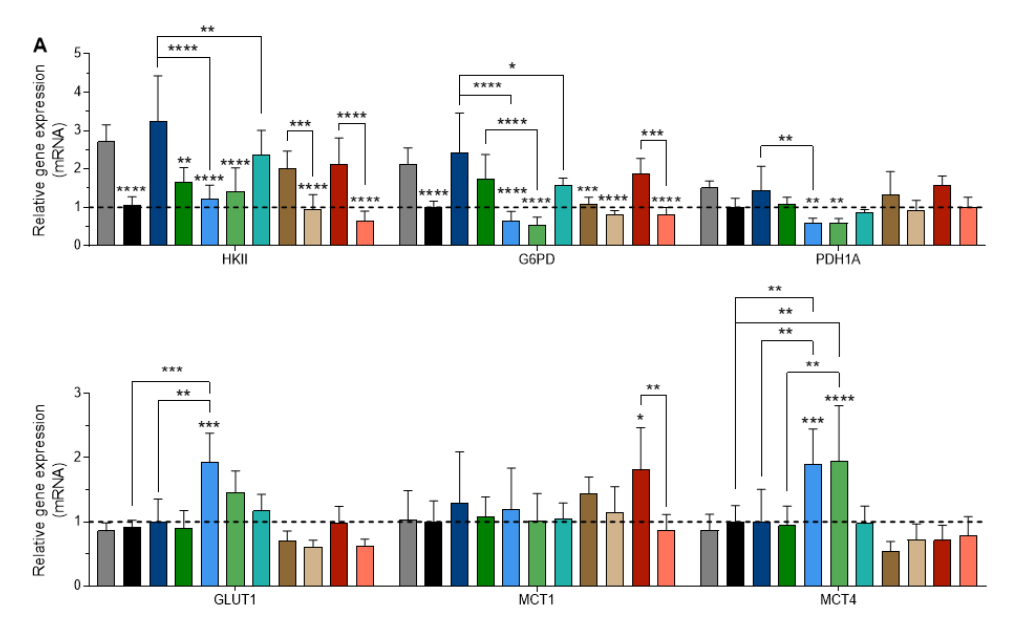


Fig 15. (Continues on the next page)

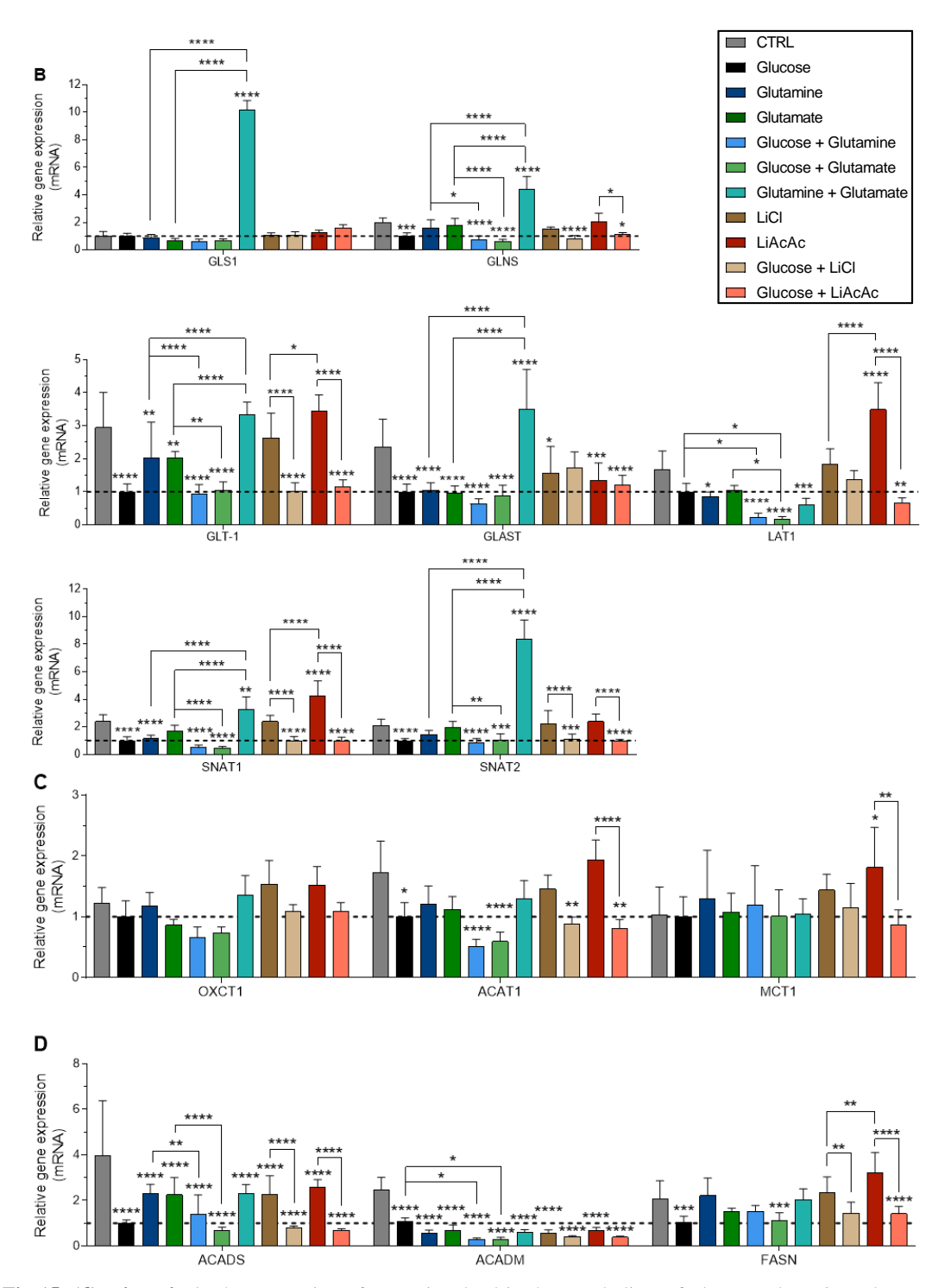


Fig 15. (Continuation) The expression of genes involved in the metabolism of glucose, glutamine, glutamate and acetoacetate (AcAc) is affected by nutrient availability in U-87 cells. We assessed the expression of genes related to (A) glucose metabolism, HKII (Hexokinase 2), G6PD (Glucose-6-Phosphate Dehydrogenase), PDHA1 (Pyruvate Dehydrogenase E1 Subunit Alpha 1), SLC2A1 (Glucose Transporter-1, GLUT1), SLC16A1 (Monocarboxylate Transporter 1, MCT1) and SLC16A4 (Monocarboxylate Transporter 4, MCT4), (B) glutamine/glutamate metabolism, GLS1 (Glutaminase 1), GLNS (Glutamine synthetase), SLC1A2 (Glutamate Transporter 1, GLT-1), SLC1A3 (Glutamate Aspartate Transporter, GLAST), SLC7A5 (L-type amino acid transporter 1, LAT1), SLC38A1 (Sodium-Coupled-Neutral-Amino-Acid-Transporter 2, SNAT2), (C) ketone bodies metabolism OXCT1 (3-Oxoacid CoA-Transferase 1), ACAT1 (Acetyl-CoA Acetyltransferase 1) and MCT1, and (D) lipid metabolism, ACADS (Acyl-CoA Dehydrogenase Short Chain), ACADM (Acyl-CoA Dehydrogenase Medium Chain) and FASN (Fatty Acid Synthase). (Continues on the next page)

Fig 15. (Continuation) Lithium chloride (LiCl) is the control for the potential effects of lithium present in Lithium acetoacetate. Cells were exposed to the experimental conditions for a period of 24 h. Results are shown as mean \pm SD. *p<0.05, **p<0.01, ***p<0.01, ****p<0.001, ****p<0.001.

Gene expression reveals differences between cell lines

To better understand the influence of gene expression (**Fig 14** and **15**) over cellular metabolism we resorted to the open-source software NetworkAnalyst. This software allowed us to obtain a network (**Fig 16** and **17**) that may translate changes in metabolism. Here, we pooled together results from each condition according to cell line and compared it to the CTRL. Even though, we are not able to distinguish between culture conditions, we can see the global metabolic changes that U-251 cells (**Fig 16**) and U-87 cells (**Fig 17**) undergo under the availability of different conditions.

The network analysis revelead differences between cell lines. In U-251 cells (**Fig 16**), we found that the main affected pathways were related to the metabolism of glucose and glutamine/glutamate. The main impacted type of metabolism corresponding to the central carbon metabolism. As such, related pathways, glycolysis and FA metabolism, are also affected, although at a lesser extent, which may suggest a special importance of the metabolism of glucose and glutamine. Furthermore, pathways directly involved in the regulation of glucose metabolism, such as insulin, glucagon and HIF-1 signalling pathways were also affected at the level of gene expression. Regarding, glutamine metabolism in specific, pathways involved with glutamate and GABA were also affected. The synthesis and oxidation of FAs were also influenced by the different culture conditions.

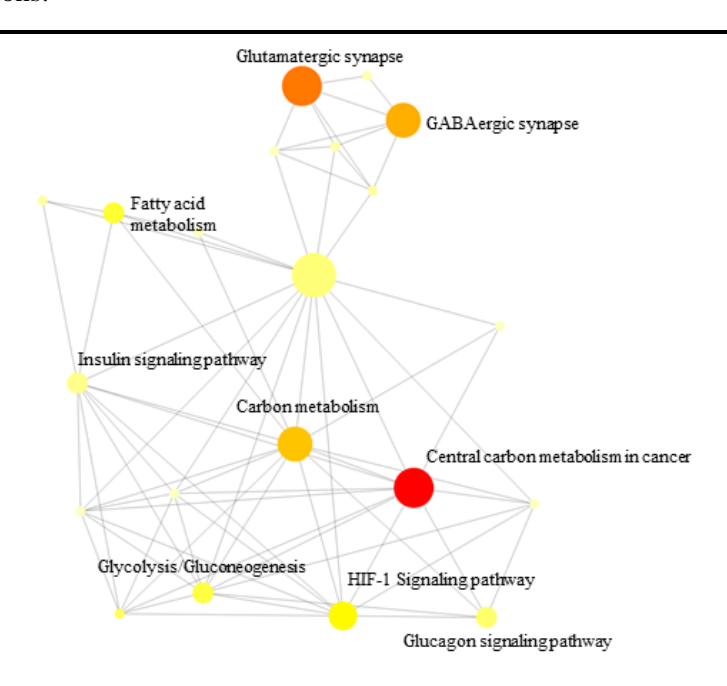


Fig 16. Influenced pathways in U-251 cells are directly linked to the metabolism of glucose and glutamine. (**Continues** on the next page)

Fig 16. (Continuation) This network is a result from the expression pattern of U-251 cells as seen in Fig 14. Genes were considered signficative when p<0.05. Red circles present lower p value and the bigger the circle the higher the importance. Cells were exposed to the experimental conditions for a period of 24 h.

U-87 cells appear to be more influenced than U-251 cells, by nutrient availability, as seen by the number of metabolic pathways (**Fig 17**). In this cell line, the most impacted pathway was glutamatergic synapse. Furthermore, commonly to U-251 cells, central carbon metabolism in cancer, carbon metabolism, insulin signaling pathway, FA metabolism and GABAergic synapse are also affected. Interestingly, the degradation of FAs appears to be important in this cell line. Furthermore, the metabolism of branched-chain amino acids (BCAAs; isoleucine, leucine and valine) was modified.

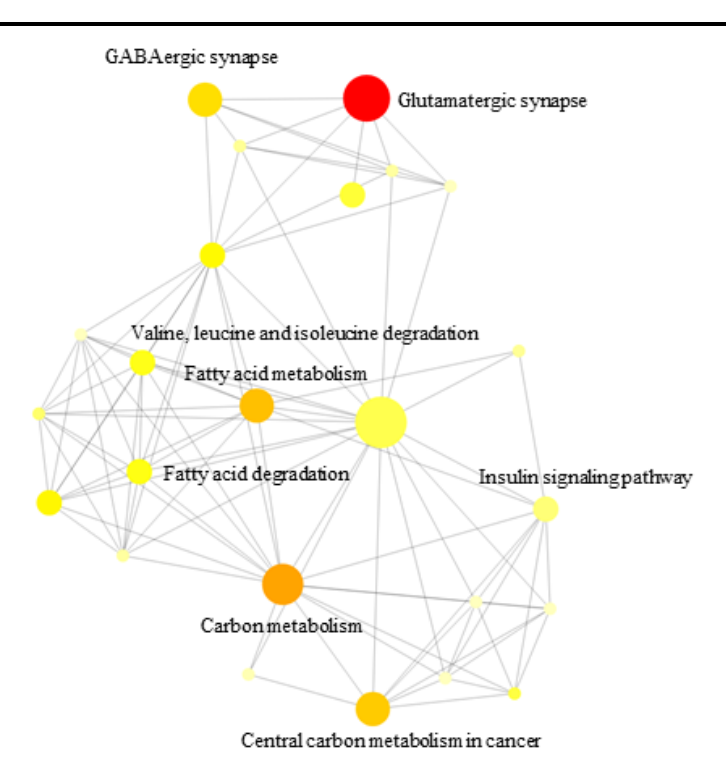


Fig 17. Gene expression of U-87 cells reveal that its metabolism may be more affected than what metabolimic analysis reveal. This network is a result from the expression pattern of U-251 cells as seen in **Fig 15.** Genes were considered significative when p < 0.05. Red circles present lower p value and the bigger the circle the higher the importance. Cells were exposed to the experimental conditions for a period of 24 h.

Discussion

Metabolism and metabolic adaptability are important phenomena of tumors ^{14,15}. Tumor metabolism is a result of cell extrinsic, and intrisinsic factors, and can confer growth advantage to cells ^{15,232}. Furthermore, it is important to consider that the metabolism of tumors is flexible and depends on the systemic and microenvironmental context ¹⁵. As such, at the nutrient level, glucose, glutamine, glutamate and AcAc are interesting in the case of GBMs.

In this thesis, we present an in vitro study exploring the metabolic rewiring of GBM cells upon different bioavailability of nutrients. Our first task was to assess whether nutrient availability affected cellular characteristics such as cell viability/cell death, cell proliferation and migration. Cell death analysis (**Fig 1A**) revealed that GBM cells were adapted to the different conditions. The only decrease in cell viability was observed when LiCl was supplied alone, but it was reverted when LiCl was supplemented in combination with glucose. In this study, we used LiCl as a control for the lithium present in LiAcAc since Vidali *et al.* (2019)²⁵⁵ reported that the anti-cancer properties of LiAcAc may be related to lithium instead of AcAc. Indeed, in LiAcAccontaining conditions total cell death does not increase. This result supports the idea that lithium may have unwanted effects on GBM cells, when utilizing LiAcAc to study the role of KBs in GBMs. Furthermore, as Vidali *et al.* (2019)²⁵⁵ suggested, to avoid these effects, other AcAc derivatives can be useful in this type of study. Nevertheless, more studies are needed to disclose the role of lithium in the control o metabolic adaptation. Since lithium presents a pivotal role in brain functioning, it may impact differently brain cell metabolism, in particular GBM cells.

Continuous proliferation is a considerable complication to tumor cells as there is a continuous need for nutrient uptake^{16,232}. As such, availability of different nutrients might affect the capacity of tumor cells to proliferate. Figure 4 showed that glucose plays a predominant role in sustaining cellular proliferation. However, it only increased proliferative rate when cells were simultaneously presented with glutamine (both cell lines, Fig 4C and H) or glutamate (U251, Fig **4D**). These results indicate that glucose may not be sufficient to completely support the metabolic bioenergetic and biosynthesic needs associated to proliferation, and require glutamine or glutamate for it to occur. These findings are in agreement with the literature. While glucose is being used to sustain biosynthetic needs, through the glycolytic pathway, cells utilize glutamine/glutamate to sustain energetic, and also synthetic, requirements associated to cell proliferation¹⁶. As such, in the control conditions glucose, glutamine and glutamate there is no significant increase in proliferation because these organic compounds have complementary functions in cancer, and are not effective in sustaining proliferation when only one is present. It is also important to state that Duraj et al. (2021)²⁵⁶ have recently demonstrated that GBM cells, including the U-87 cell line, can also be oxidative or change between a glycolytic or oxidative phenotype according to its needs. Accordingly, Figure 13 may, in part, support Duraj et al.

(2021)²⁵⁶ and our assumption that glucose is being oxidized through the glycolytic pathway. In the case of U-251 cells (**Fig 13A and B**), which have been demonstrated to have a glycolytic phenotype²⁵⁷, lactate is produced in significantly higher amounts when glucose is provided, independently of the condition. However, regarding U-87 cells, lactate production remains similar in all conditions. Furthermore, U-251 cells exposed to glucose produce more lactate than U-87 cell line in general. This may be an indicative that the two cell lines present different metabolic profiles, as it was confirmed by the PCA and PLS-DA of NMR profiles (**Fig 7**). In the specific case of extracellular glutamate (*vs* glutamine-derived glutamate) contribution to cell proliferation, this amino acid may not be involved in the TCA cycle. The expression of GLT-1 is described as being impaired in GBM cells, resulting in reduced glutamate uptake²⁵⁸⁻²⁶⁰. Our results are in agreement with this, since the expression of *GLAST* and *GLT-1* are reduced in most conditions (**Fig 14B and Fig 15B**). Therefore, as a result of impaired glutamate uptake, glutamate may instead promote proliferation through metabotropic glutamate receptors (mGlutR)²⁶¹. The metabotropic glutamate receptors are known to promote cell proliferation in GBM²⁶²⁻²⁶⁵, and GBM cell lines, including U-87 and U-251 cells, are known to express this type of receptors^{262,266}.

Cellular migration is a complex, and energetic demanding, process^{267,268}. Furthermore, in case cancer cells invade and metastasize, they are required to adapt to new microenvironmental conditions in order to survive²⁵⁴. Through the wound healing assay (**Fig 5**), we were able to assess how nutrient availability affected cell migration. The results showed us that in the presence of glucose and/or glutamine the migratory capacity of GBM cells was higher. Accordingly, glucose + glutamine achieved the highest percentage of wound closure, in both cell lines. As mentioned, the process of migration can become a pressure to cells in terms of energetic expenditure, especially because of the active cytoskeleton remodelling that occurs during cell motility²⁶⁸. As such, conditions where cells are exposed to an ideal source of energy (i.e. glucose-containing or glutamine-containing conditions), become important for migratory cells. In line with this concept, it was shown that glycolysis plays a predominant role in cell migration of prostate and breast cancer²⁶⁹. In this paper, the authors demonstrated that cell migration was significantly reduced when glycolysis was inhibited, but not when mitochondrial ATP synthesis was. This observation may be also related to the cell membrane alterations needed for cell migration, such as the formation of filopodia and lamellipodia. It is described for endothelial cells that cell migration is mainly sustained by glycolysis, since the membrane structures allowing cell motion cannot shelter mitochondria but glycolytic enzymes are associated to those structures²⁷⁰. Because of this, the participation of glutamine in the TCA cycle as a promoter of cell migration may be excluded. The presence of LiCl and LiAcAc did not affect cell migration, indicating that lithium does not impair cell migration and that AcAc may not be able to fulfil the cellular requirements associated to migration.

Tumor metabolism is a flexible network with adaptive capacity and, according to microenvironmental conditions, it allows tumors to survive in different settings^{15,16}. As such, we wanted to explore how cellular metabolism was influenced by nutrient availability. First, we assessed if the cell lines were able to be identified according to their metabolism. **Figure 7** demonstrated that U-251 cells can be clearly separated from U-87 cells. This observation underscores the metabolic heterogeneity that occurs between tumors of the same type^{271,272}. Furthermore, the fact that nutrient availability was not impactful in this analysis indicates that, at the level of nutrient availability in the TME, the tumor genetic drivers²⁷³ and individual specific features are important and limitative.

In U-251 samples, we were able to identify three main groups of cells/conditions in aqueous (Fig 8A) and supernatant (Fig 8E) samples, glucose-exposed cells, glutamine-exposed cells and cells that were not exposed to either. This result, in combination to cell proliferation and migration results, highlights the importance of glucose and glutamine for U-251 cells, as it was already seen in proliferation favoring conditions. Furthermore, the two distinct groups, glucosecontaining conditions and glutamine-containing conditions, may be a result of their different metabolic fate in this cell line. As previously described, in GBM, glucose is often found to metabolized through the glycolytic pathway and glutamine is used to fuel the TCA cycle. Indeed, Figure 13A and B emphasis the different metabolic fate since lactate is produced in significant higher amounts when glucose is available. The high importance of NAD+ observed in the separation of culture conditions may have diverse interpretations, it may result from glycolysis or other pathways. But most important it shows that those culture conditions favor the maintenance of metabolic feasibility, as NAD+ is essential for keeping metabolism on in different ways, in healthy and cancer cells²⁷⁴. Our results also reinforce the role of PPP in the different metabolic profile of these cell lines, since alanine a product of PPP²⁷⁵ was increased in U-251 cells supplemented with glucose (Fig 8C). Moreover, the dynamics of NAD+ may be an indirect indicative of PPP activity, since NADP+ produced in PPP may be converted into NAD+ depending on the oxidative cellular context and contributing both for cellular redox homeostasis^{276,277}. In pancreatic cancer, NAD kinase, responsible for the conversion of NAD+ into NADP+ is upregulated by oncogenes²⁷⁸. Although, in cancer, the role of NADP⁺ phosphatases, responsible for NADP+-NAD+ conversion, is not explored, it can be a promising research perspective. In mammalian cells MESH1, a NADP⁺ phosphatase, is pointed as relevant in the regulation of the ferroptotic cell death²⁷⁹. Whereas in cancer cells, MESH1 allows them to scape from ferroptosis²⁸⁰, which is a hot topic in cancer that deserves more attention.

Glycine is a pivotal amino acid in cell functioning, since it is an important supplier of one-carbon metabolism and it is a component of glutathione molecule, the main ROS scavenger produced in the cell²⁸¹. Our team has extensively showed the role of glutathione^{172,282–284}, cysteine

and one carbon-metabolism in cancer metabolic remodeling, accounting for survival and chemoresistance. In this study, glycine is increased in cells supplemented with glucose (**Fig 8C**) and decreased in supernatant (**Fig 8D**), suggesting that glycine is really important and it may be produced in the cell but also imported. The relevance of glycine metabolism in gliomas was already stated²⁸⁵, and it has been associated to increased proliferative capacity of glioma cells, which also agrees with our results²⁸⁶. Furthermore, we also show, that its uptake is a relevant step in glycine bioavailability and in all the related pathways functioning. Interestingly, glycine is considered important to sustain survival of glioma cells subjected to glucose²⁸⁷ and glutamine starvation²⁸⁸.

Acetate plays an important role in the regulation of cellular homestasis, since it is directly involved in the maintenance of acetyl-CoA pool by serving as its precursor²⁸⁹. Besides protein deacetylation²⁹⁰, uptake from the extracellular space and other potential sources, acetate can be synthesized de novo from pyruvate²⁹¹. Thus, as reported by Liu et al. (2018)²⁹¹, glucose contributes to the synthesis of acetate. In line with this, Figure 8C shows that cells produce significantly higher amounts of acetate when exposed to glucose. Acetate has important implications in cellular metabolism since it can be used to fuel the TCA cycle and sustain de novo lipogenesis, through the synthesis of acetyl-CoA²⁸⁹. This could, in part, justify the increased proliferation that is seen in U-251 cells when exposed to glucose + glutamine or glutamate (Fig 4B). However, since glucose does not appear to influence lipid dynamics, at the level of gene expression (Fig 14D) and lipidic constituents (Fig 10), the usage of glucose-derived acetate may be focused on sustaining energetic requirements. Indeed, the ability of acetate to sustain the TCA cycle is an alternative route for glucose to enter this pathway, since PDH is often found to be down-regulated or inhibited due to metabolic stress^{34,176,292,293} or to mutated oncogenes (e.g. TP53)²⁹⁴. Apart from cellular metabolism, acetate participates in protein acetylation (including histones), being involved in cellular signalling and regulation of gene expression²⁸⁹. In line with this, acetyl-CoA was demonstrated to be involved in the regulation of genes related to cell migration and adhesion²⁹⁵ and that it can promote migration in GBM cells²⁹⁶. Importantly, these two reports^{295,296} also demonstrated that, under limited glucose conditions, acetyl-CoA concentrations decrease, which might be related to reduced glucose-derived acetate. These observations may justify the significant increase of cellular migration when glucose is supplied together with glutamine. While glucose or glutamine are not enough to promote migration when one is absent, when both organic compounds are available it may lead to a surplus of acetyl-CoA that may be used to promote cell migration. Taken into consideration the roles of acetate in cell functioning, exactly how acetate usage is affected by nutrient availability might be an interesting topic to address.

Unlike U-251 samples, U-87 samples (**Fig 9**), aqueous and supernatant, did not cluster according to a particular nutrient. A reason for this to occur is that the metabolism of U-87 cells may respond similarly to the presence of specific nutrients, being more homogenous/stable/less plastic than the metabolism of U-251 cells. However, we also need to consider that we did not work with enough biomass (consult **Supplementary Table 2** or **3** for weight information). This can lead to lower metabolite concentration in the sample and, therefore, to higher noise-to-signal ratio, making it difficult to correctly identify organic compounds. As such, important metabolites that could help identify potential differences in the metabolism of U-87 might be absent from the results and confirmation might be necessary.

The metabolism of lipids also plays important roles in cancer progression.²⁹⁷ Furthermore, due to the inherent relationship of glucose, glutamine/glutamate and AcAc with the synthesis of lipids, we also assessed the potential impact on lipid dynamics caused by nutrient availability^{98,298}. The oxidation and synthesis of FAs are two opposing processes, though can occur simultaneously. While the first occurs when energy levels are low, the second occurs when the pool of acetyl-CoA is sufficient to support the basic needs of the cell and also lipid synthesis^{297,298}. Furthermore, FAs are involved in the synthesis of structural lipids and, in the form of triglycerides, as energy storage²⁹⁷. At the level of gene expression we found that in U-251 cells (Fig 14D), FA oxidation may be mostly unnafacted (as seen by the expression of ACADS), except in the presence of LiCl or LiAcAc. The increase in the expression of ACADS may suggest that cells are low in energy and are increasing the oxidation of FAs to satisfy their energetic needs. As such, when glucose is added, even though it may not be the ideal energy substrate in our cells, the expression of ACADS returns to control levels. However, CTRL cells are exposed to a more restrictive conditions, which might imply that lithium may be promoting the oxidation of FAs. Regarding the synthesis of FA, we saw that it may increase since the expression of FASN was upregulated in the presence of glutamine. It is known that glutamine can be used to sustain de novo lipogenesis⁸², which might indicate that glutamine is important to meet the metabolic requirements of GBM cells for FA synthesis to occur. This results however, do not fully translate into the organic fraction, of cells exposed to different conditions, as seen in Fig 10 A-E. This figure shows that the dynamics of lipids stays similar to the CTRL, the only exception occurring the phosphatidylcholine (PhCho), which increased in the presence of glutamine, glutamate and LiCl in separate. When other organic compounds were added, PhCho relative levels decreased to CTRL levels. Phosphatidylcholine is an important structural lipid, being one of the most abundant phospholipids in the cell membrane²⁹⁹. Thus, it would be to expect an increase in its synthesis when culture conditions were more favourable (e.g. glucose + glutamine). In the case of U-87 cells (Fig 15D), the expression of genes related to FA oxidation and synthesis decreased in most conditions. However, lipid dynamics at the molecular level did not change. This results should be

explored and further experiments are necessary to better understand the effects of nutrient availability over the metabolism of lipids. All in all, it is necessary to have a more targeted approach to the metabolism of lipids, of both cell lines, since the genes that we covered are only referent to a small part of it.

As mentioned before, the importance of ketone bodies metabolism is yet to be understood. Our results (Table 1) demonstrate that both cell lines are able to uptake AcAc from the extracellular environment, which is expected since MCT1 is found to be upregulated in GBM cells²⁵⁷. Interestingly, while the expression of MCT1 decreased in the presence of glucose + LiAcAc, the transport of AcAc was similar in U-251 (LiAcAc vs glucose + LiAcAc). This indicate that AcAc can be imported through other transporters (e.g. MCT2)⁹⁸ and their expression must be assessed for a better understanding. Regarding the metabolism of AcAc, we found that the enzymes involved in its oxidation and synthesis (ACAT1 and OXCT1) are mostly unnafacted by nutrient availability. Furthermore, we also found, in U251 cells, are able to produce \(\beta \)hydroxybutyrate and it is only present in conditions where AcAc is supplemented. This finding might have two explanations. The first is that AcAc is able to be metabolized, even though, in the opposite direction of acetyl-CoA, to be used as a substrate for energetic and biosynthetic reactions. However, this it is necessary to confirm this against healthy tissue; The second explanation is that β-hydroxybutyrate is being produced as a result of valine metabolism³⁰⁰, and the metabolism of ketone bodies may not be active. This explanation is less likely than the first one, since valine is available in the culture medium (Supplementary Table 1) and it was found in the aqueous extracts of all samples (Supplementary Table 2).

A network analysis of the analyzed genes (**Fig 16 and 17**) revelead information between both cell lines. As previously mentioned, the metabolism of U-251 cells was mainly affected by the presence of glucose and glutamine (**Fig 8**). Accordingly, **Figure 16** shows that the most affected pathways are involved to either glucose and glutamine, or both. Furthermore, all of these pathways are related to their metabolism^{63,298,301–303}. In the network analysis we observed that, at the level of gene expression, U-87 cells is more influenced by nutrient availability, which was not shown by NMR data. Similarly to U-251 the main affected pathways were related to glucose and glutamine. The metabolism of FAs, which was already adressed, appears to be influenced by culture conditions. Finnaly, we also found that the metabolism of BCAAs is affected. Interestingly, this metabolic pathway was described to be important to *IDH* wildtype GBM cells, U-87 cells included^{304,305}.

Conclusions

A common observation in the different results was that U-251 and U-87 were very distinct. In first place, these two cell lines were distinguishable in terms of malignancy. While U-251 cells may present a more agressive phenotype due to increased cell proliferation (Fig 4), U-87 cells are able to migrate more (Fig 5), suggesting that they are able to invade neighbouring tissue with more ease. In second place, metabolism was able to separate both cell lines (Fig 7). Furthermore, we also found that U-251 cells seem to have a higher rate of glycolysis than U-87 cells. This finding highlights the metabolic heterogeneity that is found between tumor types and sub-types^{271–273}, including gliomas, which is attributed to different oncogenic drivers despite the tissue of origin being the same. Another important metabolic pathway highlighted by this study is PPP, which might be predominant in cancer metabolism but it is still underestimated and less understood. Again, one carbon metabolism and the capacity of cancer cells to control oxidative stress are stressed as crucial in cancer cell pathophysiology. The same way the interconversion of NAD⁺↔NADP⁺ and the way it is orchestrated in cancer to allow redox homeostasis, metabolic flow and cell survival, is definitely a very interesting topic that must be pursued. Albeit all of these metabolic observations that must be deeply explored, at the scope of personalized medicine, our study shed one more light on the path, showing that specific individual features and slightly metabolic details can be relevant to follow and treat GBM.

Future Perspectives

The present thesis generated a pool of results that opens new perspectives in the metabolic adaptation of GBM cells. The most interesting queues are ought to be explored as follow:

- Explore in greater detail the role of one-carbon metabolism in GBM. Incorporation of ¹³C-Glucose and ¹³C-Glycine will clarify the importance of glucose-derived glycine and imported glycine to the cell. Also, to study the importance of glycine in cellular characteristics.
- Explore the dynamics of NAD⁺↔NADP⁺ in regards of nutrient availability, in order to disclose the role of main metabolic pathways contributing for this duality and interconversion.
- Study lipid dynamics in a targeted analysis. Complement the NMR results of lipid
 metabolism through mass spectrometry and assess the expression of genes and proteins,
 behind FA synthesis and oxidation, to find the contribution of each metabolic pathway to
 GBM metabolic fitness.
- Clarify the role of the metabolism of ketone bodies in GBM, using 13C labelled compounds in order to follow the panel of ketone bodies-derived organic compounds.

• Explore the role of lithium in the metabolic regulation and GBM pathophysiology, since some alterations were observed in cells cultured with LiCl and because of the pivotal role of lithium in the CNS physiology.

References

- World Health Organization, W. GLOBOCAN 2020: Estimated Cancer Incidence, Mortality and Prevalence Worldwide in 2020. Retrieved at December 1st, 2020 from http://gco.iarc.fr/today/home (2020).
- 2. Alberts, B. et al. Molecular Biology of the Cell. (Garland Science, 2007).
- 3. Benjamin, I., Griggs, R., Wing, E. & Fitz, G. *Andreoli and Carpenter's Cecil Essentials of Medicine*. (Saunders, 2015).
- 4. Coleman, W. B. Neoplasia. in *Molecular Pathology* 71–97 (Elsevier, 2018). doi:10.1016/B978-0-12-802761-5.00004-3.
- 5. Zilhão, R. & Neves, H. Tumor Niche Disruption and Metastasis: The Role of Epithelial-Mesenchymal Transition (EMT). in 159–189 (2019). doi:10.1007/978-3-030-11812-9_9.
- 6. Vogelstein, B. & Kinzler, K. W. Cancer genes and the pathways they control. *Nat. Med.* **10**, 789–799 (2004).
- 7. Flavahan, W. A., Gaskell, E. & Bernstein, B. E. Epigenetic plasticity and the hallmarks of cancer. *Science* (80-.). **357**, eaal2380 (2017).
- 8. Lodish, H. et al. Molecular Cell Biology. (W. H. Freeman and Company, 2016).
- 9. Friedberg, E. C. DNA damage and repair. *Nature* **421**, 436–440 (2003).
- 10. Biswas, S. & Rao, C. M. Epigenetics in cancer: Fundamentals and Beyond. *Pharmacol. Ther.* **173**, 118–134 (2017).
- 11. Nebbioso, A., Tambaro, F. P., Dell'Aversana, C. & Altucci, L. Cancer epigenetics: Moving forward. *PLOS Genet.* **14**, e1007362 (2018).
- 12. Hanahan, D. & Weinberg, R. A. The Hallmarks of Cancer. *Cell* **100**, 57–70 (2000).
- 13. Hanahan, D. & Weinberg, R. A. Hallmarks of Cancer: The Next Generation. *Cell* **144**, 646–674 (2011).
- 14. Fouad, Y. & Aanei, C. Revisiting the hallmarks of cancer. *Am. J. Cancer Res.* **7**, 1016–1036 (2017).
- 15. Faubert, B., Solmonson, A. & DeBerardinis, R. J. Metabolic reprogramming and cancer progression. *Science* (80-.). **368**, (2020).
- 16. De Berardinis, R. J. & Chandel, N. S. Fundamentals of cancer metabolism. *Sci. Adv.* **2**, (2016).
- 17. Pavlova, N. N. & Thompson, C. B. The Emerging Hallmarks of Cancer Metabolism. *Cell Metab.* **23**, 27–47 (2016).
- 18. Kroemer, G. & Pouyssegur, J. Tumor Cell Metabolism: Cancer's Achilles' Heel. *Cancer Cell* **13**, 472–482 (2008).

- 19. Thompson, C. B. Rethinking the Regulation of Cellular Metabolism. *Cold Spring Harb. Symp. Quant. Biol.* **76**, 23–29 (2011).
- 20. Du, Z. & Lovly, C. M. Mechanisms of receptor tyrosine kinase activation in cancer. *Mol. Cancer* **17**, 58 (2018).
- 21. Barthel, A. *et al.* Regulation of GLUT1 Gene Transcription by the Serine/Threonine Kinase Akt1. *J. Biol. Chem.* **274**, 20281–20286 (1999).
- 22. Wieman, H. L., Wofford, J. A. & Rathmell, J. C. Cytokine Stimulation Promotes Glucose Uptake via Phosphatidylinositol-3 Kinase/Akt Regulation of Glut1 Activity and Trafficking. *Mol. Biol. Cell* **18**, 1437–1446 (2007).
- 23. Deprez, J., Vertommen, D., Alessi, D. R., Hue, L. & Rider, M. H. Phosphorylation and Activation of Heart 6-Phosphofructo-2-kinase by Protein Kinase B and Other Protein Kinases of the Insulin Signaling Cascades. *J. Biol. Chem.* **272**, 17269–17275 (1997).
- 24. Gottlob, K. Inhibition of early apoptotic events by Akt/PKB is dependent on the first committed step of glycolysis and mitochondrial hexokinase. *Genes Dev.* **15**, 1406–1418 (2001).
- 25. Harris, A. L. Hypoxia a key regulatory factor in tumour growth. *Nat. Rev. Cancer* **2**, 38–47 (2002).
- Rankin, E. B. & Giaccia, A. J. Hypoxic control of metastasis. *Science* (80-.). 352, 175–180 (2016).
- 27. Rohlenova, K., Veys, K., Miranda-Santos, I., De Bock, K. & Carmeliet, P. Endothelial Cell Metabolism in Health and Disease. *Trends Cell Biol.* **28**, 224–236 (2018).
- 28. Belisario, D. C. *et al.* Hypoxia Dictates Metabolic Rewiring of Tumors: Implications for Chemoresistance. *Cells* **9**, 2598 (2020).
- 29. Al Tameemi, W., Dale, T. P., Al-Jumaily, R. M. K. & Forsyth, N. R. Hypoxia-Modified Cancer Cell Metabolism. *Front. Cell Dev. Biol.* **7**, (2019).
- 30. Semenza, G. L. Hypoxia-inducible factors: mediators of cancer progression and targets for cancer therapy. *Trends Pharmacol. Sci.* **33**, 207–214 (2012).
- 31. Masson, N. & Ratcliffe, P. J. Hypoxia signaling pathways in cancer metabolism: the importance of co-selecting interconnected physiological pathways. *Cancer Metab.* **2**, 3 (2014).
- 32. Samanta, D. & Semenza, G. L. Metabolic adaptation of cancer and immune cells mediated by hypoxia-inducible factors. *Biochim. Biophys. Acta Rev. Cancer* **1870**, 15–22 (2018).
- 33. Moldogazieva, N. T., Mokhosoev, I. M. & Terentiev, A. A. Metabolic Heterogeneity of Cancer Cells: An Interplay between HIF-1, GLUTs, and AMPK. *Cancers (Basel).* **12**, 862 (2020).

- 34. Kim, J., Tchernyshyov, I., Semenza, G. L. & Dang, C. V. HIF-1-mediated expression of pyruvate dehydrogenase kinase: A metabolic switch required for cellular adaptation to hypoxia. *Cell Metab.* **3**, 177–185 (2006).
- 35. Ke, Q. & Costa, M. Hypoxia-Inducible Factor-1 (HIF-1). *Mol. Pharmacol.* **70**, 1469–1480 (2006).
- 36. Semenza, G. L. HIF-1: upstream and downstream of cancer metabolism. *Curr. Opin. Genet. Dev.* **20**, 51–56 (2010).
- 37. Semenza, G. L. HIF-1 mediates metabolic responses to intratumoral hypoxia and oncogenic mutations. *J. Clin. Invest.* **123**, 3664–3671 (2013).
- 38. Elorza, A. *et al.* HIF2α Acts as an mTORC1 Activator through the Amino Acid Carrier SLC7A5. *Mol. Cell* **48**, 681–691 (2012).
- 39. Lu, H. *et al.* Chemotherapy triggers HIF-1–dependent glutathione synthesis and copper chelation that induces the breast cancer stem cell phenotype. *Proc. Natl. Acad. Sci.* **112**, E4600–E4609 (2015).
- 40. Furuta, E. *et al.* Fatty Acid Synthase Gene Is Up-regulated by Hypoxia via Activation of Akt and Sterol Regulatory Element Binding Protein-1. *Cancer Res.* **68**, 1003–1011 (2008).
- 41. Serpa, J. & Dias, S. Metabolic cues from the microenvironment act as a major selective factor for cancer progression and metastases formation. *Cell Cycle* **10**, 180–181 (2011).
- 42. Serpa, J. Metabolic Remodeling as a Way of Adapting to Tumor Microenvironment (TME), a Job of Several Holders. in 1–34 (2020). doi:10.1007/978-3-030-34025-4_1.
- 43. Fischer, K. *et al.* Inhibitory effect of tumor cell–derived lactic acid on human T cells. *Blood* **109**, 3812–3819 (2007).
- 44. Gottfried, E. *et al.* Tumor-derived lactic acid modulates dendritic cell activation and antigen expression. *Blood* **107**, 2013–2021 (2006).
- 45. Sonveaux, P. *et al.* Targeting the Lactate Transporter MCT1 in Endothelial Cells Inhibits Lactate-Induced HIF-1 Activation and Tumor Angiogenesis. *PLoS One* **7**, e33418 (2012).
- 46. Constant, J. S. *et al.* Lactate elicits vascular endothelial growth factor from macrophages: a possible alternative to hypoxia. *Wound Repair Regen.* **8**, 353–360 (2000).
- 47. Whiteside, T. L. The tumor microenvironment and its role in promoting tumor growth. *Oncogene* **27**, 5904–5912 (2008).
- 48. Ostrom, Q. T. *et al.* CBTRUS Statistical Report: Primary Brain and Other Central Nervous System Tumors Diagnosed in the United States in 2012-2016. *Neuro. Oncol.* **21**, V1–V100 (2019).
- 49. Obara-Michlewska, M. & Szeliga, M. Targeting glutamine addiction in Gliomas. *Cancers* (*Basel*). **12**, (2020).

- 50. Colman, H. Adult Gliomas. Contin. Lifelong Learn. Neurol. 26, 1452–1475 (2020).
- 51. Louis, D. N. *et al.* The 2016 World Health Organization Classification of Tumors of the Central Nervous System: a summary. *Acta Neuropathol.* **131**, 803–820 (2016).
- 52. Louis, D. N. *et al.* The 2007 WHO Classification of Tumours of the Central Nervous System. *Acta Neuropathol.* **114**, 97–109 (2007).
- 53. Aquilanti, E., Miller, J., Santagata, S., Cahill, D. P. & Brastianos, P. K. Updates in prognostic markers for gliomas. *Neuro. Oncol.* **20**, vii17–vii26 (2018).
- 54. Hartmann, C. *et al.* Type and frequency of IDH1 and IDH2 mutations are related to astrocytic and oligodendroglial differentiation and age: a study of 1,010 diffuse gliomas. *Acta Neuropathol.* **118**, 469–474 (2009).
- 55. Yao, Q. *et al.* IDH1 mutation diminishes aggressive phenotype in glioma stem cells. *Int. J. Oncol.* (2017) doi:10.3892/ijo.2017.4186.
- 56. KRAUS, J. A. *et al.* Shared Allelic Losses on Chromosomes 1p and 19q Suggest a Common Origin of Oligodendroglioma and Oligoastrocytoma. *J. Neuropathol. Exp. Neurol.* **54**, 91–95 (1995).
- 57. Deimling, A. Von *et al.* Advances in Brief Evidence for a Tumor Suppressor Gene on Chromosome 19q Associated with. *Neuropathology* 4277–4279 (1992).
- 58. Schiff, D. Low-grade Gliomas. Contin. Lifelong Learn. Neurol. 21, 345–354 (2015).
- 59. Jenkins, R. B. *et al.* A t(1;19)(q10;p10) Mediates the Combined Deletions of 1p and 19q and Predicts a Better Prognosis of Patients with Oligodendroglioma. *Cancer Res.* **66**, 9852–9861 (2006).
- 60. KOMORI, T. The 2016 WHO Classification of Tumours of the Central Nervous System: The Major Points of Revision. *Neurol. Med. Chir. (Tokyo).* **57**, 301–311 (2017).
- 61. Brito, C. *et al.* Clinical insights gained by refining the 2016 WHO classification of diffuse gliomas with: EGFR amplification, TERT mutations, PTEN deletion and MGMT methylation. *BMC Cancer* **19**, 968 (2019).
- 62. Hegi, M. E. *et al.* Clinical Trial Substantiates the Predictive Value of O-6-Methylguanine-DNA Methyltransferase Promoter Methylation in Glioblastoma Patients Treated with Temozolomide. *Clin. Cancer Res.* **10**, 1871–1874 (2004).
- 63. Dienel, G. A. Brain Glucose Metabolism: Integration of Energetics with Function. *Physiol. Rev.* **99**, 949–1045 (2019).
- 64. Cahill, G. F. Fuel Metabolism in Starvation. *Annu. Rev. Nutr.* **26**, 1–22 (2006).
- 65. Jensen, N. J., Wodschow, H. Z., Nilsson, M. & Rungby, J. Effects of Ketone Bodies on Brain Metabolism and Function in Neurodegenerative Diseases. *Int. J. Mol. Sci.* **21**, 8767 (2020).

- 66. Camandola, S. & Mattson, M. P. Brain metabolism in health, aging, and neurodegeneration. *EMBO J.* **36**, 1474–1492 (2017).
- 67. Ashrafi, G., Wu, Z., Farrell, R. J. & Ryan, T. A. GLUT4 Mobilization Supports Energetic Demands of Active Synapses. *Neuron* **93**, 606-615.e3 (2017).
- 68. Pearson-Leary, J. & McNay, E. C. Novel Roles for the Insulin-Regulated Glucose Transporter-4 in Hippocampally Dependent Memory. *J. Neurosci.* **36**, 11851–11864 (2016).
- 69. Simpson, I. A., Carruthers, A. & Vannucci, S. J. Supply and Demand in Cerebral Energy Metabolism: The Role of Nutrient Transporters. *J. Cereb. Blood Flow Metab.* **27**, 1766–1791 (2007).
- 70. Itoh, Y. *et al.* Dichloroacetate effects on glucose and lactate oxidation by neurons and astroglia in vitro and on glucose utilization by brain in vivo. *Proc. Natl. Acad. Sci.* **100**, 4879–4884 (2003).
- 71. Herrero-Mendez, A. *et al.* The bioenergetic and antioxidant status of neurons is controlled by continuous degradation of a key glycolytic enzyme by APC/C–Cdh1. *Nat. Cell Biol.* **11**, 747–752 (2009).
- 72. Shi, L., Pan, H., Liu, Z., Xie, J. & Han, W. Roles of PFKFB3 in cancer. *Signal Transduct. Target. Ther.* **2**, 17044 (2017).
- 73. Zhang, Y. *et al.* An RNA-Sequencing Transcriptome and Splicing Database of Glia, Neurons, and Vascular Cells of the Cerebral Cortex. *J. Neurosci.* **34**, 11929–11947 (2014).
- 74. Halim, N. D. *et al.* Phosphorylation status of pyruvate dehydrogenase distinguishes metabolic phenotypes of cultured rat brain astrocytes and neurons. *Glia* **58**, 1168–1176 (2010).
- 75. Bittar, P. G., Charnay, Y., Pellerin, L., Bouras, C. & Magistretti, P. J. Selective Distribution of Lactate Dehydrogenase Isoenzymes in Neurons and Astrocytes of Human Brain. *J. Cereb. Blood Flow Metab.* **16**, 1079–1089 (1996).
- 76. Magistretti, P. J. & Allaman, I. Lactate in the brain: from metabolic end-product to signalling molecule. *Nat. Rev. Neurosci.* **19**, 235–249 (2018).
- 77. Pellerin, L. & Magistretti, P. J. Glutamate uptake into astrocytes stimulates aerobic glycolysis: a mechanism coupling neuronal activity to glucose utilization. *Proc. Natl. Acad. Sci.* **91**, 10625–10629 (1994).
- 78. Laughton, J. D. *et al.* Metabolic compartmentalization in the human cortex and hippocampus: evidence for a cell- and region-specific localization of lactate dehydrogenase 5 and pyruvate dehydrogenase. *BMC Neurosci.* **8**, 35 (2007).
- 79. Morgenthaler, F. D., Kraftsik, R., Catsicas, S., Magistretti, P. J. & Chatton, J.-Y. Glucose

- and lactate are equally effective in energizing activity-dependent synaptic vesicle turnover in purified cortical neurons. *Neuroscience* **141**, 157–165 (2006).
- 80. Rouach, N., Koulakoff, A., Abudara, V., Willecke, K. & Giaume, C. Astroglial Metabolic Networks Sustain Hippocampal Synaptic Transmission. *Science* (80-.). **322**, 1551–1555 (2008).
- 81. Sada, N., Lee, S., Katsu, T., Otsuki, T. & Inoue, T. Targeting LDH enzymes with a stiripentol analog to treat epilepsy. *Science* (80-.). **347**, 1362–1367 (2015).
- 82. Altman, B. J., Stine, Z. E. & Dang, C. V. From Krebs to clinic: Glutamine metabolism to cancer therapy. *Nat. Rev. Cancer* **16**, 619–634 (2016).
- 83. DeBerardinis, R. J. *et al.* Beyond aerobic glycolysis: Transformed cells can engage in glutamine metabolism that exceeds the requirement for protein and nucleotide synthesis. *Proc. Natl. Acad. Sci. U. S. A.* **104**, 19345–19350 (2007).
- 84. Bassi, M. *et al.* Identification and characterisation of human xCT that co-expresses, with 4F2 heavy chain, the amino acid transport activity system x c -. *Pfl* egers Arch. Eur. J. *Physiol.* 442, 286–296 (2001).
- 85. Conrad, M. & Sato, H. The oxidative stress-inducible cystine/glutamate antiporter, system x c -: cystine supplier and beyond. *Amino Acids* **42**, 231–246 (2012).
- 86. Cluntun, A. A., Lukey, M. J., Cerione, R. A. & Locasale, J. W. Glutamine Metabolism in Cancer: Understanding the Heterogeneity. *Trends in Cancer* **3**, 169–180 (2017).
- 87. Curi, R. *et al.* Molecular mechanisms of glutamine action. *J. Cell. Physiol.* **204**, 392–401 (2005).
- 88. Hamberger, A., Nyström, B., Larsson, S., Silfvenius, H. & Nordborg, C. Amino acids in the neuronal microenvironment of focal human epileptic lesions. *Epilepsy Res.* **9**, 32–43 (1991).
- 89. Natarajan, S. K. & Venneti, S. Glutamine metabolism in brain tumors. *Cancers (Basel)*. **11**, (2019).
- 90. Martins, F., Gonçalves, L. G., Pojo, M. & Serpa, J. Take advantage of glutamine anaplerosis, the kernel of the metabolic rewiring in malignant gliomas. *Biomolecules* **10**, 1–25 (2020).
- 91. Bak, L. K., Schousboe, A. & Waagepetersen, H. S. The glutamate/GABA-glutamine cycle: aspects of transport, neurotransmitter homeostasis and ammonia transfer. *J. Neurochem.* **98**, 641–653 (2006).
- 92. Lanciotti, A. *et al.* Astrocytes: Emerging stars in leukodystrophy pathogenesis. *Transl. Neurosci.* **4**, (2013).
- 93. Martinez-Hernandez, A., Bell, K. & Norenberg, M. Glutamine synthetase: glial

- localization in brain. Science (80-.). 195, 1356–1358 (1977).
- 94. Yu, A. C. H., Drejer, J., Hertz, L. & Schousboe, A. Pyruvate Carboxylase Activity in Primary Cultures of Astrocytes and Neurons. *J. Neurochem.* **41**, 1484–1487 (1983).
- 95. Rothstein, J. D. *et al.* Knockout of Glutamate Transporters Reveals a Major Role for Astroglial Transport in Excitotoxicity and Clearance of Glutamate. *Neuron* **16**, 675–686 (1996).
- 96. Rothman, D. L., Behar, K. L., Hyder, F. & Shulman, R. G. In vivo NMR Studies of the Glutamate Neurotransmitter Flux and Neuroenergetics: Implications for Brain Function. *Annu. Rev. Physiol.* **65**, 401–427 (2003).
- 97. Lieth, E. *et al.* Nitrogen shuttling between neurons and glial cells during glutamate synthesis. *J. Neurochem.* **76**, 1712–1723 (2001).
- 98. Grabacka, M., Pierzchalska, M., Dean, M. & Reiss, K. Regulation of ketone body metabolism and the role of PPARα. *Int. J. Mol. Sci.* 17, (2016).
- 99. Puchalska, P. & Crawford, P. A. Multi-dimensional Roles of Ketone Bodies in Fuel Metabolism, Signaling, and Therapeutics. *Cell Metab.* **25**, 262–284 (2017).
- McGarry, J. D. & Foster, D. W. Regulation of Hepatic Fatty Acid Oxidation and Ketone Body Production. *Annu. Rev. Biochem.* 49, 395–420 (1980).
- 101. Owen, O. E. *et al.* Brain metabolism during fasting. *J. Clin. Invest.* **46**, 1589–1595 (1967).
- 102. Newman, J. C. & Verdin, E. Ketone bodies as signaling metabolites. *Trends Endocrinol. Metab.* **25**, 42–52 (2014).
- 103. Yang, H., Shan, W., Zhu, F., Wu, J. & Wang, Q. Ketone Bodies in Neurological Diseases: Focus on Neuroprotection and Underlying Mechanisms. *Front. Neurol.* **10**, (2019).
- 104. Bröer, S. et al. Comparison of Lactate Transport in Astroglial Cells and Monocarboxylate Transporter 1 (MCT 1) Expressing Xenopus laevis Oocytes. J. Biol. Chem. 272, 30096–30102 (1997).
- 105. Lee, Y. *et al.* Oligodendroglia metabolically support axons and contribute to neurodegeneration. *Nature* **487**, 443–448 (2012).
- 106. Moreira, T. J. et al. Enhanced Cerebral Expression of MCT1 and MCT2 in a Rat Ischemia Model Occurs in Activated Microglial Cells. J. Cereb. Blood Flow Metab. 29, 1273–1283 (2009).
- 107. Clouet, P. M. & Bourre, J.-M. Ketone Body Utilization for Lipid Synthesis in the Murine Sciatic Nerve: Alterations in the Dysmyelinating Trembler Mutant. *J. Neurochem.* **50**, 1494–1497 (1988).
- 108. Patel, M. S. & Owen, O. E. Effect of hyperphenylalaninaemia on lipid synthesis from ketone bodies by rat brain. *Biochem. J.* **154**, 319–325 (1976).

- 109. Taggart, A. K. P. *et al.* (d)-β-Hydroxybutyrate Inhibits Adipocyte Lipolysis via the Nicotinic Acid Receptor PUMA-G. *J. Biol. Chem.* **280**, 26649–26652 (2005).
- 110. Kimura, I. *et al.* Short-chain fatty acids and ketones directly regulate sympathetic nervous system via G protein-coupled receptor 41 (GPR41). *Proc. Natl. Acad. Sci.* **108**, 8030–8035 (2011).
- 111. Shimazu, T. *et al.* Suppression of Oxidative Stress by -Hydroxybutyrate, an Endogenous Histone Deacetylase Inhibitor. *Science* (80-.). **339**, 211–214 (2013).
- 112. Prins, M. L., Fujima, L. S. & Hovda, D. A. Age-dependent reduction of cortical contusion volume by ketones after traumatic brain injury. *J. Neurosci. Res.* **82**, 413–420 (2005).
- 113. White, H. & Venkatesh, B. Clinical review: Ketones and brain injury. *Crit. Care* **15**, 219 (2011).
- 114. Hegardt, F. G. Mitochondrial 3-hydroxy-3-methylglutaryl-CoA synthase: a control enzyme in ketogenesis. *Biochem. J.* **338** (**Pt** 3, 569–82 (1999).
- 115. Wolfrum, C., Asilmaz, E., Luca, E., Friedman, J. M. & Stoffel, M. Foxa2 regulates lipid metabolism and ketogenesis in the liver during fasting and in diabetes. *Nature* **432**, 1027–1032 (2004).
- 116. Wolfrum, C., Besser, D., Luca, E. & Stoffel, M. Insulin regulates the activity of forkhead transcription factor Hnf-3/Foxa-2 by Akt-mediated phosphorylation and nuclear/cytosolic localization. *Proc. Natl. Acad. Sci.* **100**, 11624–11629 (2003).
- 117. von Meyenn, F. *et al.* Glucagon-Induced Acetylation of Foxa2 Regulates Hepatic Lipid Metabolism. *Cell Metab.* **17**, 436–447 (2013).
- 118. McGarry, J. D. & Foster, D. W. Regulation of ketogenesis and clinical aspects of the ketotic state. *Metabolism* **21**, 471–489 (1972).
- 119. Schade, D. S. & Philip Eaton, R. Modulation of Fatty Acid Metabolism by Glucagon in Man: II. Effects in Insulin-deficient Diabetics. *Diabetes* **24**, 510–515 (1975).
- 120. Sengupta, S., Peterson, T. R., Laplante, M., Oh, S. & Sabatini, D. M. mTORC1 controls fasting-induced ketogenesis and its modulation by ageing. *Nature* **468**, 1100–1104 (2010).
- 121. Badman, M. K. *et al.* Hepatic Fibroblast Growth Factor 21 Is Regulated by PPARα and Is a Key Mediator of Hepatic Lipid Metabolism in Ketotic States. *Cell Metab.* **5**, 426–437 (2007).
- 122. Shimazu, T. *et al.* SIRT3 Deacetylates Mitochondrial 3-Hydroxy-3-Methylglutaryl CoA Synthase 2 and Regulates Ketone Body Production. *Cell Metab.* **12**, 654–661 (2010).
- 123. QUANT, P. A., TUBBS, P. K. & BRAND, M. D. Glucagon activates mitochondrial 3-hydroxy-3-methylglutaryl-CoA synthase in vivo by decreasing the extent of succinylation of the enzyme. *Eur. J. Biochem.* **187**, 169–174 (1990).

- Turko, I. V., Marcondes, S. & Murad, F. Diabetes-associated nitration of tyrosine and inactivation of succinyl-CoA:3-oxoacid CoA-transferase. *Am. J. Physiol. Circ. Physiol.* 281, H2289–H2294 (2001).
- 125. Strickland, M. & Stoll, E. A. Metabolic Reprogramming in Glioma. *Front. Cell Dev. Biol.* 5, (2017).
- 126. Bi, J. *et al.* Altered cellular metabolism in gliomas an emerging landscape of actionable co-dependency targets. *Nat. Rev. Cancer* **20**, 57–70 (2020).
- 127. Cloughesy, T. F., Cavenee, W. K. & Mischel, P. S. Glioblastoma: From Molecular Pathology to Targeted Treatment. *Annu. Rev. Pathol. Mech. Dis.* **9**, 1–25 (2014).
- 128. Lunt, S. Y. & Vander Heiden, M. G. Aerobic Glycolysis: Meeting the Metabolic Requirements of Cell Proliferation. *Annu. Rev. Cell Dev. Biol.* 27, 441–464 (2011).
- 129. Koppenol, W. H., Bounds, P. L. & Dang, C. V. Otto Warburg's contributions to current concepts of cancer metabolism. *Nat. Rev. Cancer* 11, 325–337 (2011).
- 130. Ramos-Martinez, J. I. The regulation of the pentose phosphate pathway: Remember Krebs. *Arch. Biochem. Biophys.* **614**, 50–52 (2017).
- 131. Jin, L. & Zhou, Y. Crucial role of the pentose phosphate pathway in malignant tumors (Review). *Oncol. Lett.* (2019) doi:10.3892/ol.2019.10112.
- 132. Stincone, A. *et al.* The return of metabolism: biochemistry and physiology of the pentose phosphate pathway. *Biol. Rev.* **90**, 927–963 (2015).
- 133. Patra, K. C. & Hay, N. The pentose phosphate pathway and cancer. *Trends Biochem. Sci.* **39**, 347–354 (2014).
- 134. Ahmad, F. *et al.* Nrf2-driven TERT regulates pentose phosphate pathway in glioblastoma. *Cell Death Dis.* **7**, e2213–e2213 (2016).
- 135. Kathagen-Buhmann, A. *et al.* Glycolysis and the pentose phosphate pathway are differentially associated with the dichotomous regulation of glioblastoma cell migration versus proliferation. *Neuro. Oncol.* **18**, 1219–1229 (2016).
- 136. Marin-Valencia, I. et al. Analysis of Tumor Metabolism Reveals Mitochondrial Glucose Oxidation in Genetically Diverse Human Glioblastomas in the Mouse Brain In Vivo. Cell Metab. 15, 827–837 (2012).
- 137. Koh, H.-J. *et al.* Cytosolic NADP+-dependent Isocitrate Dehydrogenase Plays a Key Role in Lipid Metabolism. *J. Biol. Chem.* **279**, 39968–39974 (2004).
- Badur, M. G. *et al.* Oncogenic R132 IDH1 Mutations Limit NADPH for De Novo Lipogenesis through (D)2-Hydroxyglutarate Production in Fibrosarcoma Cells. *Cell Rep.* 25, 1018-1026.e4 (2018).
- 139. Lee, S. -H. et al. Role of NADP + -dependent isocitrate dehydrogenase (NADP + -ICDH)

- on cellular defence against oxidative injury by γ -rays. *Int. J. Radiat. Biol.* **80**, 635–642 (2004).
- 140. Dang, L., Yen, K. & Attar, E. C. IDH mutations in cancer and progress toward development of targeted therapeutics. *Ann. Oncol.* **27**, 599–608 (2016).
- 141. Parker, S. J. & Metallo, C. M. Metabolic consequences of oncogenic IDH mutations. *Pharmacol. Ther.* **152**, 54–62 (2015).
- 142. Watanabe, T., Nobusawa, S., Kleihues, P. & Ohgaki, H. IDH1 Mutations Are Early Events in the Development of Astrocytomas and Oligodendrogliomas. *Am. J. Pathol.* **174**, 1149–1153 (2009).
- 143. Parsons, D. W. *et al.* An Integrated Genomic Analysis of Human Glioblastoma Multiforme. *Science* (80-.). **321**, 1807–1812 (2008).
- 144. Comprehensive, Integrative Genomic Analysis of Diffuse Lower-Grade Gliomas. *N. Engl. J. Med.* **372**, 2481–2498 (2015).
- 145. Losman, J.-A. & Kaelin, W. G. What a difference a hydroxyl makes: mutant IDH, (R)-2-hydroxyglutarate, and cancer. *Genes Dev.* **27**, 836–852 (2013).
- 146. Prensner, J. R. & Chinnaiyan, A. M. Metabolism unhinged: IDH mutations in cancer. *Nat. Med.* **17**, 291–293 (2011).
- 147. Han, S. *et al.* IDH mutation in glioma: molecular mechanisms and potential therapeutic targets. *Br. J. Cancer* **122**, 1580–1589 (2020).
- 148. Reitman, Z. J. *et al.* Profiling the effects of isocitrate dehydrogenase 1 and 2 mutations on the cellular metabolome. *Proc. Natl. Acad. Sci.* **108**, 3270–3275 (2011).
- 149. Biswas, S., Lunec, J. & Bartlett, K. Non-glucose metabolism in cancer cells—is it all in the fat? *Cancer Metastasis Rev.* **31**, 689–698 (2012).
- 150. Che, L. *et al.* Pathogenetic, Prognostic, and Therapeutic Role of Fatty Acid Synthase in Human Hepatocellular Carcinoma. *Front. Oncol.* **9**, (2019).
- 151. Ohka, F. *et al.* Quantitative metabolome analysis profiles activation of glutaminolysis in glioma with IDH1 mutation. *Tumor Biol.* **35**, 5911–5920 (2014).
- 152. Maus, A. & Peters, G. J. Glutamate and α -ketoglutarate: key players in glioma metabolism. *Amino Acids* **49**, 21–32 (2017).
- 153. Hensley, C. T. *et al.* Glutamine and cancer: cell biology, physiology, and clinical opportunities Find the latest version: Review series Glutamine and cancer: cell biology, physiology, and clinical opportunities. *J. Clin. Invest.* **123**, 3678–3684 (2013).
- 154. Zhao, S. *et al.* Glioma-Derived Mutations in IDH1 Dominantly Inhibit IDH1 Catalytic Activity and Induce HIF-1. *Science* (80-.). **324**, 261–265 (2009).
- 155. Mulukutla, B. C., Yongky, A., Le, T., Mashek, D. G. & Hu, W.-S. Regulation of Glucose

- Metabolism A Perspective From Cell Bioprocessing. *Trends Biotechnol.* **34**, 638–651 (2016).
- 156. Hay, N. Reprogramming glucose metabolism in cancer: can it be exploited for cancer therapy? *Nat. Rev. Cancer* **16**, 635–649 (2016).
- 157. DeBerardinis, R. J., Lum, J. J., Hatzivassiliou, G. & Thompson, C. B. The Biology of Cancer: Metabolic Reprogramming Fuels Cell Growth and Proliferation. *Cell Metab.* 7, 11–20 (2008).
- 158. Zhao, L., Mao, Y., Zhao, Y., Cao, Y. & Chen, X. Role of multifaceted regulators in cancer glucose metabolism and their clinical significance. *Oncotarget* **7**, 31572–31585 (2016).
- 159. Li, X. *et al.* PI3K/Akt/mTOR signaling pathway and targeted therapy for glioblastoma. *Oncotarget* **7**, 33440–33450 (2016).
- 160. Le Rhun, E. *et al.* Molecular targeted therapy of glioblastoma. *Cancer Treat. Rev.* **80**, 101896 (2019).
- 161. Cairns, R. A., Harris, I. S. & Mak, T. W. Regulation of cancer cell metabolism. *Nat. Rev. Cancer* 11, 85–95 (2011).
- 162. Edinger, A. L. & Thompson, C. B. Akt Maintains Cell Size and Survival by Increasing mTOR-dependent Nutrient Uptake. *Mol. Biol. Cell* 13, 2276–2288 (2002).
- 163. Chen, J.-Q. & Russo, J. Dysregulation of glucose transport, glycolysis, TCA cycle and glutaminolysis by oncogenes and tumor suppressors in cancer cells. *Biochim. Biophys. Acta Rev. Cancer* **1826**, 370–384 (2012).
- 164. Yang, H., Zhong, J.-T., Zhou, S.-H. & Han, H.-M. Roles of GLUT-1 and HK-II expression in the biological behavior of head and neck cancer. *Oncotarget* **10**, 3066–3083 (2019).
- 165. Brahimi-Horn, M. C., Chiche, J. & Pouysségur, J. Hypoxia and cancer. *J. Mol. Med.* **85**, 1301–1307 (2007).
- 166. Bhutia, Y. D. & Ganapathy, V. Glutamine transporters in mammalian cells and their functions in physiology and cancer. *Biochim. Biophys. Acta Mol. Cell Res.* **1863**, 2531–2539 (2016).
- 167. Mates, J. M. *et al.* Glutaminase Isoenzymes as Key Regulators in Metabolic and Oxidative Stress Against Cancer. *Curr. Mol. Med.* **13**, 514–534 (2013).
- Szeliga, M., Sidoryk, M., Matyja, E., Kowalczyk, P. & Albrecht, J. Lack of expression of the liver-type glutaminase (LGA) mRNA in human malignant gliomas. *Neurosci. Lett.* 374, 171–173 (2005).
- 169. Szeliga, M., Bogacińska-Karaś, M., Kuźmicz, K., Rola, R. & Albrecht, J. Downregulation of GLS2 in glioblastoma cells is related to DNA hypermethylation but not to the p53 status. *Mol. Carcinog.* **55**, 1309–1316 (2016).

- 170. Mukherjee, P. *et al.* Therapeutic benefit of combining calorie-restricted ketogenic diet and glutamine targeting in late-stage experimental glioblastoma. *Commun. Biol.* **2**, 200 (2019).
- 171. Santos, I. *et al.* Targeting Glutathione and Cystathionine β-Synthase in Ovarian Cancer Treatment by Selenium–Chrysin Polyurea Dendrimer Nanoformulation. *Nutrients* **11**, 2523 (2019).
- 172. Nunes, S. & Serpa, J. Glutathione in Ovarian Cancer: A Double-Edged Sword. *Int. J. Mol. Sci.* **19**, 1882 (2018).
- 173. Tardito, S. *et al.* Glutamine synthetase activity fuels nucleotide biosynthesis and supports growth of glutamine-restricted glioblastoma. *Nat. Cell Biol.* **17**, 1556–1568 (2015).
- 174. Kobayashi, M. *et al.* Differences in accumulation and the transport mechanism of 1- and d-methionine in high- and low-grade human glioma cells. *Nucl. Med. Biol.* **44**, 78–82 (2017).
- 175. Sidoryk, M. *et al.* Increased expression of a glutamine transporter SNAT3 is a marker of malignant gliomas. *Neuroreport* **15**, 575–578 (2004).
- 176. Gao, P. *et al.* C-Myc suppression of miR-23a/b enhances mitochondrial glutaminase expression and glutamine metabolism. *Nature* **458**, 762–765 (2009).
- 177. Wise, D. R. *et al.* Myc regulates a transcriptional program that stimulates mitochondrial glutaminolysis and leads to glutamine addiction. *Proc. Natl. Acad. Sci.* **105**, 18782–18787 (2008).
- 178. Weinberg, F. *et al.* Mitochondrial metabolism and ROS generation are essential for Krasmediated tumorigenicity. *Proc. Natl. Acad. Sci.* **107**, 8788–8793 (2010).
- 179. Gaglio, D., Soldati, C., Vanoni, M., Alberghina, L. & Chiaradonna, F. Glutamine Deprivation Induces Abortive S-Phase Rescued by Deoxyribonucleotides in K-Ras Transformed Fibroblasts. *PLoS One* **4**, e4715 (2009).
- 180. Gaglio, D. *et al.* Oncogenic K-Ras decouples glucose and glutamine metabolism to support cancer cell growth. *Mol. Syst. Biol.* **7**, 523 (2011).
- 181. Carr, E. L. *et al.* Glutamine Uptake and Metabolism Are Coordinately Regulated by ERK/MAPK during T Lymphocyte Activation. *J. Immunol.* **185**, 1037–1044 (2010).
- 182. Bryant, K. L., Mancias, J. D., Kimmelman, A. C. & Der, C. J. KRAS: feeding pancreatic cancer proliferation. *Trends Biochem. Sci.* **39**, 91–100 (2014).
- 183. Galan-Cobo, A. *et al.* LKB1 and KEAP1/NRF2 Pathways Cooperatively Promote Metabolic Reprogramming with Enhanced Glutamine Dependence in KRAS -Mutant Lung Adenocarcinoma. *Cancer Res.* **79**, 3251–3267 (2019).
- 184. Garcia-Cao, I. *et al.* Systemic Elevation of PTEN Induces a Tumor-Suppressive Metabolic State. *Cell* **149**, 49–62 (2012).

- 185. Suzuki, S. *et al.* Phosphate-activated glutaminase (GLS2), a p53-inducible regulator of glutamine metabolism and reactive oxygen species. *Proc. Natl. Acad. Sci.* **107**, 7461–7466 (2010).
- 186. Reynolds, M. R. *et al.* Control of glutamine metabolism by the tumor suppressor Rb. *Oncogene* **33**, 556–566 (2014).
- 187. Poduslo, S. E. Induction of ketone body enzymes in glial cells. *Arch. Biochem. Biophys.* **272**, 318–322 (1989).
- 188. Fredericks, M. & Ramsey, R. B. 3-Oxo acid coenzyme A transferase activity in brain and tumors of the nervous system. *J. Neurochem.* **31**, 1529–1531 (1978).
- 189. Maurer, G. D. *et al.* Differential utilization of ketone bodies by neurons and glioma cell lines: A rationale for ketogenic diet as experimental glioma therapy. *BMC Cancer* 11, (2011).
- 190. Patel, M. S., Russell, J. J. & Gershman, H. Ketone-body metabolism in glioma and neuroblastoma cells. *Proc. Natl. Acad. Sci.* **78**, 7214–7218 (1981).
- 191. Eloqayli, H., Melø, T. M., Haukvik, A. & Sonnewald, U. β-hydroxybutyrate metabolism in astrocytes and C6 glioblastoma cells. *Neurochem. Res.* **36**, 1566–1573 (2011).
- 192. De Feyter, H. M. *et al.* A ketogenic diet increases transport and oxidation of ketone bodies in RG2 and 9L gliomas without affecting tumor growth. *Neuro. Oncol.* **18**, 1079–1087 (2016).
- Chang, H. T., Olson, L. & Schwartz, K. A. Ketolytic and glycolytic enzymatic expression profiles in malignant gliomas: implication for ketogenic diet therapy. *Nutr. Metab. (Lond)*. 10, 47 (2013).
- 194. Poff, A. *et al.* Targeting the Warburg effect for cancer treatment: Ketogenic diets for management of glioma. *Semin. Cancer Biol.* **56**, 135–148 (2019).
- 195. Allen, B. G. *et al.* Ketogenic Diets Enhance Oxidative Stress and Radio-Chemo-Therapy Responses in Lung Cancer Xenografts. *Clin. Cancer Res.* **19**, 3905–3913 (2013).
- 196. Stafford, P. et al. The ketogenic diet reverses gene expression patterns and reduces reactive oxygen species levels when used as an adjuvant therapy for glioma. Nutr. Metab. (Lond).
 7, 74 (2010).
- 197. Lussier, D. M. *et al.* Enhanced immunity in a mouse model of malignant glioma is mediated by a therapeutic ketogenic diet. *BMC Cancer* **16**, 310 (2016).
- 198. Xia, S. *et al.* Prevention of Dietary-Fat-Fueled Ketogenesis Attenuates BRAF V600E Tumor Growth. *Cell Metab.* **25**, 358–373 (2017).
- 199. Bonuccelli, G. *et al.* Ketones and lactate "fuel" tumor growth and metastasis. *Cell Cycle* **9**, 3506–3514 (2010).

- 200. Stupp, R. *et al.* Radiotherapy plus Concomitant and Adjuvant Temozolomide for Glioblastoma. *N. Engl. J. Med.* **352**, 987–996 (2005).
- 201. Haj, A. *et al.* Extent of Resection in Newly Diagnosed Glioblastoma: Impact of a Specialized Neuro-Oncology Care Center. *Brain Sci.* **8**, 5 (2017).
- 202. Rajesh, Y. *et al.* Insights into molecular therapy of glioma: current challenges and next generation blueprint. *Acta Pharmacol. Sin.* **38**, 591–613 (2017).
- 203. Tanase, C. *et al.* Anti-cancer Therapies in High Grade Gliomas. *Curr. Proteomics* **10**, 246–260 (2013).
- 204. Bush, N. A. O., Chang, S. M. & Berger, M. S. Current and future strategies for treatment of glioma. *Neurosurg. Rev.* **40**, 1–14 (2017).
- 205. Stupp, R. et al. Effect of Tumor-Treating Fields Plus Maintenance Temozolomide vs Maintenance Temozolomide Alone on Survival in Patients With Glioblastoma. JAMA 318, 2306 (2017).
- 206. Stupp, R. *et al.* Maintenance Therapy With Tumor-Treating Fields Plus Temozolomide vs Temozolomide Alone for Glioblastoma. *JAMA* **314**, 2535 (2015).
- 207. Chinot, O. L. *et al.* Bevacizumab plus Radiotherapy–Temozolomide for Newly Diagnosed Glioblastoma. *N. Engl. J. Med.* **370**, 709–722 (2014).
- 208. Gilbert, M. R. *et al.* A Randomized Trial of Bevacizumab for Newly Diagnosed Glioblastoma. *N. Engl. J. Med.* **370**, 699–708 (2014).
- 209. Norden, A. D. *et al.* Bevacizumab for recurrent malignant gliomas: Efficacy, toxicity, and patterns of recurrence. *Neurology* **70**, 779–787 (2008).
- 210. Mathupala, S. P., Ko, Y. H. & Pedersen, P. L. Hexokinase-2 bound to mitochondria: Cancer's stygian link to the "Warburg effect" and a pivotal target for effective therapy. *Semin. Cancer Biol.* **19**, 17–24 (2009).
- 211. Zhao, S. *et al.* miR-143 inhibits glycolysis and depletes stemness of glioblastoma stem-like cells. *Cancer Lett.* **333**, 253–260 (2013).
- 212. Boado, R. J., Black, K. L. & Pardridge, W. M. Gene expression of GLUT3 and GLUT1 glucose transporters in human brain tumors. *Mol. Brain Res.* 27, 51–57 (1994).
- 213. Guo, H. *et al.* miRNA-451 inhibits glioma cell proliferation and invasion by downregulating glucose transporter 1. *Tumor Biol.* **37**, 13751–13761 (2016).
- 214. Han, W., Shi, J., Cao, J., Dong, B. & Guan, W. Emerging Roles and Therapeutic Interventions of Aerobic Glycolysis in Glioma. *Onco. Targets. Ther.* **Volume 13**, 6937–6955 (2020).
- 215. Cheng, T. *et al.* Pyruvate carboxylase is required for glutamine-independent growth of tumor cells. *Proc. Natl. Acad. Sci.* **108**, 8674–8679 (2011).

- 216. Martín-Rufián, M. *et al.* Both GLS silencing and GLS2 overexpression synergize with oxidative stress against proliferation of glioma cells. *J. Mol. Med.* **92**, 277–290 (2014).
- 217. Franceschi, S. *et al.* Mitochondrial enzyme GLUD2 plays a critical role in glioblastoma progression. *EBioMedicine* **37**, 56–67 (2018).
- 218. Majewska, E., Márquez, J., Albrecht, J. & Szeliga, M. Transfection with GLS2 Glutaminase (GAB) Sensitizes Human Glioblastoma Cell Lines to Oxidative Stress by a Common Mechanism Involving Suppression of the PI3K/AKT Pathway. *Cancers (Basel)*. 11, 115 (2019).
- 219. Szeliga, M. *et al.* Transfection with liver-type glutaminase cDNA alters gene expression and reduces survival, migration and proliferation of T98G glioma cells. *Glia* **57**, 1014–1023 (2009).
- 220. Szeliga, M., Zgrzywa, A., Obara-Michlewska, M. & Albrecht, J. Transfection of a human glioblastoma cell line with liver-type glutaminase (LGA) down-regulates the expression of DNA-repair gene MGMT and sensitizes the cells to alkylating agents. *J. Neurochem.* 123, 428–436 (2012).
- 221. Wahi, K. & Holst, J. ASCT2: a potential cancer drug target. *Expert Opin. Ther. Targets* 23, 555–558 (2019).
- Dranoff, G., Elion, G. B., Friedman, H. S., Campbell, G. L. & Bigner, D. D. Influence of glutamine on the growth of human glioma and medulloblastoma in culture. *Cancer Res.* 45, 4077–81 (1985).
- 223. Oizel, K. *et al.* Efficient mitochondrial glutamine targeting prevails over glioblastoma metabolic plasticity. *Clin. Cancer Res.* **23**, 6292–6305 (2017).
- 224. Martin-McGill, K. J., Srikandarajah, N., Marson, A. G., Tudur Smith, C. & Jenkinson, M. D. The role of ketogenic diets in the therapeutic management of adult and paediatric gliomas: a systematic review. *CNS Oncol.* 7, CNS17 (2018).
- 225. Poff, A. M., Ari, C., Seyfried, T. N. & D'Agostino, D. P. The Ketogenic Diet and Hyperbaric Oxygen Therapy Prolong Survival in Mice with Systemic Metastatic Cancer. *PLoS One* **8**, e65522 (2013).
- 226. Martuscello, R. T. *et al.* A Supplemented High-Fat Low-Carbohydrate Diet for the Treatment of Glioblastoma. *Clin. Cancer Res.* **22**, 2482–2495 (2016).
- 227. Abdelwahab, M. G. *et al.* The Ketogenic Diet Is an Effective Adjuvant to Radiation Therapy for the Treatment of Malignant Glioma. *PLoS One* **7**, e36197 (2012).
- 228. Scheck, A. C. *et al.* Mechanistic studies of the ketogenic diet as an adjuvant therapy for malignant gliomas. in *Experimental and Molecular Therapeutics* 638–638 (American Association for Cancer Research, 2010). doi:10.1158/1538-7445.am10-638.

- 229. Champ, C. E. *et al.* Targeting metabolism with a ketogenic diet during the treatment of glioblastoma multiforme. *J. Neurooncol.* **117**, 125–131 (2014).
- 230. Strowd, R. E. et al. Glycemic modulation in neuro-oncology: experience and future directions using a modified Atkins diet for high-grade brain tumors. *Neuro-Oncology Pract.* 2, 127–136 (2015).
- 231. RIEGER, J. *et al.* ERGO: A pilot study of ketogenic diet in recurrent glioblastoma. *Int. J. Oncol.* **44**, 1843–1852 (2014).
- 232. Boroughs, L. K. & DeBerardinis, R. J. Metabolic pathways promoting cancer cell survival and growth. *Nat. Cell Biol.* **17**, 351–9 (2015).
- 233. Commisso, C. *et al.* Macropinocytosis of protein is an amino acid supply route in Rastransformed cells. *Nature* **497**, 633–637 (2013).
- 234. Lopes-Coelho, F., André, S., Félix, A. & Serpa, J. Breast cancer metabolic cross-talk: Fibroblasts are hubs and breast cancer cells are gatherers of lipids. *Mol. Cell. Endocrinol.* 462, 93–106 (2018).
- Serpa, J. et al. Butyrate-rich Colonic Microenvironment Is a Relevant Selection Factor for Metabolically Adapted Tumor Cells. J. Biol. Chem. 285, 39211–39223 (2010).
- 236. van Engeland, M., Nieland, L. J. W., Ramaekers, F. C. S., Schutte, B. & Reutelingsperger, C. P. M. Annexin V-Affinity assay: A review on an apoptosis detection system based on phosphatidylserine exposure. *Cytometry* 31, 1–9 (1998).
- 237. Koopman, G. *et al.* Annexin V for flow cytometric detection of phosphatidylserine expression on B cells undergoing apoptosis. *Blood* **84**, 1415–20 (1994).
- 238. Kay, J. G. & Fairn, G. D. Distribution, dynamics and functional roles of phosphatidylserine within the cell. *Cell Commun. Signal.* **17**, 126 (2019).
- 239. Leventis, P. A. & Grinstein, S. The Distribution and Function of Phosphatidylserine in Cellular Membranes. *Annu. Rev. Biophys.* **39**, 407–427 (2010).
- 240. Crowley, L. C., Marfell, B. J., Scott, A. P. & Waterhouse, N. J. Quantitation of Apoptosis and Necrosis by Annexin V Binding, Propidium Iodide Uptake, and Flow Cytometry. *Cold Spring Harb. Protoc.* **2016**, pdb.prot087288 (2016).
- 241. Jiang, L. *et al.* Monitoring the progression of cell death and the disassembly of dying cells by flow cytometry. *Nat. Protoc.* **11**, 655–663 (2016).
- 242. Riccardi, C. & Nicoletti, I. Analysis of apoptosis by propidium iodide staining and flow cytometry. *Nat. Protoc.* **1**, 1458–1461 (2006).
- 243. Poon, I. K. H., Hulett, M. D. & Parish, C. R. Molecular mechanisms of late apoptotic/necrotic cell clearance. *Cell Death Differ.* 17, 381–397 (2010).
- 244. Grada, A., Otero-Vinas, M., Prieto-Castrillo, F., Obagi, Z. & Falanga, V. Research

- Techniques Made Simple: Analysis of Collective Cell Migration Using the Wound Healing Assay. *J. Invest. Dermatol.* **137**, e11–e16 (2017).
- 245. Maddocks, S. & Jenkins, R. Quantitative PCR. in *Understanding PCR* 45–52 (Elsevier, 2017). doi:10.1016/B978-0-12-802683-0.00004-6.
- 246. Hoy, M. A. DNA Amplification by the Polymerase Chain Reaction. in *Insect Molecular Genetics* 307–372 (Elsevier, 2013). doi:10.1016/B978-0-12-415874-0.00008-1.
- 247. Fairfax, M. R., Bluth, M. H. & Salimnia, H. Diagnostic Molecular Microbiology. *Clin. Lab. Med.* 38, 253–276 (2018).
- 248. Emwas, A.-H. *et al.* NMR Spectroscopy for Metabolomics Research. *Metabolites* **9**, 123 (2019).
- 249. Wishart, D. S. NMR metabolomics: A look ahead. J. Magn. Reson. 306, 155–161 (2019).
- 250. Amiel, A. *et al.* Proton NMR enables the absolute quantification of aqueous metabolites and lipid classes in unique mouse liver samples. *Metabolites* **10**, 1–20 (2020).
- 251. Nunes, S. C. Tumor Microenvironment Selective Pressures Boosting Cancer Progression. in 35–49 (2020). doi:10.1007/978-3-030-34025-4_2.
- 252. Trepat, X., Chen, Z. & Jacobson, K. Cell Migration. in *Comprehensive Physiology* 2369–2392 (Wiley, 2012). doi:10.1002/cphy.c110012.
- 253. Pascual, G., Domínguez, D. & Benitah, S. A. The contributions of cancer cell metabolism to metastasis. *Dis. Model. Mech.* **11**, (2018).
- Hipólito, A., Martins, F., Mendes, C., Lopes-Coelho, F. & Serpa, J. Molecular and Metabolic Reprogramming: Pulling the Strings Toward Tumor Metastasis. *Front. Oncol.* 11, (2021).
- 255. Vidali, S. *et al.* Lithium and Not Acetoacetate Influences the Growth of Cells Treated with Lithium Acetoacetate. *Int. J. Mol. Sci.* **20**, 3104 (2019).
- 256. Duraj, T. *et al.* Beyond the Warburg Effect: Oxidative and Glycolytic Phenotypes Coexist within the Metabolic Heterogeneity of Glioblastoma. *Cells* **10**, 202 (2021).
- 257. Miranda-Gonçalves, V. et al. MCT1 Is a New Prognostic Biomarker and Its Therapeutic Inhibition Boosts Response to Temozolomide in Human Glioblastoma. Cancers (Basel).
 13, 3468 (2021).
- 258. Ye, Z.-C., Rothstein, J. D. & Sontheimer, H. Compromised Glutamate Transport in Human Glioma Cells: Reduction–Mislocalization of Sodium-Dependent Glutamate Transporters and Enhanced Activity of Cystine–Glutamate Exchange. *J. Neurosci.* 19, 10767–10777 (1999).
- 259. de Groot, J. F., Liu, T. J., Fuller, G. & Yung, W. K. A. The Excitatory Amino Acid Transporter-2 Induces Apoptosis and Decreases Glioma Growth In vitro and In vivo.

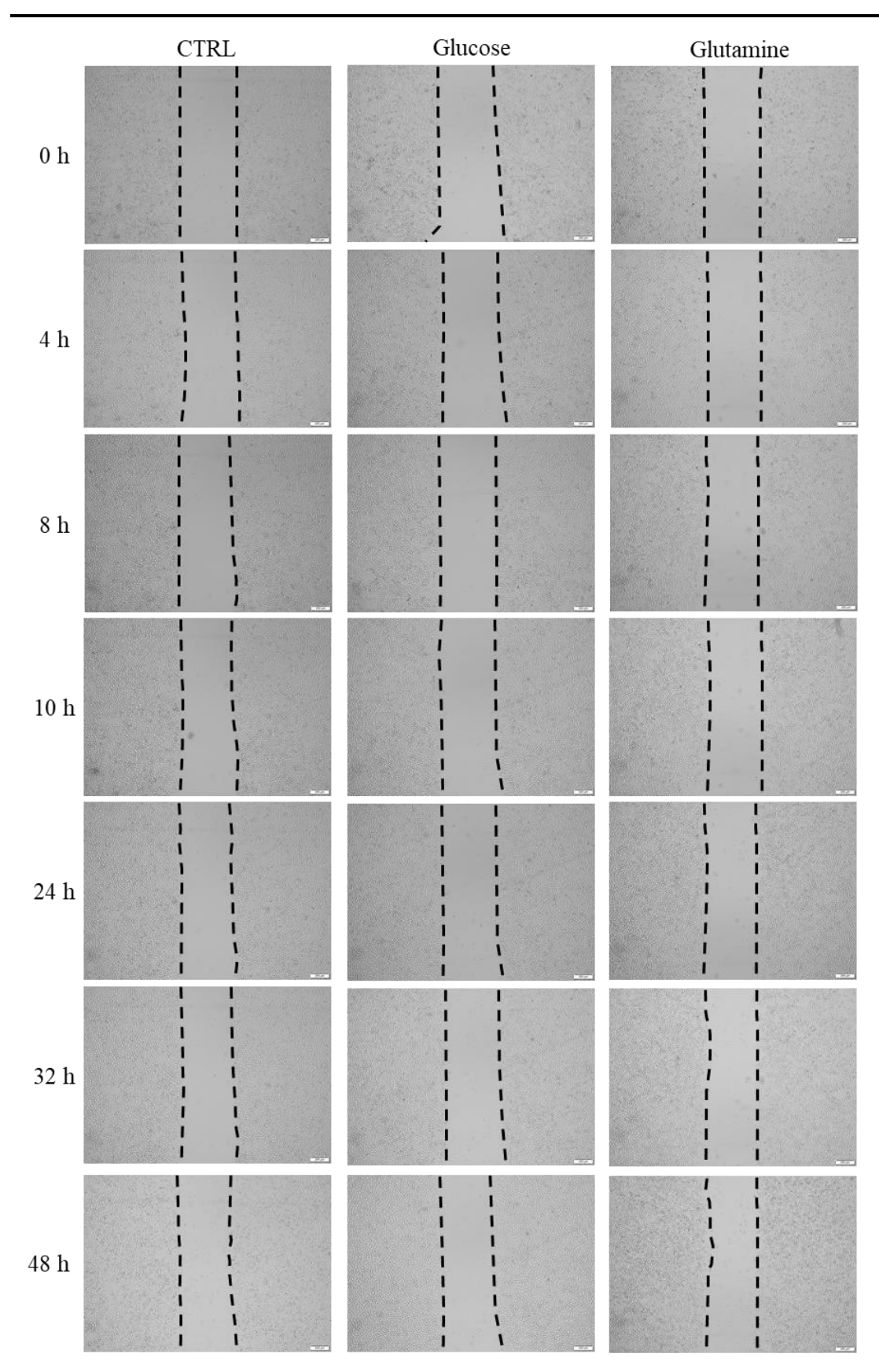
- Cancer Res. 65, 1934–1940 (2005).
- 260. Buccoliero, A. M. *et al.* Angiocentric glioma-associated seizures: The possible role of EATT2, pyruvate carboxylase and glutamine synthetase. *Seizure* **86**, 152–154 (2021).
- 261. Corsi, L., Mescola, A. & Alessandrini, A. Glutamate Receptors and Glioblastoma Multiforme: An Old "Route" for New Perspectives. *Int. J. Mol. Sci.* **20**, 1796 (2019).
- 262. Arcella, A. *et al.* Pharmacological blockade of group II metabotropic glutamate receptors reduces the growth of glioma cells in vivo. *Neuro. Oncol.* **7**, 236–245 (2005).
- 263. Yelskaya, Z. *et al.* Synergistic Inhibition of Survival, Proliferation, and Migration of U87 Cells with a Combination of LY341495 and Iressa. *PLoS One* **8**, e64588 (2013).
- 264. Dalley, C. B., Wroblewska, B., Wolfe, B. B. & Wroblewski, J. T. The Role of Metabotropic Glutamate Receptor 1 Dependent Signaling in Glioma Viability. J. Pharmacol. Exp. Ther. 367, 59–70 (2018).
- 265. Zhang, C. et al. Anti-Cancer Effect of Metabotropic Glutamate Receptor 1 Inhibition in Human Glioma U87 Cells: Involvement of PI3K/Akt/mTOR Pathway. Cell. Physiol. Biochem. 35, 419–432 (2015).
- 266. Stepulak, A. *et al.* Expression of glutamate receptor subunits in human cancers. *Histochem. Cell Biol.* **132**, 435–445 (2009).
- 267. Han, T. *et al.* How does cancer cell metabolism affect tumor migration and invasion? *Cell Adh. Migr.* **7**, 395–403 (2013).
- 268. Guak, H. & Krawczyk, C. M. Implications of cellular metabolism for immune cell migration. *Immunology* **161**, 200–208 (2020).
- 269. Shiraishi, T. *et al.* Glycolysis is the primary bioenergetic pathway for cell motility and cytoskeletal remodeling in human prostate and breast cancer cells. *Oncotarget* **6**, 130–143 (2015).
- 270. De Bock, K. *et al.* Role of PFKFB3-Driven Glycolysis in Vessel Sprouting. *Cell* **154**, 651–663 (2013).
- 271. Kim, J. & DeBerardinis, R. J. Mechanisms and Implications of Metabolic Heterogeneity in Cancer. *Cell Metab.* **30**, 434–446 (2019).
- 272. Cuperlovic-Culf, M., Ferguson, D., Culf, A., Morin, P. & Touaibia, M. 1H NMR Metabolomics Analysis of Glioblastoma Subtypes. *J. Biol. Chem.* **287**, 20164–20175 (2012).
- 273. Arthurs, A. L., Keating, D. J., Stringer, B. W. & Conn, S. J. The Suitability of Glioblastoma Cell Lines as Models for Primary Glioblastoma Cell Metabolism. *Cancers* (*Basel*). **12**, 3722 (2020).
- 274. Xie, N. et al. NAD+ metabolism: pathophysiologic mechanisms and therapeutic potential.

- Signal Transduct. Target. Ther. 5, 227 (2020).
- 275. Brekke, E. M. F., Walls, A. B., Schousboe, A., Waagepetersen, H. S. & Sonnewald, U. Quantitative Importance of the Pentose Phosphate Pathway Determined by Incorporation of 13 C from [2- 13 C]- and [3- 13 C]Glucose into TCA Cycle Intermediates and Neurotransmitter Amino Acids in Functionally Intact Neurons. *J. Cereb. Blood Flow Metab.* 32, 1788–1799 (2012).
- 276. Stubberfield, C. R. & Cohen, G. M. Interconversion of NAD(H) TO NADP(H). *Biochem. Pharmacol.* **38**, 2631–2637 (1989).
- 277. Xiao, W., Wang, R.-S., Handy, D. E. & Loscalzo, J. NAD(H) and NADP(H) Redox Couples and Cellular Energy Metabolism. *Antioxid. Redox Signal.* **28**, 251–272 (2018).
- 278. Schild, T. *et al.* NADK is activated by oncogenic signaling to sustain pancreatic ductal adenocarcinoma. *Cell Rep.* **35**, 109238 (2021).
- 279. Ding, C.-K. C. *et al.* MESH1 is a cytosolic NADPH phosphatase that regulates ferroptosis. *Nat. Metab.* **2**, 270–277 (2020).
- 280. Lin, C.-C. *et al.* The regulation of ferroptosis by MESH1 through the activation of the integrative stress response. *Cell Death Dis.* **12**, 727 (2021).
- 281. Serpa, J. Cysteine as a Carbon Source, a Hot Spot in Cancer Cells Survival. *Front. Oncol.* **10**, (2020).
- 282. Nunes, S. C. *et al.* Cysteine allows ovarian cancer cells to adapt to hypoxia and to escape from carboplatin cytotoxicity. *Sci. Rep.* **8**, 9513 (2018).
- Nunes, S. C. *et al.* Cysteine boosters the evolutionary adaptation to CoCl2 mimicked hypoxia conditions, favouring carboplatin resistance in ovarian cancer. *BMC Evol. Biol.* 18, 97 (2018).
- 284. Lopes-Coelho, F. *et al.* HNF1β drives glutathione (GSH) synthesis underlying intrinsic carboplatin resistance of ovarian clear cell carcinoma (OCCC). *Tumor Biol.* **37**, 4813–4829 (2016).
- 285. Maudsley, A. A. *et al.* Mapping of Glycine Distributions in Gliomas. *Am. J. Neuroradiol.* **35**, S31–S36 (2014).
- 286. Tiwari, V. *et al.* Glycine by MR spectroscopy is an imaging biomarker of glioma aggressiveness. *Neuro. Oncol.* **22**, 1018–1029 (2020).
- 287. Noch, E. *et al.* P13.07 Cysteine induces glioblastoma cytotoxicity through mitochondrial reductive stress. *Neuro. Oncol.* **23**, ii33–ii34 (2021).
- 288. Tanaka, K. *et al.* Glioma cells require one-carbon metabolism to survive glutamine starvation. *Acta Neuropathol. Commun.* **9**, 16 (2021).
- 289. Bose, S., Ramesh, V. & Locasale, J. W. Acetate Metabolism in Physiology, Cancer, and

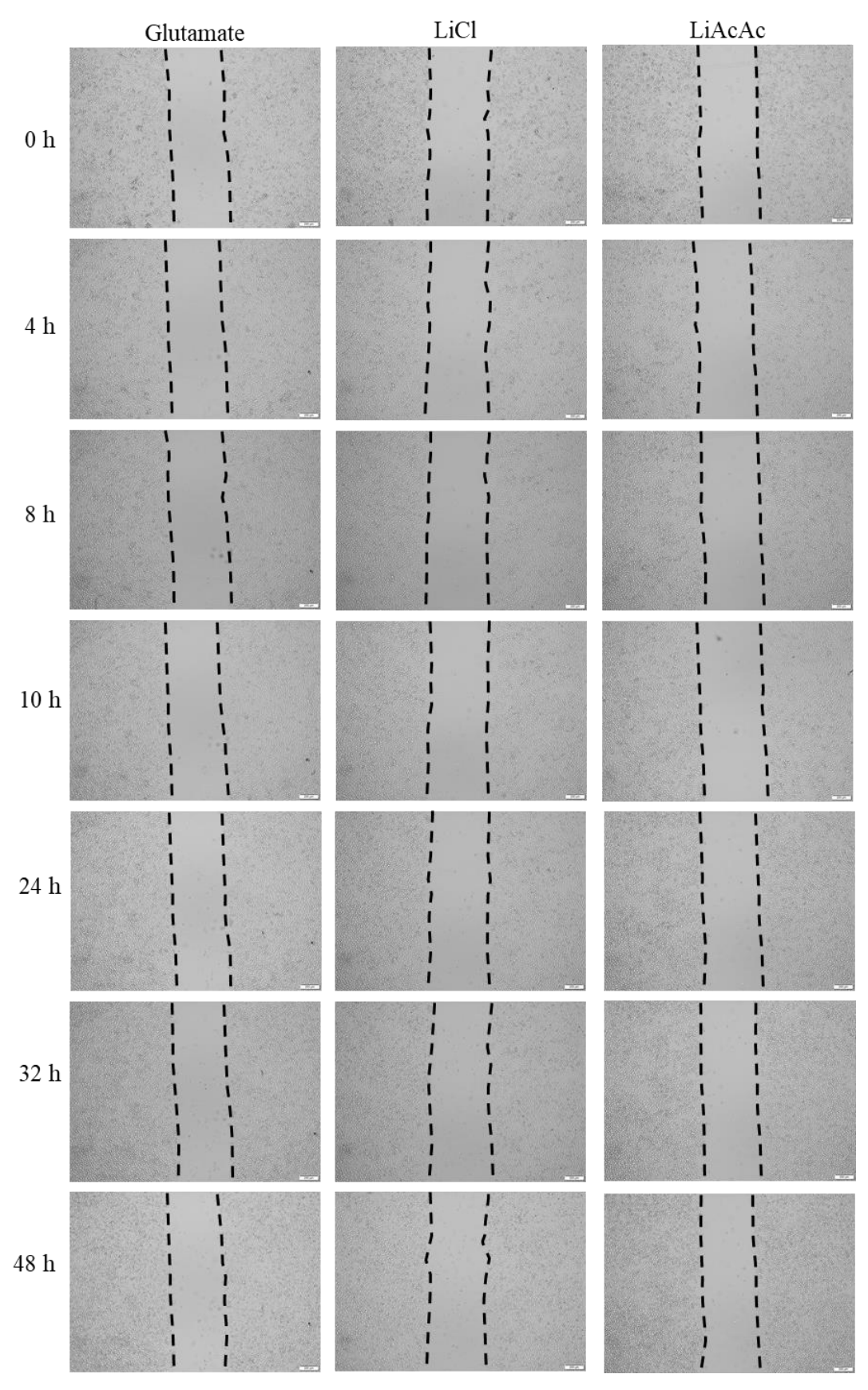
- Beyond. Trends Cell Biol. 29, 695–703 (2019).
- 290. Ye, C. & Tu, B. P. Sink into the Epigenome: Histones as Repositories That Influence Cellular Metabolism. *Trends Endocrinol. Metab.* **29**, 626–637 (2018).
- 291. Liu, X. *et al.* Acetate Production from Glucose and Coupling to Mitochondrial Metabolism in Mammals. *Cell* **175**, 502-513.e13 (2018).
- 292. Spriet, L. L. *et al.* Pyruvate dehydrogenase activation and kinase expression in human skeletal muscle during fasting. *J. Appl. Physiol.* **96**, 2082–2087 (2004).
- 293. Schug, Z. T., Vande Voorde, J. & Gottlieb, E. The metabolic fate of acetate in cancer. *Nat. Rev. Cancer* **16**, 708–717 (2016).
- 294. Lacroix, M., Riscal, R., Arena, G., Linares, L. K. & Le Cam, L. Metabolic functions of the tumor suppressor p53: Implications in normal physiology, metabolic disorders, and cancer. *Mol. Metab.* **33**, 2–22 (2020).
- 295. Lee, J. V. *et al.* Akt-Dependent Metabolic Reprogramming Regulates Tumor Cell Histone Acetylation. *Cell Metab.* **20**, 306–319 (2014).
- 296. Lee, J. V. *et al.* Acetyl-CoA promotes glioblastoma cell adhesion and migration through Ca 2+ –NFAT signaling. *Genes Dev.* **32**, 497–511 (2018).
- 297. Maan, M., Peters, J. M., Dutta, M. & Patterson, A. D. Lipid metabolism and lipophagy in cancer. *Biochem. Biophys. Res. Commun.* **504**, 582–589 (2018).
- 298. Currie, E., Schulze, A., Zechner, R., Walther, T. C. & Farese, R. V. Cellular Fatty Acid Metabolism and Cancer. *Cell Metab.* **18**, 153–161 (2013).
- 299. van der Veen, J. N. *et al.* The critical role of phosphatidylcholine and phosphatidylethanolamine metabolism in health and disease. *Biochim. Biophys. Acta Biomembr.* **1859**, 1558–1572 (2017).
- 300. Cole, J. T. Metabolism of BCAAs. in *Branched Chain Amino Acids in Clinical Nutrition* 13–24 (Springer New York, 2015). doi:10.1007/978-1-4939-1923-9_2.
- 301. Wong, T. L., Che, N. & Ma, S. Reprogramming of central carbon metabolism in cancer stem cells. *Biochim. Biophys. Acta Mol. Basis Dis.* **1863**, 1728–1738 (2017).
- 302. Nagao, A., Kobayashi, M., Koyasu, S., Chow, C. C. T. & Harada, H. HIF-1-Dependent Reprogramming of Glucose Metabolic Pathway of Cancer Cells and Its Therapeutic Significance. *Int. J. Mol. Sci.* **20**, 238 (2019).
- 303. Lee, Y. H., Wang, M.-Y., Yu, X.-X. & Unger, R. H. Glucagon is the key factor in the development of diabetes. *Diabetologia* **59**, 1372–1375 (2016).
- 304. Tönjes, M. *et al.* BCAT1 promotes cell proliferation through amino acid catabolism in gliomas carrying wild-type IDH1. *Nat. Med.* **19**, 901–908 (2013).
- 305. Zhang, B. et al. Regulation of branched-chain amino acid metabolism by hypoxia-

inducible factor in glioblastoma. Cell. Mol. Life Sci. 78, 195–206 (2021).

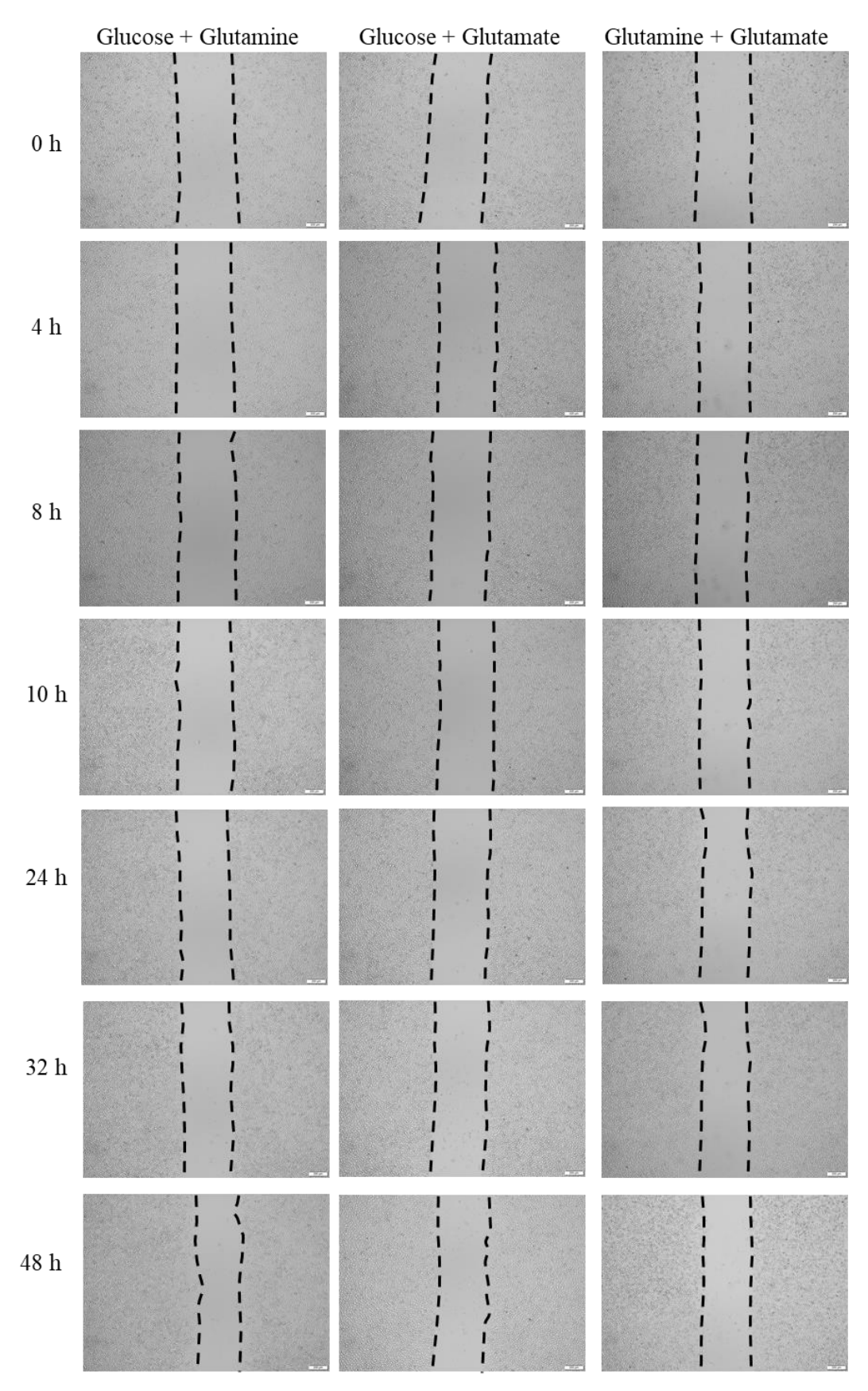
Supplementary Figures and Tables



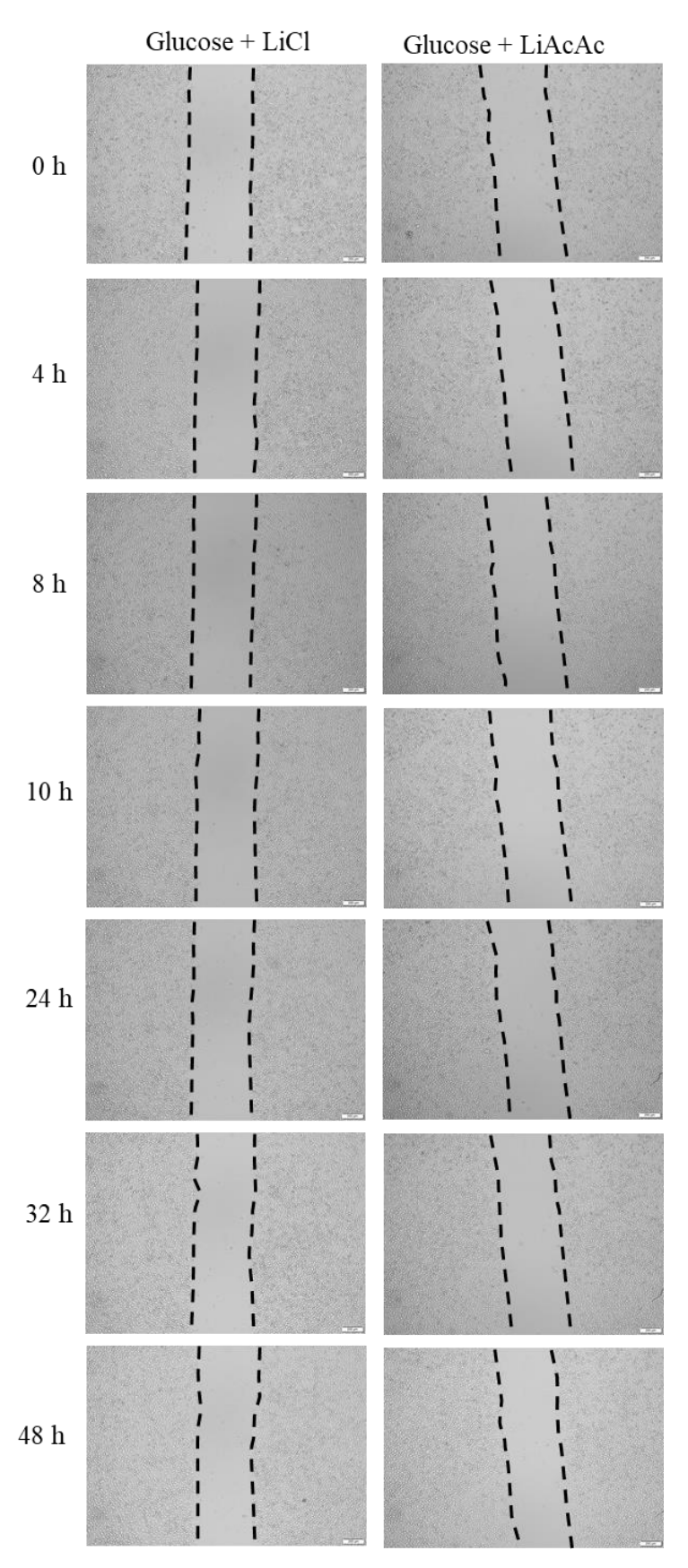
Supplementary Figure 1. (Continues on the next page)



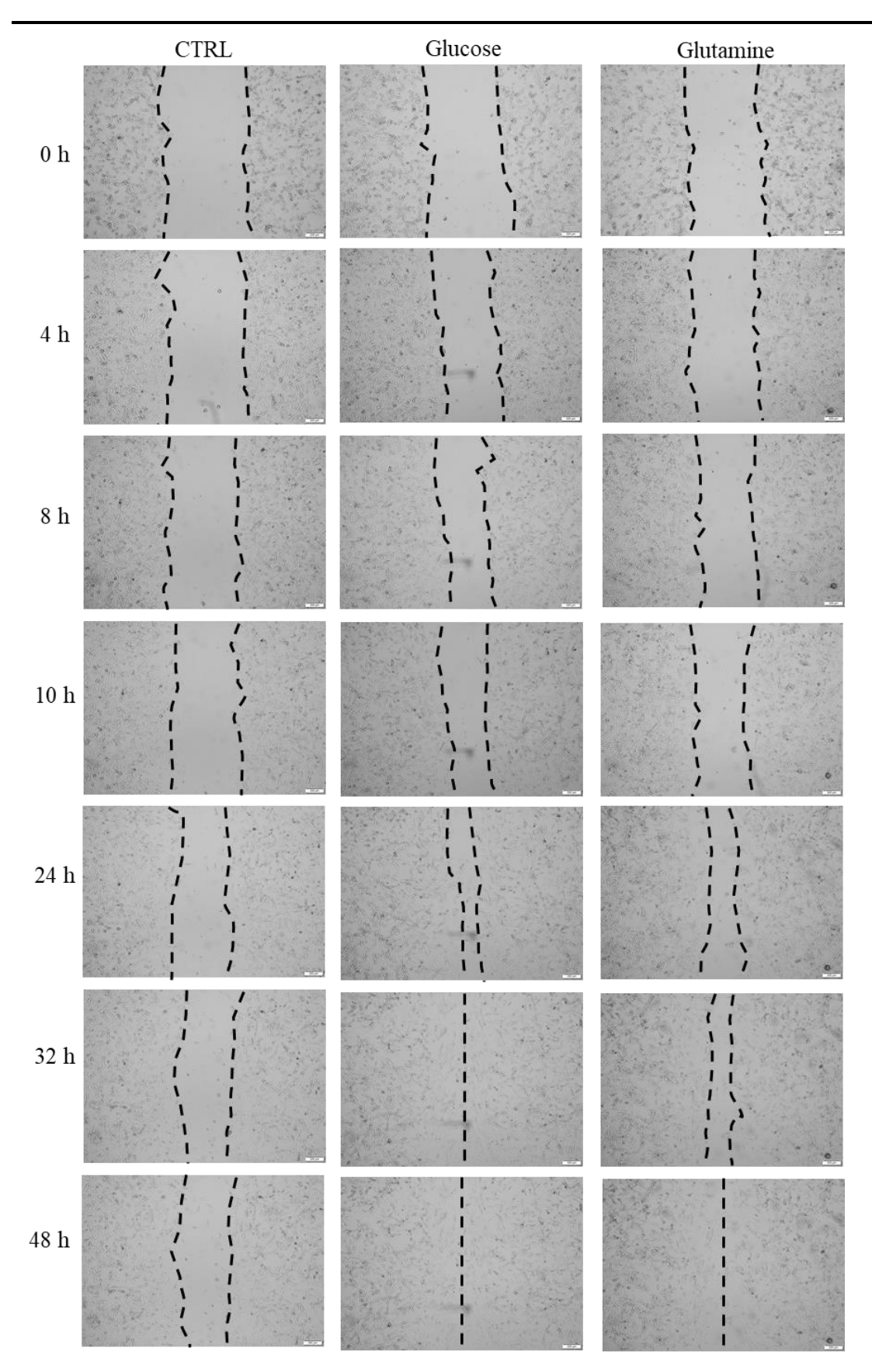
Supplementary Figure 1. (Continues on the next page)



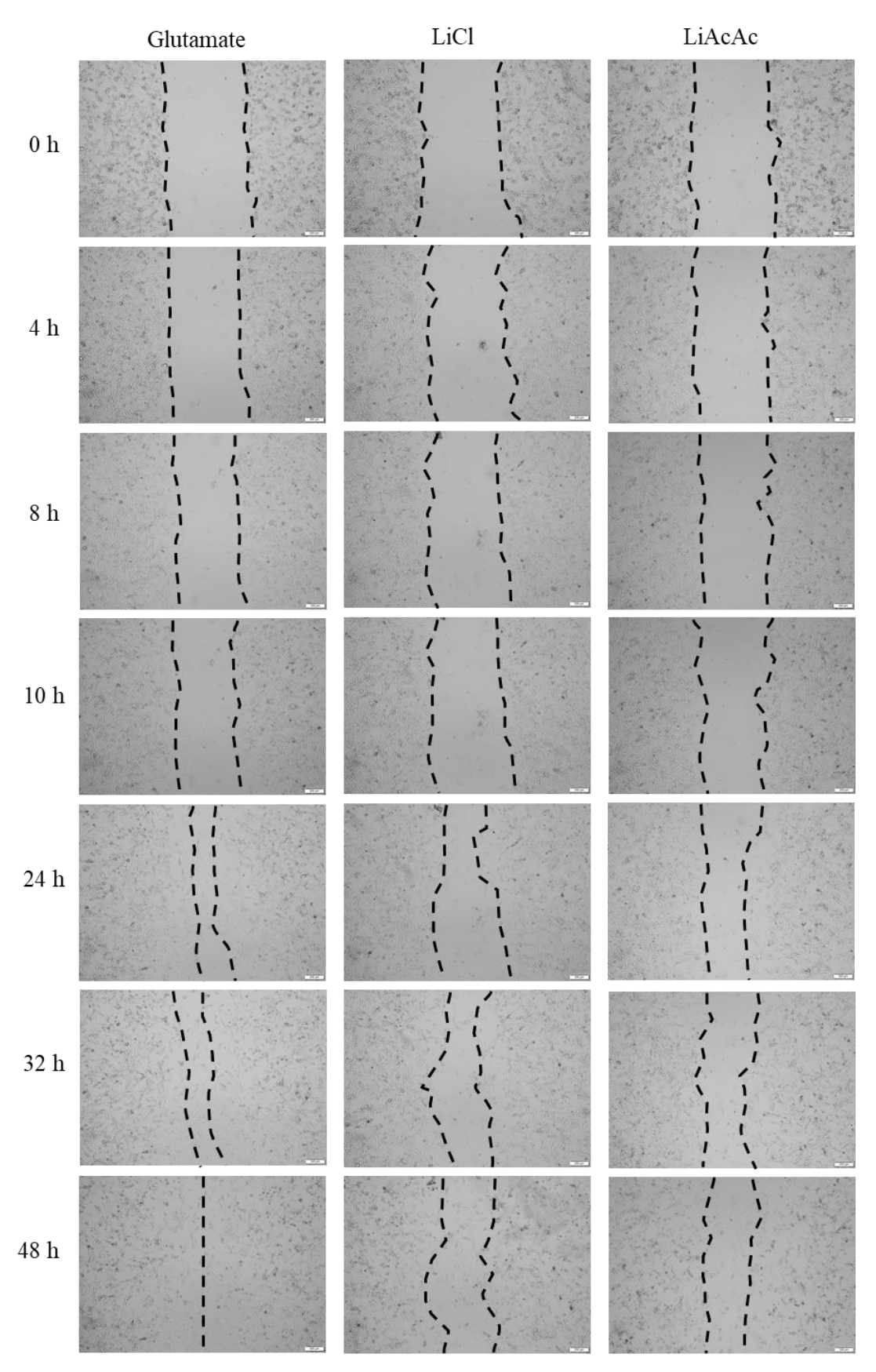
Supplementary Figure 1. (Continues on the next page)



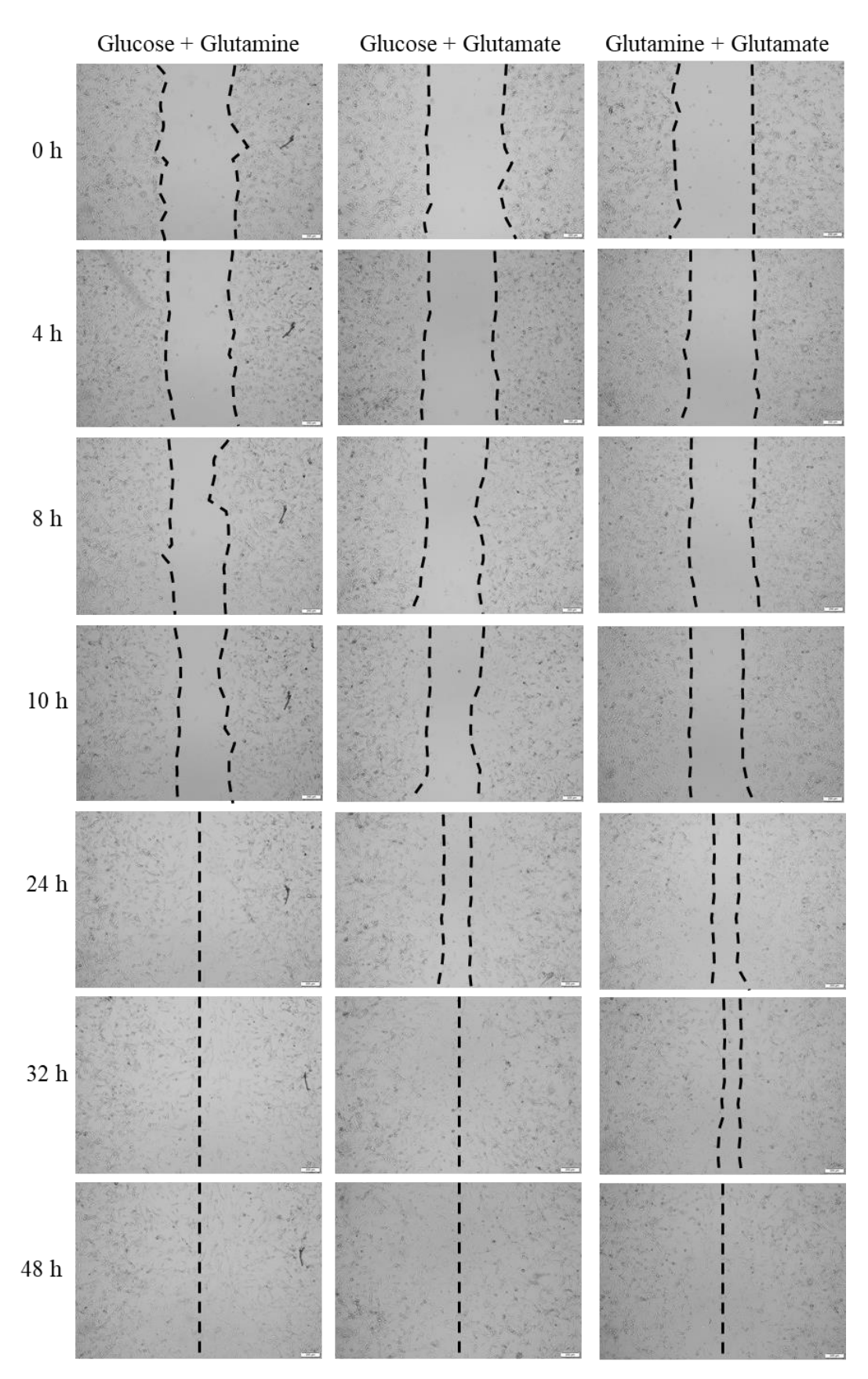
Supplementary Figure 1. (Continuation) Wound healing process of U-251 cells.



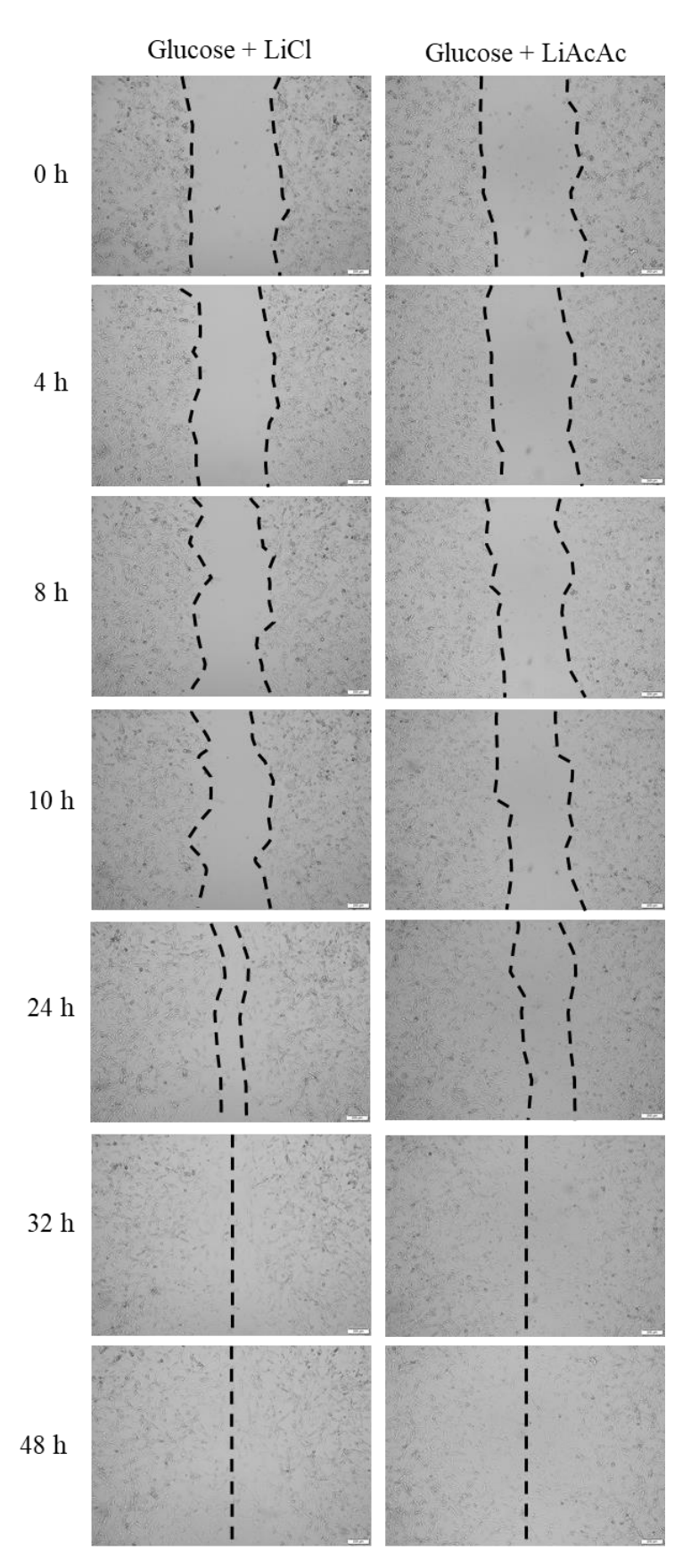
Supplementary Figure 2. (Continues on the next page)



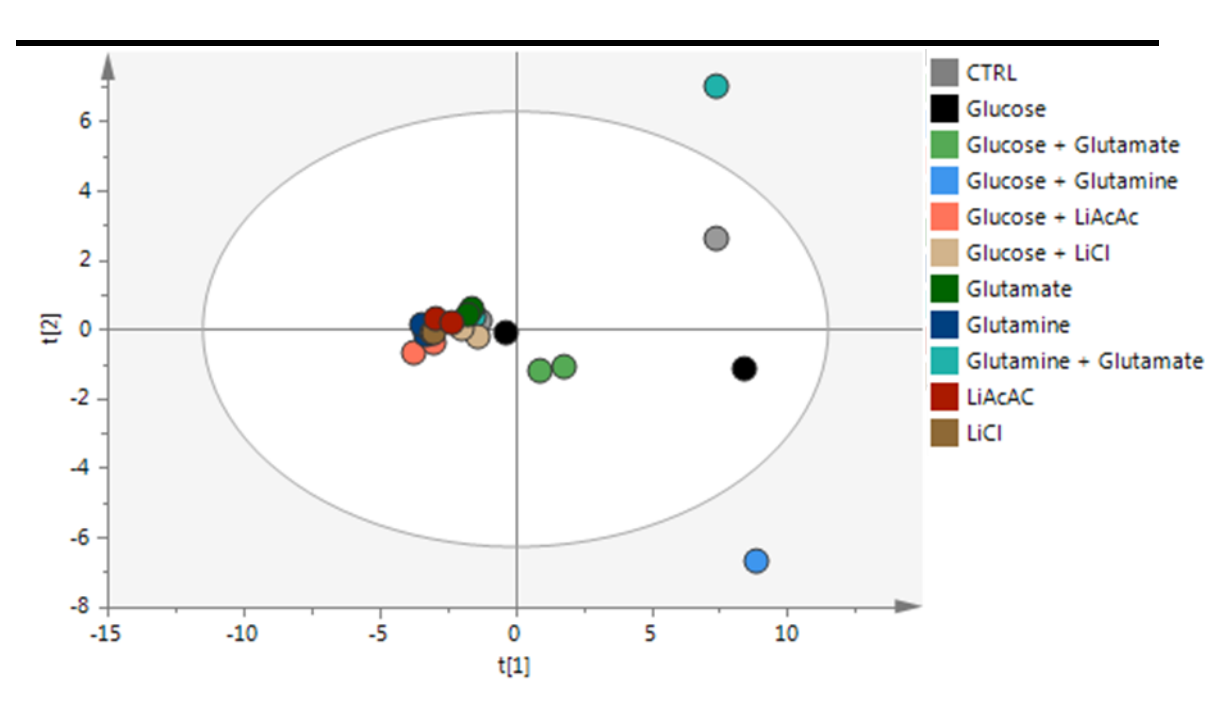
Supplementary Figure 2. (Continues on the next page)



Supplementary Figure 2. (Continues on the next page)



Supplementary Figure 2. Wound healing process of U-87 cells.



Supplementary Figure 3. Principal Component Analysis (PCA) score plot of U-87 aqueous samples with outliers. Due to the high variability in these four samples, we decided to exclude them from our analysis.

Supplementary Table 1. Formulation of the DMEM/F12 used during experimental conditions.

	DMEM/F12 w/o glucose, w/o glutamine Formulation	mg/L					
	Glycine	18.75					
	L-Alanine	4.45					
	L-Alany l-L-Glutamine (Glutamine stable)	0					
	L-Arginine Monohy drochloride	147.5					
	L-Asparagine Monohydrate	7.5					
	L-Aspartic acid	6.65					
	L-Cysteine Monohydrochloride Monohydrate	17.56					
	L-Cysteine Dihydrochloride	31.29					
	L-Glutamic Acid	7.35					
Amino Acids	L-Glutamine	0					
10 A	L-Histidine Monohy drochloride Monohy drate	31.48					
√ min	L-Isoleucine	54.57					
7	L-Leucine	59.05					
	L-Ly sine Monohy drochloride	91.25					
	L-Methionine	17.24					
	L-Pheny lalanine	35.48					
	L-Proline	17.25					
	L-Serine	26.25					
	L-Threonine	53.45					
	L-Tryptophan	9.02					
	L-Tyrosine Disodium Slat Dihydrate L-Valine	55.79					
		52.85					
	Calcium Cholride Dihydrate	154.5					
	Cupric Sulfate Pentahy drate	0.0013					
	Ferric Nitrate Nonahydrate	0.05					
	Ferrous Sulfate Heptahydrate	0.417					
alts	Magnesium Chloride Anhydrous	61.2					
Inorganic Salts	Magnesium Chloride Hexahy drate Magnesium Sulfate Anhy drous	61.2 48.84					
orga	Potassium Chloride						
Inc	Potassium Chloride Sodium Bicarbonate						
	Sodium Chloride	2438 6996					
	Sodium Phosphate Dibasic Anhydrous	71.02					
	Sodium Phosphate Monobasic Anhydrous	54.3					
	Zinc Sulfate Heptahy drate	0.432					
	Choline Chloride	8.98					
	D-Biotin	0.0035					
	D-Ca Pantothenate	2.24					
	Folic Acid	2.66					
s,	Myo-inositol	12.6					
Vitamins	Nicotinamide	2.2					
V its	Pyridoxal Hydrochloride	2					
	Py ridoxine Hy drochloride	0.031					
	Riboflavin	0.219					
	Thiamine Hydrochloride	2.17					
	VitamineB12	0.68					
	D-Glucose Anhydrous	0					
	Hepes Free Acid	0					
ıts	Hypoxanthine	2.1					
Other Components	Linoleic Acid	0.042					
dwo	Phenol Red Sodium Salt	8.63					
er C	Putrescine+2HCL	0.081					
Oth	Sodium Pyruvate	55					
	Thioctic Acid	0.105					
	Thymidine	0.365					

Supplementary Table 2. Quantity (nmol), per gram of biomass), of the organic compounds found in aqueous samples. Samples highlighted in red were excluded from analysis. (Continues on the next page)

Cell line	Condition	Weight (g)	3-Hydroxyis ovalerate	ADP	AMP	Acetate	Acetoacetate	Adenine	Alanine	Aspartate	Benzoate	Caprate	Choline	Creatine	Dimethyl sulfone
	CTRL	0.0873	0	39.863	154.639	1376.632	0	90.034	98.969	214.433	93.471	0	96.907	110.653	46.735
	CTRL	0.067	0	66.269	269.552	1538.507	0	100.299	112.836	0	80.597	0	135.224	152.239	57.313
	Glucose	0.0881	0	105.562	213.167	1595.006	0	84.449	609.535	0	154.597	0	162.089	202.951	55.165
	Glucose	0.0846	0	78.014	182.270	1318.440	0	86.525	507.801	0	144.681	0	170.213	136.879	46.809
	Glutamine	0.0919	0	41.785	142.982	272.905	0	45.702	120.131	879.434	16.322	0	60.065	40.479	16.975
	Glutamine	0.09	0	114.000	288.000	257.333	0	82.667	273.333	2215.333	20.000	0	105.333	106.000	37.333
	Glutamate	0.0548	0	60.219	104.015	286.861	0	71.168	61.314	373.358	21.898	0	153.285	72.263	24.088
	Glutamate	0.0718	0	116.992	233.983	201.393	0	68.524	68.524	490.529	20.056	0	114.485	0	31.755
	LiCl	0.0606	0	90.099	203.960	275.248	0	113.861	44.554	108.911	0	0	158.416	64.356	25.743
	LiCl	0.0784	0	60.459	234.949	257.143	0	71.173	42.092	151.531	0	0	113.265	68.112	40.561
U-251	LiAcAC	0.0745	0	63.624	167.517	397.852	22.550	76.510	178.792	379.329	25.772	0	253.691	0	41.879
Ü	LiAcAc	0.0687	0	45.415	151.092	220.961	10.480	45.415	110.044	327.511	16.594	0	134.498	72.489	27.074
	Glucose + Glutamine	0.0873	29.553	153.952	414.433	1522.337	0	159.450	1744.330	1357.388	81.787	0	199.313	172.509	50.859
	Glucose + Glutamine	0.1282	0	71.139	443.214	2143.058	0	94.072	1865.991	2253.978	78.159	0	283.619	270.983	0
	Glucose + Glutamate	0.1121	0	84.567	155.219	1256.735	0	74.398	845.138	261.195	67.440	0	166.459	168.064	50.312
	Glucose + Glutamate	0.1049	0	64.633	188.179	1229.171	0	92.660	684.652	348.904	30.887	0	141.849	122.974	42.898
	Glutamine + Glutamate	0.0678	0	66.372	256.637	1480.531	0	99.115	447.788	1835.398	198.230	0	151.327	130.973	33.628
	Glutamine + Glutamate	0.0554	3517.690	48.736	266.426	1326.715	0	74.729	363.899	1474.007	154.874	0	129.964	94.224	28.159
	Glucose + LiCl	0.0742	0	90.566	249.057	1445.822	0	102.695	468.194	0	114.016	0	128.571	126.954	39.623
	Glucose + LiCl	0.0675	0	91.556	180.444	1266.667	0	82.667	422.222	0	190.222	0	130.667	134.222	42.667
	Glucose + LiAcAc	0.0912	20.395	0	136.842	1833.553	25.000	50.658	651.316	0	154.605	0	103.947	203.947	61.842
	Glucose + LiAcAc	0.0831	15.162	129.964	145.126	1867.148	0	64.982	585.560	0	123.466	0	103.971	109.747	44.765
	CTRL	0.0396	18.182	15.152	0	254.545	0	53.030	34.848	0	0	0	54.545	0	21.212
	CTRL	0.0386	0	31.088	0	279.793	0	0	9.326	0	40.415	0	6.218	4.663	4.663
	Glucose	0.0326	29.448	71.779	27.607	220.859	0	0	60.736	0	62.577	0	22.086	0	14.724
	Glucose	0.044	4.091	23.182	0	196.364	0	16.364	12.273	0	25.909	0	9.545	0	5.455
	Glutamine	0.0437	4.119	0	0	182.609	0	0	8.238	0	20.595	70.023	5.492	2.746	0
	Glutamine	0.0401	2.993	0	0	167.581	0	0	7.481	25.436	29.925	77.805	4.489	2.993	0
	Glutamate	0.0506	0	0	0	166.008	0	0	11.858	34.387	35.573	46.245	7.115	4.743	5.929
	Glutamate	0.0444	0	0	0	177.027	0	0	10.811	52.703	24.324	104.054	14.865	0	0
	LiCl	0.0489	0	0	0	165.644	0	0	7.362	0	25.767	67.485	12.270	0	4.908
U-87	LiCl	0.0448	0	0	0	163.393	0	0	10.714	0	21.429	73.661	6.696	0	5.357
∄	LiAcAC	0.0711	0	0	0	169.620	0	0	7.595	0	21.097	67.511	5.907	5.907	3.376
	LiAcAc			0 125 532		180.220			8.791		23.077	67.033	12.088		
	Glucose + Glutamine	0.0282	8.511	120.002	46.809	189.362	0	0	174.468	70.213	29.787	0	14.894	0	12.766
	Glucose + Glutamate	0.0347 0.0554	32.853	32.853 57.401	5.187	167.723	0	0	38.040	0	24.207	0	12.104 9.747	0	6.916 9.747
	Glucose + Glutamate		0 8.136	36.610	19.495	213.357			24.910 107.797	174.915	21.661 77.288				9.747
	Glutamine + Glutamate	0.0295	5.1.0.0	11.823	0	264.407	0	85.424	11.823			0	40.678 10.345	10.169	
	Glutamine + Glutamate	0.0406	0		-	195.074	0	0		0	22.167	0		0	5.911
	Glucose + LiCl	0.0404	0	0	0	196.040	0	0	10.396	0	37.129	0	7.426	0	8.911
	Glucose + LiCl		7.634			206.107	-	0	0	-	22.901	132.824	7.634		7.634
	Glucose + LiAcAc	0.0627	1.914	0	0	163.636	44.019	0	7.122	0	29.665	64.115	2.871	0	0
	Glucose + LiAcAc	0.0674	0	0	0	167.359	8.902	0	7.122	0	24.036	0	3.561	2.671	1.780

Supplementary Table 2 (Continuation)

Cell line	Condition	Ethanol	Ethylene glycol	Formate	Fumarate	Glucose	Glutamate	Glutamine	Glutathione	Glycerol	Glycine	Glycolate	Histidine	Hypoxanthine
	CTRL	0	51.546	7225.430	0	0	0	0	610.309	263.918	610.997	35.052	0	172.509
	CTRL	0	51.940	9530.149	0	0	428.060	0	862.388	187.164	1009.254	0	0	197.910
	Glucose	0	70.148	8492.622	11.578	0	1074.007	0	954.143	546.198	1283.768	81.044	0	186.606
	Glucose	0	59.574	7014.184	7.092	0	940.426	0	1011.348	358.865	1100.709	0	0	110.638
	Glutamine	0	22.851	3221.980	0	0	1435.691	178.890	514.472	114.255	48.313	32.644	0	0
	Glutamine	0	24.000	3086.000	0	80.667	3086.000	134.667	894.000	273.333	589.333	25.333	0	36.000
	Glutamate	28.467	8.759	4322.628	0	0	236.496	0	379.927	218.978	64.599	27.372	0	131.387
	Glutamate	0	12.535	2841.226	0	0	266.574	0	962.674	171.309	427.019	0	0	71.866
	LiCl	0	11.881	3710.891	0	0	133.663	0	581.188	194.059	71.287	26.733	32.673	115.842
	LiCl	0	15.306	3727.806	0	56.633	0	0	144.643	233.418	423.980	0	0	67.347
U-251	LiAcAC	0	18.523	3357.584	0	0	612.886	0	225.503	358.389	134.497	0	0	56.376
Ĕ	LiAcAc	0	7.860	2793.886	0	0	643.668	0	229.694	193.013	348.472	0	0	56.769
	Glucose + Glutamine	0	67.354	7901.718	23.368	0	5652.921	709.278	2024.055	472.165	885.223	0	0	285.223
	Glucose + Glutamine	0	81.903	10003.900	22.465	0	6532.605	0	2107.956	607.020	1180.811	0	0	137.598
	Glucose + Glutamate	0	6.958	6228.546	21.945	0	1530.776	0	1127.208	295.986	1074.755	0	0	251.026
	Glucose + Glutamate	0	57.769	7295.520	22.879	0	1303.527	0	1146.806	471.878	837.941	0	0	144.709
	Glutamine + Glutamate	0	52.212	9115.929	6.195	0	4538.938	0	1413.274	309.735	869.912	0	0	109.735
	Glutamine + Glutamate	0	50.903	8291.697	9.747	0	3828.520	0	999.639	298.917	728.881	0	0	110.469
	Glucose + LiCl	0	56.604	9224.798	5.660	0	999.461	0	907.278	401.078	1259.838	0	0	85.714
	Glucose + LiCl	0	59.556	7574.222	6.222	0	839.111	0	805.333	216.000	1026.667	0	0	114.667
	Glucose + LiAcAc	0	62.500	2296.053	12.500	0	1215.789	0	1319.079	317.105	1405.921	117.105	0	66.447
	Glucose + LiAcAc	0	53.430	2427.437	17.329	0	538.628	0	606.498	231.769	836.101	70.036	0	101.083
	CTRL	0	25.758	4739.394	0	0	130.303	0	175.758	286.364	168.182	0	0	0
	CTRL	0	0	5777.720	0	0	0	0	0	152.332	26.425	0	0	0
	Glucose	66.258	42.331	6007.362	0	0	219.018	0	270.552	362.577	16.564	0	0	0
	Glucose	40.909	19.091	4651.364	0	109.091	76.364	47.727	0	117.273	5.455	0	0	0
	Glutamine	19.222	4.119	4536.384	0	0	54.920	126.316	0	155.149	15.103	0	0	0
	Glutamine	22.444	4.489	5013.965	0	0	64.339	119.701	0	170.574	14.963	0	0	0
	Glutamate	17.787	7.115	3646.245	0	0	201.581	0	0	246.640	33.202	0	0	0
	Glutamate	21.622	6.757	4321.622	0	0	233.784	0	0	162.162	0	0	0	0
	LiCl	19.632	3.681	4226.994	0	0	0	0	0	150.920	20.859	0	0	0
15	LiCl	18.750	4.018	4364.732	0	0	0	0	0	147.321	22.768	20.089	0	0
U-87	LiAcAC	15.190	3.376	3722.363	0	0	32.911	0	0	144.304	25.316	0	0	0
	LiAcAc	17.582	4.396	3890.110	0	0	0	0	0	112.088	31.868	0	0	0
	Glucose + Glutamine	80.851	51.064	5955.319	0	0	497.872	0	408.511	368.085	178.723	0	0	68.085
	Glucose + Glutamate	114.121	20.749	4694.524	0	48.415	254.179	0	48.415	288.761	86.455	0	0	0
	Glucose + Glutamate	0	29.242	4895.307	0	61.733	223.105	0	47.653	238.267	57.401	0	0	0
	Glutamine + Glutamate	32.542	22.373	6099.661	4.068	0	683.390	0	0	1462.373	16.271	0	0	0
	Glutamine + Glutamate	0	5.911	4239.901	0	0	363.547	118.227	0	214.286	29.557	22.167	0	0
	Glucose + LiCl	22.277	0	5027.228	0	112.871	0	0	0	219.802	31.188	0	0	0
	Glucose + LiCl	0	0	5319.084	0	108.397	0	0	0	154.198	22.901	0	0	0
	Glucose + LiAcAc	20.096	2.871	3309.091	0	125.359	0	0	0	87.081	0	0	0	0
	Glucose + LiAcAc	0	4.451	3327.596	0	129.080	0	0	0	163.798	24.036	0	0	0

Supplementary Table 2 (Continuation)

Cell line	Condition	Inosine	Isoleucine	Lactate	Leucine	Lysine	Malonate	Methanol	NAD+	NADP+	O-Phosphocholine	Pantothenate	Phenylalanine	Proline
	CTRL	0	0	476.289	151.890	0	296.220	56.357	6.873	16.495	2225.430	135.395	87.973	140.206
	CTRL	0	115.522	645.672	172.836	0	407.463	74.328	12.537	16.119	3214.925	159.403	129.851	340.299
	Glucose	0	136.209	4143.473	277.185	0	352.100	68.104	0	0	2714.642	120.545	162.770	438.593
	Glucose	0	175.887	3238.298	276.596	0	302.837	66.667	10.638	0	2590.780	111.348	212.766	359.574
	Glutamine	0	67.247	166.485	81.610	0	105.767	28.074	20.892	13.058	545.811	24.157	56.801	112.296
	Glutamine	97.333	135.333	526.667	92.000	114.000	229.333	72.667	26.000	28.000	1026.667	46.667	96.667	241.333
	Glutamate	0	114.964	404.015	122.628	0	133.577	584.672	20.803	12.044	2186.496	40.511	117.153	117.153
	Glutamate	68.524	72.702	300.000	101.950	59.331	254.875	74.373	36.769	20.056	2207.799	47.632	105.292	81.058
	LiCl	14.851	91.089	379.208	139.604	65.347	151.485	49.505	23.762	16.832	2087.129	32.673	154.455	172.277
	LiCl	104.082	66.582	350.510	91.837	89.541	286.990	65.051	16.837	19.898	2286.735	44.388	94.133	110.969
U-251	LiAcAC	127.248	86.980	792.483	72.483	111.946	304.430	901.208	39.463	16.107	2491.812	50.738	167.517	165.101
E E	LiAcAc	49.782	62.009	639.301	41.048	136.245	0	47.162	47.162	11.354	1579.913	50.655	86.463	144.105
	Glucose + Glutamine	0	140.206	16158.076	319.588	0	323.711	739.519	0	0	1446.735	129.897	152.577	548.454
	Glucose + Glutamine	0	272.387	2680.811	494.228	0	477.847	293.448	0	0	1363.339	152.574	182.059	682.371
	Glucose + Glutamate	0	133.274	5172.525	194.291	0	319.001	350.580	8.029	0	1742.730	99.554	188.403	430.330
	Glucose + Glutamate	0	132.126	5305.052	215.634	256.244	275.119	339.180	9.152	0	1645.567	68.637	161.868	351.764
	Glutamine + Glutamate	0	99.115	5456.637	209.735	0	241.593	403.540	0	0	1280.531	47.788	98.230	463.717
	Glutamine + Glutamate	0	101.805	2529.964	192.780	0	189.531	62.816	0	0	731.047	43.321	97.473	325.993
	Glucose + LiCl	0	135.040	2795.418	198.922	237.736	255.526	221.563	20.216	0	2581.132	70.350	163.342	500.539
	Glucose + LiCl	0	144.000	3442.667	201.778	111.111	268.444	67.556	16.000	10.667	2013.333	64.000	175.111	378.667
	Glucose + LiAcAc	0	155.263	10464.474	227.632	203.289	395.395	67.105	21.711	0	2788.158	84.211	226.974	317.763
	Glucose + LiAcAc	0	129.964	7623.827	205.776	414.440	261.372	195.668	18.773	0	2422.383	59.206	215.162	389.892
	CTRL	87.879	28.788	384.848	39.394	60.606	127.273	113.636	37.879	0	89.394	0	31.818	43.939
	CTRL	0	15.544	175.648	12.435	0	29.534	46.632	0	0	26.425	10.881	0	0
	Glucose	57.055	23.926	2111.043	44.172	36.810	88.344	82.822	53.374	0	82.822	11.043	31.288	64.417
	Glucose	23.182	13.636	460.909	17.727	30.000	57.273	50.455	28.636	0	25.909	5.455	0	0
	Glutamine	0	13.730	177.117	6.865	0	19.222	98.856	0	0	4.119	0	0	0
	Glutamine	0	10.474	92.768	7.481	0	20.948	50.873	0	0	5.985	0	0	0
	Glutamate	17.787	14.229	231.225	8.300	27.273	48.617	34.387	15.415	0	20.158	0	0	14.229
	Glutamate	21.622	17.568	206.757	8.108	0	60.811	35.135	17.568	0	28.378	0	0	0
	LiCl	0	12.270	142.331	12.270	0	35.583	42.945	0	0	6.135	0	0	19.632
	LiCl	10.714	9.375	151.339	12.054	0	32.143	48.214	0	0	17.411	0	0	0
U-87	LiAcAC	10.970	12.658	96.203	11.814	14.346	27.848	77.637	6.751	0	13.502	0	0	13.502
	LiAcAc	15.385	19.780	154.945	29.670	0	46.154	39.560	0	0	35.165	0	0	0
	Glucose + Glutamine	21.277	29.787	2895.745	0	0	76.596	131.915	70.213	0	63.830	12.766	0	157.447
	Glucose + Glutamate	0	20.749	1155.043	13.833	31.124	50.144	58.790	19.020	0	15.562	0	0	0
	Glucose + Glutamate	19.495	16.245	934.657	24.910	35.740	57.401	44.404	41.155	0	25.993	0	14.079	22.744
	Glutamine + Glutamate	0	30.508	512.542	26.441	0	85.424	67.119	50.847	0	40.678	0	32.542	83.390
	Glutamine + Glutamate	11.823	20.690	227.586	19.212	0	32.512	44.335	10.345	0	2.956	0	0	0
	Glucose + LiCl	0	10.396	436.634	17.822	0	51.980	106.931	28.218	0	23.762	0	0	0
	Glucose + LiCl	0	16.794	381.679	18.321	0	51.908	51.908	13.740	0	12.214	0	0	0
	Glucose + LiAcAc	0	12.440	176.077	7.656	0	23.923	129.187	0	0	5.742	0	0	0
	Glucose + LiAcAc	0	13.353	267.953	8.012	0	18.694	45.401	0	0	7.122	0	8.012	0

Supplementary Table 2 (Continuation)

Cell line	Condition	Propionate	Propylene glycol	Succinate	Threonine	Tyrosine	UDP-N-Acetylglucosamine	Uracil	Uridine	Valine	cis-Aconitate	myo-Inositol	sn-Glycero-3-phosphocholine	π-Methylhistidine
	CTRL	0	9.622	33.677	218.557	79.725	37.113	47.423	17.869	96.907	0	656.357	4.124	35.739
	CTRL	0	13.433	42.985	460.299	154.925	63.582	56.418	23.284	63.582	0	794.328	103.881	65.373
	Glucose	0	14.983	204.994	903.746	249.262	135.528	134.847	63.337	225.426	0	1089.671	96.708	121.226
	Glucose	0	13.475	170.922	609.929	212.766	138.298	147.518	87.234	304.255	0	1008.511	158.156	87.234
	Glutamine	0	0	26.768	103.156	52.884	22.198	26.115	0	80.958	0	225.245	32.644	35.256
	Glutamine	0	0	75.333	217.333	102.000	43.333	70.000	18.000	162.000	0	443.333	67.333	66.667
	Glutamate	0	0	29.562	244.161	130.292	0	75.547	0	119.343	0	596.715	41.606	75.547
	Glutamate	0	0	38.440	277.437	122.006	0	32.591	20.056	124.513	0	439.554	66.852	62.674
	LiCl	0	0	22.772	313.861	100.990	50.495	65.347	0	171.287	0	570.297	109.901	0
	LiCl	0	0	26.020	228.061	96.429	47.449	37.500	20.663	81.122	0	564.796	114.796	19.898
J-251	LiAcAC	0	0	93.423	484.027	198.926	0	131.275	0	63.624	0	865.772	62.819	128.054
ğ	LiAcAc	0	0	79.476	185.153	103.930	16.594	70.742	21.834	96.943	0	396.507	62.882	0
	Glucose + Glutamine	0	17.182	408.935	503.093	158.076	261.168	127.148	70.103	138.832	0	1568.385	148.454	101.031
	Glucose + Glutamine	0	0	304.212	591.576	174.571	265.835	222.777	140.406	198.908	0	1883.775	0	0
	Glucose + Glutamate	0	16.057	278.323	814.630	198.573	169.670	95.807	103.836	175.022	0	1327.921	168.064	117.217
	Glucose + Glutamate	0	14.871	260.248	724.690	179.600	130.410	80.076	80.076	235.081	0	934.032	136.702	109.247
	Glutamine + Glutamate	0	9.735	107.080	321.239	113.274	0	84.071	38.938	172.566	0	673.451	72.566	47.788
	Glutamine + Glutamate	0	0	86.643	230.686	88.809	0	87.726	14.079	163.538	0	662.816	47.653	57.401
	Glucose + LiCl	0	12.129	152.830	754.447	190.027	114.825	104.313	55.795	138.275	0	1301.078	197.305	91.375
	Glucose + LiCl	0	13.333	138.667	474.667	176.000	104.889	108.444	0	142.222	0	1197.333	175.111	72.000
	Glucose + LiAcAc	0	10.526	415.789	998.026	236.842	165.132	24.342	45.395	336.184	0	1626.974	385.526	143.421
	Glucose + LiAcAc	0	10.108	311.191	0	223.105	152.347	56.318	69.314	214.440	0	916.968	200.000	127.076
	CTRL	0	0	15.152	69.697	25.758	0	22.727	0	43.939	0	0	327.273	18.182
	CTRL	0	0	7.772	0	0	0	0	0	18.653	0	0	63.731	0
	Glucose	0	0	12.883	79.141	29.448	0	27.607	0	42.331	0	22.086	548.466	22.086
	Glucose	0	0	4.091	0	10.909	0	0	0	24.545	0	0	245.455	9.545
	Glutamine	8.238	0	6.865	0	0	0	0	0	13.730	0	0	32.952	0
	Glutamine	0	0	4.489	0	0	0	0	0	14.963	0	0	40.399	0
	Glutamate	0	0	7.115	0	10.672	0	0	0	18.972	0	8.300	99.605	0
	Glutamate	0	0	8.108	0	0	0	0	0	21.622	0	0	143.243	9.459
	LiCl	0	0	6.135	0	0	0	0	0	14.724	0	0	52.761	0
78-1	LiCl	0	0	6.696	0	10.714	0	0	0	12.054	0	0	88.393	0
ă	LiAcAC	0	0	5.063	0	6.751	0	0	0	12.658	0	0	62.447	0
	LiAcAc	0	0	5.495	0	0	0	0	0	21.978	0	0	114.286	0
	Glucose + Glutamine	0	0	19.149	0	0	0	14.894	0	44.681	0	48.936	682.979	0
	Glucose + Glutamate	0	0	12.104	0	12.104	0	0.000	0	27.666	0	17.291	242.075	0
	Glucose + Glutamate	0	0	8.664	0	11.913	23.827	0.000	0	22.744	0	17.329	393.141 298.983	11.913
	Glutamine + Glutamate	, ,	Ü	34.576	0	0	Ů.	24.407	·	38.644		-	2, 0, 0, 0	Ü
	Glutamine + Glutamate	0	0	13.300	0		0		0	22.167	13.300	0	54.680	0
	Glucose + LiCl Glucose + LiCl	0	0	8.911 4.580	0	0	0	0	0	14.851 30.534	0	0	234.653 125.191	0
		0	0	3.828	0	0	0	0	0	14.354	0	0	44.019	0
	Glucose + LiAcAc	0	0	3.828	0	7.122	0	0	0	14.354	0	16,914	93.472	0
	Glucose + LiAcAc	U	U	3.301	U	7.122	U	U	U	10.024	U	10.914	93.472	U

Supplementary Table 3. Concentrarion (µmol/L) of the organic compounds found in supernatant samples. (Continues on the next page)

Cell line	Condition	Weight (g)	1-Methylnicotinamide	2-Hvdroxvbutvrate	2-Oxoisocaproate	3-Hvdroxybutyrate	3-Hydroxyisobutyrate	Acetate	Acetoacetate	Alanine	Arginine	Aspartate	Choline	Citrate	Formate	Fumarate	Glucose
	CTRL	0.0873	14.444	101.444	73.333	0	61.333	87.444	0	10.667	267.667	0	31.333	40.556	644.333	3.222	0
	CTRL	0.067	13.000	80.000	72.444	0	55.000	39.778	0	10.667	317.333	0	25.000	32.667	451.778	2.556	0
	Glucose	0.0881	10.000	110.333	78.889	0	54.889	30.111	0	105.333	282.889	0	18.889	112.778	150.111	5.556	874.111
	Glucose	0.0846	8.778	94.333	68.667	0	43.333	35.333	0	86.000	291.000	0	16.444	82.778	125.333	4.222	1018.333
	Glutamine	0.0919	10.444	31.889	14.222	0	20.000	70.222	0	348.333	327.333	184.222	87.444	56.556	351.556	5.444	0
	Glutamine	0.09	10.556	33.444	0	0	57.111	33.444	0	332.000	216.889	244.889	48.889	0	336.667	5.889	0
	Glutamate	0.0548	12.556	67.667	49.222	0	44.444	27.778	0	13.111	358.111	128.111	35.778	37.222	546.222	2.778	0
	Glutamate	0.0718	11.222	56.778	42.889	0	54.111	28.556	0	24.778	274.889	115.889	38.444	43.222	374.222	3.222	0
	LiCl	0.0606	10.333	81.778	61.111	0	31.556	89.667	0	11.667	212.000	0	27.667	37.778	533.667	2.333	0
	LiCl	0.0784	11.111	78.556	56.333	0	38.444	53.889	0	15.778	338.000	49.444	26.667	36.889	437.778	1.889	0
U251	LiAcAc	0.0745	10.444	114.444	83.889	253.111	66.556	478.778	2931.111	20.333	306.333	0	19.111	107.667	369.000	4.444	0
ū	LiAcAc	0.0687	10.333	89.333	73.889	222.889	56.778	461.222	2783.111	69.222	222.444	0	24.333	103.889	241.222	4.444	0
	Glucose + Glutamine	0.0873	9.111	38.111	12.667	0	21.444	24.222	0	795.333	328.444	95.444	31.333	84.000	89.111	11.667	107.333
	Glucose + Glutamine	0.1282	11.444	35.444	10.000	0	29.111	25.111	0	910.556	225.778	88.889	22.889	112.444	68.444	14.556	37.444
	Glucose + Glutamate	0.1121	8.778	38.111	59.444	0	63.778	0	0	177.667	336.778	85.222	24.222	127.333	148.333	7.778	274.222
	Glucose + Glutamate	0.1049	10.333	91.889	83.000	0	57.889	29.000	0	202.556	289.444	78.778	24.222	114.889	156.444	7.667	340.556
	Glutamine + Glutamate	0.0678	11.444	35.000	12.556	0	19.444	43.444	0	405.222	384.000	278.556	53.889	0	406.111	6.000	0
	Glutamine + Glutamate	0.0554	9.556	27.889	10.222	0	13.444	17.222	0	297.111	306.444	238.333	43.667	0	350.444	5.333	0
	Glucose + LiCl	0.0742	8.333	107.111	79.000	0	36.000	31.222	0	97.889	260.000	0	18.444	86.778	158.667	4.444	595.667
	Glucose + LiCl	0.0675	10.556	105.889	78.222	0	40.333	28.667	0	99.667	313.667	0	19.444	112.333	189.000	5.444	397.222
	Glucose + LiAcAc	0.0912	8.667	114.556	82.444	291.111	50.000	417.111	2790.889	109.111	331.111	0	25.333	137.889	223.889	6.889	1327.000
	Glucose + LiAcAc	0.0831	8.778	107.667	101.556	266.000	44.333	461.111	2829.444	128.444	617.000	0	20.556	131.000	206.111	7.222	1097.667
	CTRL	0.0396	0	42.778	19.889	0	0	169.222	0	98.556	403.000	57.000	68.667	0	139.111	1.444	1075.889
	CTRL	0.0386	0	30.222	10.778	0	0	226.111	0	84.889	454.111	64.000	75.778	0	89.667	0	375.222
	Glucose	0.0326	0	38.778	32.222	0	0	179.111	0	112.111	665.778	69.222	77.444	0	129.556	2.333	3439.000
	Glucose	0.044	0	32.111	15.111	0	0	225.000	0	99.333	632.333	63.556	78.333	0	74.000	0	5041.222
	Glutamine	0.0437	0	26.556	13.667	0	0	163.556	0	92.556	533.333	50.000	72.778	25.000	59.556	1.111	357.889
	Glutamine	0.0401	0	27.000	14.889	0	0	174.556	0	97.889	693.222	73.778	75.667	19.000	61.778	1.222	332.889
	Glutamate	0.0506	0	34.333	26.000	0	0	117.000	0	101.556	536.889	93.333	76.333	0	91.444	1.111	476.111
	Glutamate	0.0444	0	30.333	23.222	0	0	142.111	0	96.333	541.556	79.778	70.000	0	78.667	0	372.889
	LiCl	0.0489	0	29.222	11.444	0	0	163.667	0	95.667	464.444	65.333	69.111	0	76.444	0	346.889
_	LiCl	0.0448	0	32.111	20.222	0	0	154.889	0	90.778	557.333	65.667	70.000	0	89.222	0	313.778
187	LiAcAc	0.0711	0	32.000	12.556	0	0	797.444	4428.556	119.444	536.222	66.778	85.556	23.000	75.333	0.778	440.000
	LiAcAc	0.0546	0	31.222	21.333	0	0	768.667	4415.111	90.889	487.111	60.667	153.778	21.111	77.111	0.889	453.667
	Glucose + Glutamine	0.0282	0	8.778	11.444	0	0	115.333	0	98.333	539.000	46.111	57.222	0	66.000	1.889	3697.111
	Glucose + Glutamine	0.028	0	54.667	39.000	0	0	294.556	0	233.667	1320.333	191.111	139.000	0	132.000	3.111	8858.556
	Glucose + Glutamate	0.0347	0	25.667	24.222	0	0	124.444	0	100.889	539.667	77.444	61.778	0	68.444	1.667	3892.333
	Glucose + Glutamate	0.0554	0	30.444	20.889	0	0	175.333	0	105.556	500.333	74.444	63.889	0	79.222	0.778	3513.222
	Glutamine + Glutamate	0.0295	0	27.889	10.667	0	0	118.667	0	132.889	491.889	103.778	63.333	0	98.000	2.111	0
	Glutamine + Glutamate	0.0406	0	23.111	9.444	0	0	139.889	0	88.333	403.333	54.333	59.222	13.111	59.000	0	250.556
	Glucose + LiCl	0.0404	0	26.222	11.111	0	0	183.667	0	78.222	583.778	76.889	62.000	0	59.111	0	4353.333
	Glucose + LiAcAc	0.0627	0	19.444	21.556	0	0	717.333	4221.778	74.444	575.444	80.333	61.889	19.667	60.778	0.889	4351.778
	Glucose + LiAcAc	0.0674	0	33.778	13.444	0	0	714.556	4534.778	103.667	607.333	38.222	62.556	20.444	57.889	1.222	3874.000

Supplementary Table 3. (Continuation)

Cell line	Condition	Glutamate	Glutamine	Glycine	Histidine	Hypoxanthine	Isobutyrate	Isoleucine	Lactate	Leucine	Lysine	Methionine	Nicotinate	Ornithine
	CTRL	0	0	614.444	29.444	13.667	44.111	162.889	183.111	146.111	372.667	79.111	5.444	110.444
	CTRL	0	0	435.778	66.778	8.778	43.222	139.667	310.111	138.000	336.667	80.444	5.667	89.333
	Glucose	0	0	199.778	65.222	0	50.667	100.444	7032.222	110.667	373.556	51.889	3.111	85.111
	Glucose	0	0	185.556	49.667	0	44.222	100.444	6266.889	107.111	194.667	46.667	0	65.111
	Glutamine	470.444	1882.333	328.889	62.889	3.444	9.111	235.778	537.889	234.222	384.667	64.333	4.000	195.111
	Glutamine	465.889	1849.222	312.889	62.333	4.111	10.556	328.778	446.556	228.000	331.778	70.778	5.111	264.000
	Glutamate	4628.667	0	496.444	75.778	7.222	30.333	150.111	90.444	99.778	373.111	45.778	5.000	102.000
	Glutamate	4177.333	0	356.556	37.222	3.111	25.111	136.444	358.889	114.778	337.444	35.778	4.889	100.333
	LiCl	0	0	512.111	65.222	8.667	38.222	163.889	250.333	167.778	410.444	74.111	6.222	126.000
	LiCl	162.222	0	444.000	36.111	3.667	36.111	151.556	172.222	155.889	355.333	71.778	5.222	118.333
U251	LiAcAc	0	0	355.333	49.111	1.667	53.111	100.556	378.000	113.556	368.778	59.000	4.667	88.667
23	LiAcAc	170.556	0	275.556	31.889	0	47.778	125.111	1063.667	112.889	340.778	60.667	6.000	107.333
	Glucose + Glutamine	0	2473.333	139.222	45.000	0	12.111	177.000	8962.778	150.889	197.333	39.000	0	96.333
	Glucose + Glutamine	374.111	1727.222	82.667	22.556	0	11.000	133.778	7542.667	100.000	164.667	27.111	0	108.778
	Glucose + Glutamate	4036.667	0.000	167.556	69.889	0	38.000	77.444	7519.333	66.778	294.222	49.000	0	120.778
	Glucose + Glutamate	4295.333	0.000	183.778	15.444	0	42.000	99.778	8266.222	87.000	343.778	83.667	0	77.667
	Glutamine + Glutamate	5364.778	2470.889	411.000	51.111	4.444	9.444	294.444	533.222	292.000	149.889	87.444	5.889	219.444
	Glutamine + Glutamate	4500.222	1832.000	335.778	52.000	3.556	6.778	220.556	482.667	154.444	203.000	55.444	4.778	147.000
	Glucose + LiCl	0	0	213.667	7.667	0	50.111	104.556	7091.333	115.333	345.667	50.778	5.111	93.222
	Glucose + LiCl	0	0	231.889	32.222	0	49.778	91.111	7473.667	102.000	340.000	49.889	0	123.889
	Glucose + LiAcAc	0	0	243.556	21.778	0	53.222	87.222	6528.889	90.333	341.333	46.111	0	102.444
	Glucose + LiAcAc	107.111	0	225.778	34.111	0	65.333	86.889	7324.667	95.333	352.778	46.444	0	85.889
	CTRL	0	0	328.444	68.667	12.333	15.000	323.889	3339.000	332.000	467.222	84.000	19.222	114.333
	CTRL	0	0	314.222	116.333	16.889	8.000	385.333	1585.556	376.889	398.222	88.222	18.000	94.444
	Glucose	0	0	343.111	28.556	11.111	12.556	424.889	5206.222	361.667	88.222	99.667	20.889	0
	Glucose	0	0	341.111	80.444	13.667	6.778	414.000	4228.111	415.000	461.667	97.889	21.111	0
	Glutamine	0	3520.222	263.111	42.111	12.667	4.556	364.000	1371.444	374.889	468.222	106.111	18.000	0
	Glutamine	132.111 5071.556	3569.111	272.667	40.222 83.111	13.444	247.444 8.778	311.889 375.444	1716.667 2388.333	392.556 372.778	589.000 502.000	106.889	16.333 16.778	32.111
	Glutamate Glutamate	4949.667	0	318.667 293.333	28.000	14.000 13.889	7.333	374.778		348.667	458.222	126.444 122.778	17.333	55.667
	LiCl	131.222	0	295.556	27.889	12.222	7.222	379.778	1697.778 2297.778	344.333	458.222	134.556	17.333	27.889
	LiCl	77.889	0	304.000	21.444	13.889	8.111	379.778	2227.667	367.667	477.667	84.889	18.667	28.222
	LiAcAc	0	0	304.889	18.667	11.556	6.889	380.556	2085.667	392.889	577.778	108.444	15.667	0
U87	LiAcAc	151.222	0	296.333	22.000	13.333	7.000	437.111	1699.000	378.000	449.222	105.556	14.222	27.667
	Glucose + Glutamine	0	4064.778	236.000	46.222	8.889	4.889	301.667	3823.333	288.333	362.444	87.222	14.222	47.000
	Glucose + Glutamine	425.000	7626.667	540.444	0	15.778	0	717.667	9981.222	783.444	964.000	235.333	39.000	0
	Glucose + Glutamate	4393.444	0	247.111	47.111	9.444	6.333	310.667	3718.222	309.000	432.111	66.222	16.667	42.111
	Glucose + Glutamate	4846.778	0	283.111	7.889	9.667	7.444	335.000	5188.889	333.444	427.667		16.000	64.667
												74.778		
	Glutamine + Glutamate	4324.889 3809.889	3841.444 2984.000	254.333 226.000	70.222 50.444	9.333 10.000	8.222 5.111	298.333	2299.444 1311.333	305.556 287.000	440.889 347.444	88.333	13.111 13.111	55.111 0
	Glutamine + Glutamate							279.444				80.778	16.222	0
	Glucose + LiCl	0	0	280.111	116.444	12.000	5.667	359.333	2873.444	351.778	459.333	105.222		
	Glucose + LiAcAc	0	0	256.111	56.667	11.333	6.889	328.556	3068.111	317.000	448.556	101.556	17.333	0
	Glucose + LiAcAc	0	0	243.444	34.889	10.000	5.667	337.778	3079.778	327.000	322.111	99.556	16.333	0

Supplementary Table 3. (Continuation)

Cell line	Condition	Phenylalanine	Proline	Pyroglutamate	Pyruvate	Serine	Threonine	Tryptophan	Tyrosine	Uracil	Valine	myo-Inositol
	CTRL	178.778	188.556	217.111	4.111	96.778	376.000	25.111	159.111	32.000	226.000	77.333
	CTRL	180.111	147.111	210.778	17.111	92.778	330.333	19.444	149.778	20.000	210.778	68.889
	Glucose	139.778	186.000	229.556	202.333	109.222	300.444	22.444	135.000	16.000	154.667	81.889
	Glucose	114.333	108.333	190.444	186.778	84.444	284.556	6.000	117.111	11.222	150.667	72.222
	Glutamine	144.444	244.778	516.556	42.778	225.444	335.667	24.667	152.556	21.778	280.111	68.667
	Glutamine	168.000	270.000	463.222	27.778	202.111	296.556	27.333	179.333	23.000	271.556	69.556
	Glutamate	158.222	169.444	201.889	19.111	86.667	372.778	27.667	160.000	26.000	218.667	73.889
	Glutamate	144.222	170.556	236.222	17.778	94.889	313.333	29.222	142.444	19.222	196.556	65.333
	LiCl	157.667	199.333	207.444	21.111	0	378.111	27.556	156.222	28.778	252.000	64.000
	LiCl	166.000	158.667	191.333	18.222	0	341.222	29.556	152.889	21.556	237.000	67.556
U251	LiAcAc	139.222	151.333	249.667	46.778	164.444	328.889	22.000	145.556	16.111	163.222	69.111
n n	LiAcAc	125.333	137.778	246.333	85.222	139.667	295.444	23.889	175.000	12.778	178.111	61.444
	Glucose + Glutamine	107.889	188.889	365.111	301.889	88.889	299.111	21.111	127.889	13.222	220.222	58.556
	Glucose + Glutamine	131.111	239.000	323.222	244.778	55.111	239.778	8.889	111.778	13.667	168.667	56.333
	Glucose + Glutamate	150.889	0	205.556	230.444	81.111	259.889	10.778	109.222	13.667	106.778	68.444
	Glucose + Glutamate	146.667	156.333	232.778	279.667	95.667	259.111	12.444	121.000	14.667	169.222	56.333
	Glutamine + Glutamate	148.778	264.333	553.111	29.000	243.556	388.222	26.111	205.333	21.444	342.000	78.778
	Glutamine + Glutamate	117.444	236.778	452.889	18.333	195.000	293.556	19.222	130.222	19.556	257.000	59.333
	Glucose + LiCl	122.889	138.889	170.556	173.333	0	309.222	17.333	127.000	14.000	182.222	58.444
	Glucose + LiCl	120.222	170.444	196.667	179.111	142.667	314.444	15.444	127.556	0	148.222	50.667
	Glucose + LiAcAc	125.000	134.889	224.556	285.778	114.333	277.889	15.556	172.667	8.000	145.111	52.889
	Glucose + LiAcAc	119.444	172.222	226.000	328.667	103.889	285.889	20.667	151.778	13.222	147.778	54.889
	CTRL	194.111	199.333	141.111	329.556	215.333	390.889	12.889	180.000	0	380.444	82.889
	CTRL	171.556	158.111	120.889	457.444	188.000	412.889	31.556	180.000	0	394.333	76.778
	Glucose	235.444	183.444	163.111	467.222	218.667	351.333	25.667	219.556	0	420.889	103.222
	Glucose	213.000	153.444	134.778	513.778	281.111	462.778	45.444	206.333	0	450.667	101.444
	Glutamine	174.111	256.333	471.778	430.000	214.889	274.111	13.556	189.333	0	361.333	83.000
	Glutamine	196.778	149.667	490.667	463.111	209.222	364.889	29.667	199.333	0	378.889	101.111
	Glutamate	195.444	198.222	157.889	384.111	200.222	372.667	42.556	181.889	0	420.111	86.000
	Glutamate	185.111	179.111	127.778	388.667	189.667	366.111	8.667	155.333	0	402.111	72.667
	LiCl	229.556	157.222	146.556	460.556	201.444	341.222	32.444	171.778	0	355.111	82.778
	LiCl	184.667	150.111	113.667	449.222	194.111	359.778	42.000	178.000	0	349.333	91.556
U87	LiAcAc	197.333	157.778	119.444	519.111	205.556	376.889	30.556	184.778	0	354.667	75.222
	LiAcAc	194.778	152.111	125.889	483.000	213.333	373.000	31.000	176.444	0	381.444	81.000
	Glucose + Glutamine	168.000	216.778	401.333	357.444	167.889	343.000	24.000	188.222	0	334.444	73.333
	Glucose + Glutamine	426.556	340.000	1282.556	879.222	0	677.222	42.333	411.222	0	761.889	229.444
	Glucose + Glutamate	173.778	168.556	102.778	341.667	195.889	345.000	26.778	164.000	0	344.111	73.111
	Glucose + Glutamate	179.556	192.556	110.444	311.667	223.889	390.000	5.222	169.556	0	384.222	79.222
	Glutamine + Glutamate	164.000	163.778	377.778	183.222	171.000	322.222	31.556	168.222	0	332.333	69.778
	Glutamine + Glutamate	158.111	139.333	441.444	232.889	192.778	307.000	22.667	146.333	0	312.444	67.778
	Glucose + LiCl	207.111	164.889	126.222	426.111	164.222	391.000	28.667	170.000	0	337.778	50.667
	Glucose + LiAcAc	168.889	144.111	118.444	414.778	171.444	346.222	33.333	123.444	0	356.889	86.667
	Glucose + LiAcAc	180.556	155.778	76.222	444.444	212.222	278.778	5.000	166.333	0	295.444	82.000